Doctoral Thesis

Immunogenicity of pluripotent stem cells and their differentiation products

In partial fulfillment of the requirements for the degree

"Doctor rerum naturalium (Dr. rer. nat.)"

in the Molecular Medicine Study Program

at the Georg-August University Göttingen

submitted by

Sebastian Monecke

born in

Heilbad Heiligenstadt, Germany

Göttingen, December 2012

Members of the thesis committee

First member of the thesis committee:

Prof. Dr. Jürgen Wienands

Department of Cellular and Molecular Immunology
University Medical Center
Georg-August University Göttingen

Second member of the thesis committee:

Prof. Dr. Ahmed Mansouri

Department of Molecular Cell Biology
Max-Planck-Institute for Biophysical Chemistry Göttingen

Third member of the thesis committee:

Prof. Dr. Walter Paulus

Department of Clinical Neurophysiology
University Medical Center
Georg-August University Göttingen

Advisor:

Prof. Dr. Ralf Dressel

Department of Cellular and Molecular Immunology
University Medical Center
Georg-August University Göttingen

Date of Disputation:

Affidavit

Here I declare that my doctoral thesis entitled

“Immunogenicity of pluripotent stem cells and their differentiation products”

has been written independently with no other sources and aids than quoted.

_____ _____

Date Signature

Danksagung

Ich möchte mich herzlich bei Herrn Prof. Dr. Jürgen Wienands bedanken, der mir die Möglichkeit gab in der Abteilung Zelluläre und Molekulare Immunologie meine Doktorarbeit anzufertigen und in meinen *Thesis Committee meetings,* sowie in jedem Donnerstagsseminar meine Fähigkeit wissenschaftlich relevante Fragen zu stellen schulte.

Mein größter Dank gilt Herrn Prof. Dr. Ralf Dressel, da er mir nicht nur dieses Thema stellte, sondern ebenso Hilfestellungen gab, wo es nur möglich war und jederzeit für Diskussionen offen war. Als Ansprechpartner bei aufgetretenen Problemen war er jederzeit für mich da, dafür vielen Dank!

Ebenfalls möchte ich mich bei den Mitgliedern meines *Thesis Committees,* Herrn Prof. Dr. Ahmed Mansouri und Herrn Prof. Dr. Walter Paulus für ihre Unterstützung und die rege Teilnahme an meinen *Thesis Committee meetings* bedanken. Außerdem danke ich Herrn Prof. Dr. Ahmed Mansouri und besonders Sharif Mahsur für die Möglichkeit die Stammzellkultur zu erlernen.

Mein Dank gilt auch Herrn Prof. Dr. Wolfgang Engel, Dr. Kaomei Guan-Schmidt und ihren Mitarbeitern für zahlreiche Hilfestellungen und für viele zur Verfügung gestellte Zelllinien.

Des Weiteren danke ich allen Kollegen, besonders Leslie Elsner, Niklas Engels, Henrike Fischer, Antje Isernhagen und Andreas Kahlmeyer. Ohne euch wären die langen Aufenthalte in der Zellkultur und die Mittagspausen sehr langweilig gewesen.

Meinen Eltern, Harry und Ursula Monecke, gilt mein besonderer Dank, da mir beide jederzeit zur Seite standen und schon immer an mich geglaubt haben.

Meiner Freundin Maria Wiese danke ich besonders für ihre aufmunternden Worte, Ihre Hilfe bei wissenschaftlichen Fragen und Western Blots und nicht zuletzt dafür, dass Sie so ist wie Sie ist.

Table of Contents

List of Figures

List of tables

Abstract

Embryonic stem cells (ESCs) hold great promises for regenerative medicine since they are able to differentiate into any cell type of an adult body. However, transplantation of these cells is associated with at least two severe risks: the risk of tumor formation in the recipient and the risk of an immune rejection. Since ESCs have to be transplanted in an allogeneic setting, major histocompatibility complex (MHC) mismatch could lead to rapid immune rejection of these cells. Recently, the usage of autologous pluripotent stem cells for transplantation became conceivable by description of induced pluripotent stem cells (iPSCs) and multipotent adult germline stem cells (maGSCs). But even autologous transplantations could lead to immune rejection, caused by the expression of differentiation antigens that act as mHC antigens, leading to immunogenicity of these cells.

This PhD thesis aims to further characterize the immunological properties of pluripotent stem cells (PSCs) and differentiated cells derived from them. In addition, the different types of PSCs were systematically compared. In particular, the impact of mHC antigens on the susceptibility of PSCs to cytotoxic T cells (CTLs) was analyzed. Moreover, the immunogenicity of different PSCs types was studied, involving the assessment of their ability to activate the immune system as well as their potential to suppress immune functions.

In previous studies our group has shown that PSCs can be killed by CTLs, although they were negative for MHC class I expression in flow cytometry. In these experiments, PSCs were pulsed with an antigenic peptide before they were exposed to activated, peptide-specific CTLs. In this thesis endogenously expressed Ovalbumin (OVA) was used as model antigen and CTLs, transgenic for a T cell receptor (TCR) that is specific for an OVA-derived peptide, were used to assess the capability of PSCs to process and present antigens. The analysis of two different, OVA-expressing ESC lines and an iPSC line revealed that they were not able to present OVA-derived antigens, whereas an analyzed maGSC line exhibited a weak antigen presentation capability. Gene expression studies of several proteins that are part of the peptide loading complex revealed that the transporter associated with antigen processing (TAP) genes were only low expressed in pluripotent stem cells. Since peptide loading is crucial for MHC class I stability and also for the transport to cell membrane, this could explain the failure of most stem cells to present antigens. Furthermore, co-culture of OVA-expressing PSCs with naïve OVA-specific $CD8^+$ and $CD4^+$ T cells revealed that PSC were not only unable to stimulate those cells but actively inhibited their proliferation. Transplantation studies with OVA-expressing iPSCs in syngeneic hosts revealed that the expression of OVA as a model of a mHC antigen render these cells immunogenic. The transplanted iPSC OVA cells were rejected or tumor growth was significantly impeded in immunocompetent but not in immunodeficient hosts. CTLs could have contributed to this result since OVA-specific CTLs, which were able to kill OVA-expressing RMA cells, were found in the majority of the hosts, especially in those which successfully rejected the OVA-expressing iPSCs.

List of Abbreviations

Abbreviations

°C	Celsius
aa	amino acid
APC	antigen presenting cell
APS	ammonium persulphate
Arg1	Arginase 1
bp	base pairs
BD	Becton Dickinson
BSA	bovine serum albumine
Calr	Calreticulin
Canx	Calnexin
CD	cluster of differentiation
CIP	calf intestine phosphatase
Con A	concanavalin A
CMV	cytomegalovirus
cpm	counts per minute
ct	cycle threshold
CTL	cytotoxic T lymphocyte
Cts	Cathepsin
DB	database
dH_2O	destilled water
DMEM	Dulbecco's modified Eagle's medium
DMSO	dimethylsulfoxide
DNA	desoxyribonucleic acid
dNTPs	deoxynucleotide triphosphates
DTT	dithiotreitol
E	efficiency
EB	Embryoid Bodies
E. coli	Escherichia coli
ECL	enhanced chemoluminescence
EDTA	ethylendiamine tetraacetic acid
EGTA	ethylene glycol tetraacetic acid
ELISA	Enzyme-Linked Immunosorbent Assay
ER	endoplasmatic reticulum
ESC	embryonic stem cell
EtOH	ethanol

FACS	fluorescence activated cell sorting
FasL	Fas ligand
FCS	fetal calf serum
FITC	fluoresceinisothiocyanate
Gal	Galectin
GAPDH	Glyceraldehyde 3-phosphate dehydrogenase
geo	geometric
GFP	green fluorescence protein
Gr	granzyme
HCl	hydrochloric acid
Hepes	4-(2-hydroxyethyl)-1-piperazineethanesulfonic acid
HPRT	Hypoxanthine-guanine phosphoribosyltransferase
hr/hrs	hour/hours
HRP	horseradish peroxidase
ID	Identity
IDO	Indoleamine 2,3-dioxygenase
IFN	interferon
IL-2	interleukin-2
iPSC	induced pluripotent stem cell
ISQAVHAAHAEINEAGR	OVA peptide aa 323–339
kb	kilo base pairs
kDa	kilo Dalton
LEAF	low endotoxin, Azide-free
LIF	leukemia inhibitory factor
LMP	low molecular weight protein
µCi	micro Curie
µF	micro Farad
µl	micro liter
µM	micro molar
M	gene stability measure
maGSC	multipotent adult germline stem cell
MEF	mouse embryonic fibroblast
MFI	mean fluorescence intensity
$MgCl_2$	magnesium chloride
mHC	minor histocompatibility
MHC	major histocompatibility complex
min	minutes
mRNA	messenger RNA
MTG	monothioglycerol

$NaHCO_3$	sodium bicarbonate
NaCl	sodium chloride
NaOH	sodium hydroxide
NEAA	non essential amino acids
NEB	New England Biolabs
NH_4OAc	ammonium acetate
NK	natural killer
o/n	over night
OVA	Ovalbumin (Gallus gallus)
PAGE	polyacrylamide gel electrophoresis
PBMC	peripheral blood mononuclear cell
PBS	phosphate-buffered saline
PCR	polymerase chain reaction
PE	(red) phycoerythrin
PEG	polyethylene glycol
PFA	paraformaldehyde
pH	potentium hydrogenii
PI	propidium iodide
PSC	pluripotent stem cell
PS	phosphatidylserine
qPCR	quantitative real-time PCR
RCAS1	receptor binding cancer antigen expressed on SiSo cells
RNA	ribonucleic acid
rpm	rounds per minute
RT	room temperature
SC	stem cell
SSC	spermatogonial stem cell
SD	standard deviation
SEM	standard error of the mean
SDS	sodium dodecyl sulphate
Sema	Semaphorin
SIINFEKL	OVA peptide aa 257–264
SOC	super optimal broth medium + glucose
SPI-6	serine peptidase inhibitor 6
TAE	Tris/acetate/EDTA
TAP	transporter associated with antigen processing
TAPBP	TAP binding protein
TBE	Tris/borate/EDTA
TC	tri-colour

TCR	T cell receptor
TEMED	N,N,N,N-tetramethyl-ethane-1,2-diamine
Tris	Tris(hydroxymethyl)-aminomethane
UBC	Ubiquitin C
UTR	untranslated region
UV	ultraviolet
V	variation
v/v	volume/volume
w/v	weight/volume
wt	wild type
x g	accelaration of gravity

Amino acid one-letter code

one-letter code	amino acid
A	Alanine
C	Cysteine
D	Aspartic acid
E	Glutamic acid
F	Phenylalanine
G	Gylcine
H	Histidine
I	Isoleucine
K	Lysine
L	Leucine
N	Asparaginine
P	Proline
Q	Glutamine
R	Arginine
S	Serine
T	Threonine
V	Valine
W	Trypthophane
Y	Tyrosine

1 Introduction

1.1 Pluripotent stem cells – a prospect for transplantation medicine

The future medicine is facing severe challenges – a lack of transplant donors and a population that constantly ages. Currently the united network for organ sharing (UNOS) reports that about 116000 candidates in the USA are waiting for a transplant, while only about 19000 transplants were available from January to August 2012. In addition, the frequency of age-related diseases such as heart and liver failure or Parkinson's disease will rise within the next decades. Until 2050, the number of people aged 65 or older is expected to rise from now 11 % to 26 % in low-fertility countries like Germany (DESA/PD, 2011). For these reasons, pluripotent stem cells (PSCs) hold great promises for regenerative medicine, since they possess the ability to self-renew and develop into virtually any desired cell type (see 1.2). Thus, PSCs could provide the basis for cell or tissue transplants, as well as the treatment of age-related diseases associated with irreversible tissue injury.

However, for successful stem cell transplantation several immunological hurdles have to be overcome, similar to classical transplantations. Embryonic stem cells (ESCs) are usually derived from other individuals than the potential recipients and could be rapidly rejected by the immune system if the major histocompatibility complex (MHC) of transplanted cells is mismatched or minor histocompatibility (mHC) antigens are expressed (see 1.5). In addition, the use of ESCs is restricted due to ethical concerns, since isolation of human ESCs destroys human embryos. For this reason other pluripotent or multipotent cells, such as induced pluripotent stem cells (iPSCs) and multipotent adult germline stem cells (maGSCs) have became attractive for medical research. In addition to the fact, that using these cells is not ethically objectionable, further potential advantages might be associated with their medical use. These cells or their differentiation products could be transplanted in an autologous setting, associated with a lower risk for rejection after transplantation. However, even these MHC-matched cells could potentially induce an immune rejection in the recipient due to the expression of mHC antigens to which no tolerance has been established in the recipient (see 1.5.2). Immune reactions due to mHC antigen expression could also limit the success of the proposed establishment of MHC-matched PSC biobanks. Especially, the impact of mHC antigen expression on successful stem cell transplantation has not been addressed sufficiently.

A second major problem, also significantly limiting possible studies in humans, is the risk of teratoma formation in the recipient due to the capability of PSCs to proliferate virtually indefinitely. Teratomas are tumors which comprise cells derived from all three germ-layers. In fact

this property is frequently used as a proof of pluripotency of stem cells (Brivanlou et al, 2003). As few as 2 murine or 245 human ESCs have been reported to be sufficient to induce teratoma growth in immunodeficient hosts (Hentze et al, 2009; Lawrenz et al, 2004). Differentiation into the desired cell type *in vitro* could solve this problem, since terminally differentiated cells lose their tumorigenic potential (Kolossov et al, 2006). However, prolonged *in vitro* culture could lead to uptake of xenogeneic or allogeneic antigens thereby increasing the immunogenicity of PSCs. Stringent quality tests would be needed to ensure the purity of ESC-derived cells gained from *in vitro* culture. Furthermore, differentiation could also reduce the ability of the grafted cells to get functionally integrated into the host's tissue. Currently, mouse models provide the best possibility to further analyze these immunological issues and allow the characterization of PSCs in transplantation studies.

1.2 Immunology of pluripotent stem cells

1.2.1 Embryonic stem cells

Embryonic stem cells (ESCs) are undifferentiated cells from the inner cell mass of the early blastocyst (Evans & Kaufman, 1981; Martin, 1981). The most prominent characteristic of ESCs is their potential to differentiate into virtually any adult cell type including germline (Figure 1) (Bradley et al, 1984). For developmental reasons, trophoblast cells represent the only cell type ESCs are unable to differentiate into. The second important characteristic of ESCs is their ability to self renew almost incessantly. Therefore, human ESCs, since their first description in 1998, got into the focus of regenerative medicine (Thomson et al, 1998).

Compared to other pluripotent cell types, the immunogenicity of ESCs is probably best characterized, since they have been studied for the longest time. Differences between human ESCs (hESCs) and murine ESCs (mESCs) in MHC class I expression, IFNγ responsiveness and further immunological properties were reported. Since in this thesis especially murine PSCs were studied, this section focuses primarily on the immunology of mESCs.

Using standard flow cytometry, neither MHC class I nor MHC class II complexes were detected on the cell surface of mESCs (Magliocca et al, 2006; Tian et al, 1997). However, even very few MHC class I complexes on target cells are sufficient to induce transient calcium signaling and killing activity in cytotoxic T cells (CTLs) (Brower et al, 1994) and the ability of CTLs to kill mESCs was shown *in vitro* (Dressel et al, 2009). Since mESCs became targets of CTLs the amount of MHC class I molecules expressed on the surface of mESCs must be under the detection limit of flow cytometry.

The presence of MHC class I molecules on mESCs was also demonstrated utilizing lacZ-inducible, antigen/MHC class I specific T cell hybridomas (Abdullah et al, 2007). These T cell hybridomas comprised a lacZ reporter gene under control of the IL-2 promoter. Following TCR-dependent activation upon co-culture with αPIG ESCs, the T cell hybridomas were positively stained with a β-galactosidase staining kit. In addition, T cell-mediated responses against mESCs were demonstrated *in vivo* (Boyd & Wood, 2009; Dressel et al, 2009; Robertson et al, 2007; Wu et al, 2008).

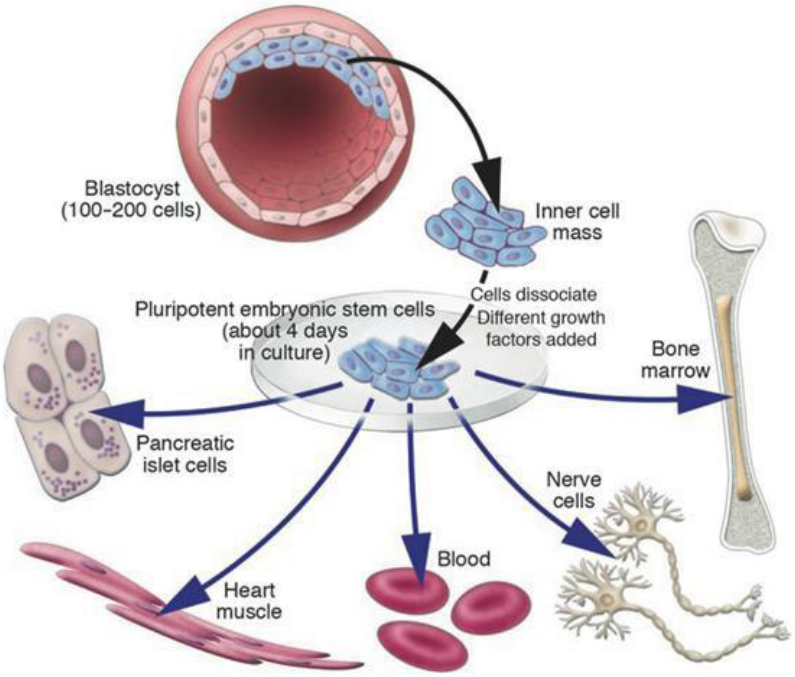

Figure 1: Differentiation capacity of embryonic stem cells (ESCs)
ESCs, derived from the inner cell mass of the early blastocyst-staged embryo, can be cultured and differentiated into various cell types *in vitro* (Fischbach & Fischbach, 2004).

Conflicting data were published regarding the ability of mESCs to respond to IFNγ signaling. One the one hand it was reported that the expression of MHC class I molecules was not enhanced after IFNγ treatment, neither on transcript nor on protein level (Abdullah et al, 2007; Nussbaum et al, 2007; Tian et al, 1997). On the other hand Bonde and Zavazava reported that MHC class I molecule expression raised after IFNγ treatment in mESCs (Bonde & Zavazava, 2006). Likewise, it remains uncertain how the expression of MHC class I molecules changes upon differentiation of mESCs. It was reported that MHC class I molecules were generally up-regulated when mESC differentiate into teratomas *in vivo* (Nussbaum et al, 2007). Another study suggests that mESCs only transiently, between day 4 and day 6 of differentiation, slightly up-regulate the MHC class I

expression (Abdullah et al, 2007). Also regarding the susceptibility of mESCs to the cytotoxic activity of natural killer (NK) cells conflicting results were published. Several groups were able to show that mESCs are efficiently killed. This was most likely due to low MHC class I molecule expression, which serve as ligand for inhibitory NK cell receptors, combined with expression of ligands for activating NK cell receptors (Dressel et al, 2010; Dressel et al, 2008; Frenzel et al, 2009). However, other groups reported that mESCs or their derivatives were resistant to NK cell-mediated cytotoxicity (Abdullah et al, 2007; Bonde & Zavazava, 2006; Koch et al, 2008; Mammolenti et al, 2004). The reasons for these discrepancies are unknown, but most likely result from the analysis of different stem cell lines, cell culture conditions and the experimental set up e.g. whether NK cells were activated prior to the assay or not. For this reason, during this thesis several PSC lines derived from different mouse strains were analyzed in order to validate the results. In summary, the findings published so far suggest that ESCs are probably more immunogenic than initially proposed in many early studies, in which a general immune privilege of ESCs was suggested (Bonde & Zavazava, 2006; Koch et al, 2008; Li et al, 2004; Magliocca et al, 2006).

1.2.2 Multipotent adult germline stem cells

Multipotent adult germline stem cells (maGSCs) are PSCs derived from spermatogonial stem cells (SSCs) of the testis. SSCs are located at the basal membrane of the tubuli seminiferi and are responsible for the generation of sperms during whole life-time of adults. The SSCs arise from primordial germ cells (PGCs) during embryonic development. The pluripotency of PGCs derived from embryos between 8.5 and 12.5 days post coitum was first demonstrated in 1992 (Matsui et al, 1992; Resnick et al, 1992). In 2004, SSCs were generated from neonatal mouse testis and for the first time pluripotency of these cells was achieved using specific cell culture conditions (Kanatsu-Shinohara et al, 2004). However, for clinical applications SSCs need to be generated also from adult testis. In 2006 SSCs from adult mouse testis were isolated and gave rise to pluripotent maGSCs for the first time following culture under ESC conditions. Pluripotency of these cells was shown *in vivo* by injection into immunodeficient hosts. MaGSCs formed teratomas consisting of cells derived from all 3 germ layers. Moreover, maGSCs were successfully differentiated *in vitro* using embryoid body (EB) formation. Resulting cells were positive for specific markers of all 3 primary germ layers (Guan et al, 2006). Subsequently, even more specialized cell types were generated *in vitro* from maGSCs including cardiomyocytes, functional endothelial cells as well as functional neurons and glia cells (Cheng et al, 2012; Glaser et al, 2008; Guan et al, 2007;

Streckfuss-Bömeke et al, 2009). Epigenetics of maGSCs were analyzed and compared to ESCs. DNA methylation status and chromatin state as well as the gene expression pattern resemble those of ESCs, further confirming their pluripotent nature (Khromov et al, 2011; Meyer et al, 2010; Zechner et al, 2009). Moreover, maGSCs and ESCs have similar miRNA and proteomic profiles (Dihazi et al, 2009; Zovoilis et al, 2008).

MaGSCs and maGSC-derived differentiated cells could potentially be transplanted in an autologous setting, what reduces immunological barriers of transplantation. However, the immunological properties of this relative new pluripotent cell type are insufficiently characterized and the expression of differentiation antigens could increase the immunogenicity of these cells. Furthermore, in clinical applications only male patients could benefit. In previous studies our group demonstrated, that maGSCs were negative for the MHC class I molecules H2K and H2D in flow cytometry similarly to ESCs. Moreover, maGSCs were susceptible to the cytotoxicity of IL-2 activated NK cells *in vitro*, most likely resulting from the combination of low MHC class I expression and expression of ligands for activating NK cell receptors. However, not all maGSC lines tested in this study were positive for ligands of activating NK cell receptors, suggesting that the low expression of MHC class I molecules might be sufficient to render maGSCs susceptible to killing by NK cells. In addition, the susceptibility of maGSCs was analyzed *in vivo*. Following injection into SCID mice, that lack T and B cells but possess functional NK cells, teratomas were formed in six of six animals. In contrast, after NK cell activation *in vivo* using poly (I:C) injection teratomas formed only in four of six animals. These results suggest, that only proper activated NK cells are able to kill maGSCs (Dressel et al, 2010). In addition, maGSCs were also moderately killed by antigen-specific CTLs *in vitro* (Dressel et al, 2009).

1.2.3 Induced pluripotent stem cells

Induced pluripotent stem cells (iPSCs) are somatic cells that are reprogrammed to pluripotency by expression of a set of defined transcription factors. IPSCs were generated for the first time in 2006 by retroviral transfection of fibroblasts with expression constructs of the transcription factors Oct4, Sox2, c-Myc and Klf4 (Takahashi & Yamanaka, 2006). These iPSCs resembled ESCs in terms of morphology and differentiation potential, which was shown by teratoma growth assays in immunodeficient mice. The iPSCs formed tumors consisting of cells of all three primary germ-layers. Moreover, their DNA methylation and chromatin state as well as their global gene expression pattern were similar to those of ESCs albeit minor differences exist depending on the generation method (Li et al, 2011; Liu et al, 2012). IPSCs can form viable chimeras, contribute to

the germline and – the gold standard proof of pluripotency – they generate living embryos when injected into tetraploid blastocysts (Okita et al, 2007; Takahashi & Yamanaka, 2006; Wernig et al, 2007). However, in 20 % of firstly generated iPSC chimeras tumors arose, due to overexpression of the proto-oncogene c-Myc. Shortly after this observation, a first report demonstrated successful reprogramming of somatic cells in the absence of c-Myc (Nakagawa et al, 2008). Utilizing a G9a histone methyltransferase inhibitor and an L-type calcium channel agonist further reduced the number of crucial transcription factors. Introduction of Oct4 and Klf4 alone was in this combination sufficient to generate iPSCs (Shi et al, 2008). However, these iPSC lines still have alterations in their genomes due to integration of the used retroviral vector. In between even more elegant methods to reprogram somatic cells into iPSCs were reported. IPSCs were generated by the use of non-integrating adenoviral vectors or by repeated transfection of non-viral expression vectors (Okita et al, 2008; Stadtfeld et al, 2008). Another advance is the generation of iPSCs using recombinant proteins for transfection. Polyarginine protein transduction domains fused to Oct4, Sox2, c-Myc and Klf4 proteins enables their transport into the cell and the nucleus (Zhou et al, 2009).

The immunogenicity of iPSCs is less well characterized compared to ESCs. Like maGSCs these cells or their differentiation products could theoretically give rise to autologous transplants thereby avoiding a MHC mismatch. However, especially after retroviral transfection the alterations in the genome could lead to expression of minor histocompatibility antigens, thereby possibly inducing rejection of transplanted cells. Furthermore, the risk of teratoma formation might increase in autologous transplantations due to reduced immune surveillance. However, studies addressing these questions are rare. For murine iPSCs it was shown that MHC class I expression is not detectable. Moreover, it was demonstrated that these cells can become targets of CTLs and NK cells (Dressel et al, 2009; Dressel et al, 2008). In addition, also human iPSCs express only low amounts of HLA molecules in addition to weak or absent expression of genes that are part of the peptide loading complex (see 1.4.1). Suarez-Alvarez et al. therefore concluded that the deficiencies in peptide loading combined with the lack of β2-microglobulin (β2m) limited the expression of MHC class I molecules on the cell surface. Furthermore, they demonstrated that epigenetic mechanisms may be responsible for these findings. The absence of *HLA-DR* and *HLA-G* was mediated by DNA methylation while the chromatin structure of the *HLA-B* and *β2m* gene acquired the H3K4me3 modification to inhibit their transcription. In addition, expression of the NKG2D ligands MICA and MICB was observed, but the functional relevance of these molecules was not investigated (Suarez-Alvarez et al, 2010). Zhao and colleagues compared the immunogenicity of murine iPSCs either generated by retroviral transfection (ViPSCs) or by an episomal approach (EiPSCs) without genomic integration. They found that ViPSCs were mostly

immune-rejected from syngeneic hosts and generally unable to form teratomas. In contrast, EiPSCs efficiently formed teratomas but showed infiltration of T cells and tumor regression in 10 % of the recipients. Analysis of both iPSC lines revealed a variety of abnormally expressed genes including tumor antigens. The authors concluded that these abnormally expressed proteins could induce T cell-mediated immune responses, even when iPSCs are not genomically altered (Zhao et al, 2011). In a previous study of our group it was shown that murine iPSCs, generated by retroviral transfection of tail-tip fibroblasts, can become targets of activated NK cells. After transplantation into SCID mice, which lack T and B cells but possess functional NK cells, teratomas formed in six of six animals. However, teratomas formed only in three of six SCID mice, in which NK cells were activated by poly (I:C) injection prior to transplantation, demonstrating that activated NK cells can contribute to the rejection of iPSCs. This finding was confirmed by *in vitro* killing assays, in which this iPSC line was highly susceptible to killing by IL-2-activated NK cells (Dressel et al, 2010).

1.3 Immune-modulating properties of PSCs

In addition to the proposed immune privilege of PSCs due to undetectable MHC class I expression further mechanisms of PSCs to evade immune responses were reported. Such mechanisms are evolutionary reasonable for ESCs since these cells, derived from the early blastocyst, need immune escape mechanisms to evade the maternal immune response (Trowsdale & Betz, 2006). Abdullah et al. reported that murine ESCs are protected against immune responses, due to high expression of serpin 6 (Abdullah et al, 2007). This protein is an endogenous inhibitor of granzyme B, the serine protease that enables NK cells and CTLs to lyse target cells via the granule exocytosis pathway (Medema et al, 2001a). However, previous studies of our group did not confirm these observations for other PSCs. Various PSC lines, including ESCs, maGSCs and iPSCs from different genetic backgrounds were analyzed but no expression of serpin 6 was detectable in western blots and only low amounts of serpin 6 mRNAs were detectable by qPCR (Dressel et al, 2010).

Another known protective protein against cellular cytotoxicity is Cathepsin B. Cathepsin B is a protease that inactivates the pore-forming activity of perforin, thereby inhibiting the transport of granzyme B into target cells. It was shown that CTLs protect themselves against perforin of their own cytotoxic granules by transient exposure of membrane bound Cathepsin B (Balaji et al, 2002). In previous studies, our group was able to demonstrate that Cathepsin B was indeed expressed in a maGSC line, an iPSC line and four different ESC lines. However, a functional relevance of Cathepsin B was not detected, since the expression of Cathepsin B did not correlate with the resistance to cytotoxic T cells (Dressel et al, 2010).

Furthermore, it was reported that expression of Fas ligand (FasL) on murine ESCs play a crucial role for their immune escape (Bonde & Zavazava, 2006). FasL is a transmembrane protein on cytotoxic cells that induces apoptosis in Fas receptor expressing cells. In addition to the granzyme B pathway, the expression of FasL is a mechanism of CTLs to induce apoptosis in target cells (Nagata, 1996). Cells of immune privileged areas such as testis or cornea express FasL, thereby avoiding the cytotoxic activity of infiltrating CTLs by a counter attack (Ferguson & Griffith, 1997; Griffith & Ferguson, 1997; van Parijs et al, 1998). Accordingly, Bonde et al. reported that 75 % of pre-activated T cells became apoptotic following exposure to murine ESCs and apoptosis was inhibited by addition of a FasL neutralizing antibody in a dose dependent manner (Bonde & Zavazava, 2006). However, in other studies no FasL expression on several murine ESCs was detected (Brunlid et al, 2007; Frenzel et al, 2009). In addition, no FasL expression was detected on human ESCs (Drukker et al, 2006; Grinnemo et al, 2006).

Yachimovich-Cohen et al. reported that the expression of Arginase I in hESCs and mESCs inhibits the activation of T cells. Arginase I is an enzyme responsible for the degradation of L-arginine from the cellular microenvironment. Depletion of L-arginine leads to reduced expression of the CD3 ζ chain of the T cell receptor (TCR) thereby inhibiting T cell activation (Bronte & Zanovello, 2005). ESCs were cultured together with peripheral blood mononuclear cells (PBMCs) and IFNγ production as well as proliferation of CFSE-stained PBMCs was used to monitor activation. Separation of hESCs and PBMCs with a permeable membrane did not restore T cell activation, suggesting a contact independent mechanism. Moreover, the supplementation of the culture medium with L-arginine restored PBMC activation in a dose dependent manner (Yachimovich-Cohen et al, 2010).

Koch et al. reported that ESCs evade the immune response by secretion of TGFβ. It is well established that TGFβ, released by regulatory T cells, inhibits the activation of naive T cells. The release of TGFβ by ESCs (R1 and 129SvJ ESC line) was demonstrated using ELISA and ESC-conditioned medium was able to suppress proliferation of CD4 positive T cells. Proliferation was largely restored after addition of a TGFβ sRII/Fc fusion protein or addition of a TGFβ neutralizing antibody (Koch et al, 2008).

It was reported that Indoleamine 2,3-dioxygenase (IDO), a tryptophan-catabolizing enzyme, suppress immune reactions. T cell proliferation is inhibited by tryptophan depletion from the cellular microenvironment and further studies demonstrated that the tryptophan catabolite kynurenine induces apoptosis in T cells by activation of caspase-8 (Fallarino et al, 2002; Mellor & Munn, 1999; Munn et al, 1999). Plumas et al. reported that IDO expression in adult mesenchymal stem cells (MSCs) induces apoptosis of activated T cells (Plumas et al, 2005). However, contribution of IDO to the immune suppressive activity of ESCs was not confirmed in another

study (Han et al, 2011). In summary, many possible mechanisms to avoid immune responses were reported for single ESC or MSC lines but a contribution of these mechanisms in other PSC lines often cannot be confirmed. Cell line specific variations or different cell culture conditions could provide an explanation for the conflicting findings, generated in independent studies. However, up to now comparative studies of different PSC lines are largely missing and investigations of immune suppressive mechanisms in iPSCs or maGSCs are rare.

1.4 Antigen presentation

The antigen processing pathway has evolved as part of the adaptive immune system and is responsible for the presentation of antigens to T cells. Antigen presentation pathways can be divided into the MHC class I and the MHC class II pathway. The MHC class I molecules are expressed on nearly every nucleated cell and display intracellular antigens, i. e. peptides generated almost exclusively in the cytoplasm of the cell, to CTLs. In contrast, MHC class II molecules are restricted to professional antigen presenting cells of the immune system, i.e. macrophages, dendritic cells and B cells. In addition to presentation of antigens derived from peptides generated in the cytoplasm, these cells capture antigens from extracellular space in order to display them to $CD4^+$ T helper cells via MHC class II molecules.

1.4.1 MHC class I pathway

Under non-pathological conditions MHC class I molecules continuously present peptides derived from endogenous proteins. These peptides are generated mainly in the cytoplasm of the cell by the ubiquitin-proteasome pathway. After viral infection or malignant transformation an additional set of peptides is generated from the pathogens or tumor antigens. This mechanism enables CTLs to recognize and kill pathologic cells. The peptides generated by the proteasome have a size distribution of 3 to 30 amino acids (Ehring et al, 1996; Kisselev et al, 1999). Upon stimulation with IFNγ the catalytical β-subunits of the proteasome are exchanged for β_i-subunits, also known as LMP 2 and LMP 7 (low molecular mass peptides). This exchange leads to the formation of the immunoproteasome that exhibits a different cleavage pattern and creates more suitable peptides for MHC class I binding (Rock & Goldberg, 1999). Especially peptides with hydrophobic and basic C-termini are preferred in binding to MHC class I molecules but also for transport by the transporter associated with antigen processing (TAP). Proteasomally generated peptides which have bound to TAP are subsequently transported into the lumen of the endoplasmatic reticulum

(ER) in an ATP-driven process. It was shown that cells lacking TAP exhibit strongly reduced levels of MHC class I molecules on their cell surface (Ljunggren et al, 1990; Townsend et al, 1989). In the lumen of the ER the N-termini of the peptides are further trimmed by aminopeptidases (Beninga et al, 1998). The resulting peptides consist of 8 to 10 amino acids. The length of peptides is crucial for binding since N- and C- termini interact with structures at the ends of the MHC class I molecule binding pocket.

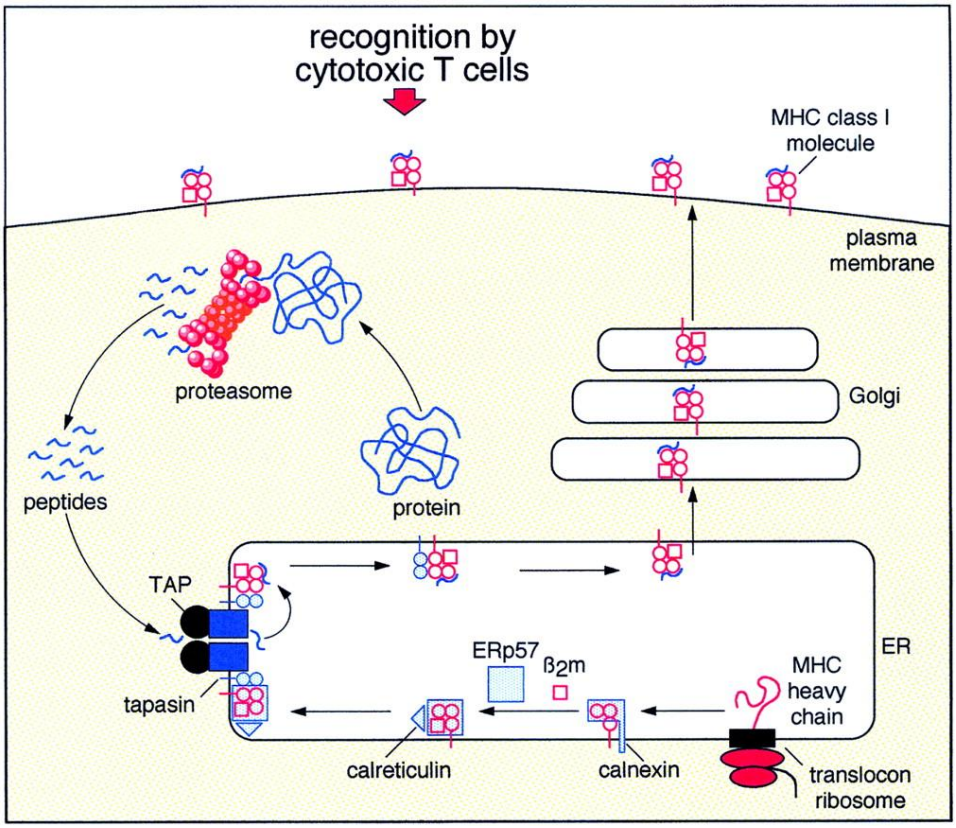

Figure 2: Antigen processing and presentation via the MHC class I pathway
Newly synthesized MHC class I molecules are loaded within the ER with antigenic peptides generated by proteasomal degradation of endogenously expressed proteins. The transporter associated with antigen processing mediates the transport of these peptides from the cytoplasm into the lumen of the ER. There, TAPBP (or tapasin) mediates the peptide loading onto MHC class I molecules. Subsequently, the transport of assembled MHC class I molecules to the cell surface via the Golgi apparatus is initiated.
(Lankat-Buttgereit & Tampe, 2002)

The MHC class I molecule is a dimer consisting of a transmembrane heavy chain (HC) and β2-microglobulin (β2m). MHC class I proteins are cotranslationally translocated into the lumen of the ER, where this dimer is stabilized by the membrane-bound chaperone Calnexin. Calnexin is subsequently exchanged for another chaperone - Calreticulin. The soluble Calreticulin together with its co-factor ERp57, a thiol reductase that assists in the generation of disulfide bonds, further stabilizes the MHC class I molecule. Both chaperones are also known to be involved in quality

control. They bind incomplete or misfolded proteins and prevent them from being exported via the golgi apparatus. The TAP binding protein (TAPBP) mediates the interaction of TAP and the MHC class I molecules and assists in loading peptides onto the MHC class I molecules (Sadasivan et al, 1996). TAPBP is furthermore involved in retention and stabilization of MHC class I molecules (Grandea & Van Kaer, 2001). In addition, TAPBP is responsible for the optimization of the peptide cargo, accelerates the dissociation of low-affinity peptides and favors the binding of high-affinity peptides to MHC class I molecules (Praveen et al, 2010). Upon peptide binding, the MHC class I molecule is stabilized, Calreticulin is released and the transport to the cell surface via the Golgi apparatus is initiated (Lankat-Buttgereit & Tampe, 2002; Pamer & Cresswell, 1998). There, the peptides (antigens) are presented to CTLs that recognize structures of the MHC class I molecule binding pocket in combination with the peptide structure with their T cell receptor (TCR). A schematic overview of the MHC class I antigen processing pathway is shown in Figure 2.

Antigens captured from the extracellular space can also be presented to CTLs on MHC class I molecules. This process is termed cross-presentation and mediated by professional antigen presenting cells (APCs), particularly macrophages and dendritic cells (Rock et al, 1993). This important mechanism enables the adaptive immune system to respond to viruses that do not infect APCs or against tumor cells which not act as APCs themselves. Antigens of virally infected or malignantly transformed cells that become necrotic or apoptotic are taken up by phagocytosis or macropinocytosis. Subsequently, antigens are translocated into the cytosol for entry into the proteasome- and TAP-dependent MHC class I pathway (Kovacsovics-Bankowski & Rock, 1995; Norbury et al, 1995). Additional pathways for cross-presentation were suggested. Instead of protein translocation into the cytosol for proteasomal degradation and subsequent translocation into the ER, it was suggested that parts of the ER, including TAP and MHC class I transporters, are incorporated into the phagosomes and lysosomes (Ackerman et al, 2006). In this model, antigens are proposed to enter the cytosol and re-enter the phagosome/ER compartment following proteasomal degradation (Guermonprez et al, 2003; Houde et al, 2003). In addition, a cross-presentation pathway was described, which functions independently of proteasome activity or TAP transporters. In this pathway proteases such as Cathepsin S generate antigens, which are suitable for loading on MHC class I molecules, within the phagosomes. MHC class I molecules are also present in these compartments and can be loaded directly (Pfeifer et al, 1993; Shen et al, 2004).

1.4.2 MHC class II pathway

As mentioned before the MHC class II pathway enables professional antigen presenting cells (APCs) to display antigens, mainly captured from the extracellular space, to $CD4^+$ T cells. Professional APCs are mainly dendritic cells (DCs) but also macrophages and B cells. Furthermore, stimulation with IFNγ can induce the expression of MHC class II molecules on the surface of non-professional APCs such as endothelial and epithelial cells as well as fibroblasts. Professional APCs mainly capture antigens via endocytosis and process them in the endosomal/lysosomal pathway. However, also antigens derived from endogenously expressed proteins have access to the MHC class II antigen presentation pathway (Schmid et al, 2007; Zhou et al, 2005). The main proteases mediating the processing of antigens in the endosomal/lysosomal pathway are cathepsins (Colbert et al, 2009). In general, peptides bound by MHC class II molecules have a size of 12 to 19 amino acids, but also the binding of longer peptides was reported (Davidson et al, 1991; Engelhard, 1994; Moss et al, 2007).

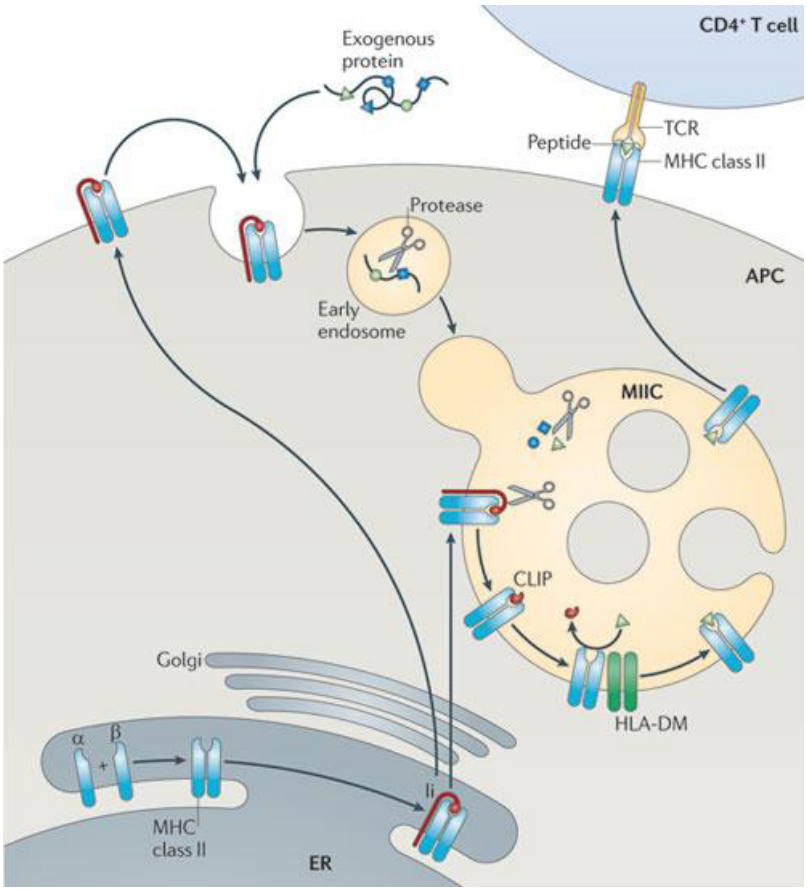

Figure 3: Antigen processing and presentation via the MHC class II pathway
Antigen presentation via MHC class II molecules is mainly mediated by professional APCs. The professional APCs are able to capture proteins from the extracellular space. These proteins are degraded by proteases in endosomes and the resulting antigenic peptides are loaded on MHC class II molecules in specialized cellular organelles called MIIC. (adapted from(Neefjes et al, 2011))

MHC class II complexes are assembled in the ER and consist of an α- and a β-chain. This dimer is stabilized by binding of the chaperone molecule invariant chain (Ii) (Cresswell, 1996; Sant & Miller, 1994). The invariant chain exhibits a cytoplasmic tail containing a motif that targets the Ii-MHC class II complexes to endosomal/lysosomal compartments. There, Ii is degraded by acidic proteases to the class II-associated invariant chain peptide (CLIP), a fragment which remains associated with the MHC class II peptide binding groove (Maric et al, 1994; Riese et al, 1996). The MHC class II-like chaperone DM catalyzes the removal of CLIP and further stabilizes the MHC class II complex (Denzin & Cresswell, 1995; Sherman et al, 1995). Moreover, DM catalyzes the association of antigenic peptides to MHC class II molecules by altering MHC class II conformation (Narayan et al, 2009). Thereby, DM is also able to mediate the dissociation of sub-optimal peptides from the MHC class II binding groove (Kropshofer et al, 1996). Another class II MHC-like chaperone called DO regulates the activity of DM. DO probably has an inhibitory function in order to broaden the range of possible presented peptides (Watts, 2012). This process occurs in a specialized cellular organelle, the MHC class II compartment (MIIC) (Pieters, 1997). The endosomal/lysosomal compartments, containing antigenic peptides intersect MIICs which contain the pre-assembled MHC class II molecules. Upon antigen binding, MHC class II molecules are transported to the cells surface and display antigens to $CD4^+$ T cells (see Figure 3).
Recently, additional pathways for MHC class II antigen presentation were reported including macroautophagy and chaperone-mediated autophagy as well as a TAP-dependent pathway and intercellular antigen transfer (Crotzer & Blum, 2009; Taylor et al, 2006; Tewari et al, 2005).

1.5 Immune rejection pathways

1.5.1 MHC mismatch

MHC class I as well as MHC class II molecules are polygenic and co-dominantly expressed. Mice, depending on the different strains, comprise up to three MHC class I allels (one H2-K, -D, -L from each parent) encoding the α chain that build the MHC class I molecule together with the invariant β2-microglobulin. The MHC class II molecules in mice consist of a α chain and a β chain each, which are encoded in two allel pairs (one H2-A- and -E from each parent). Moreover, the MHC genes are highly polymorphic and several hundreds of different alleles exist within the population. Due to the polymorphic nature of the MHC molecules, CTLs are able to discriminate between self and non-self or host and donor, respectively, since CTLs not only recognize the antigens presented via MHC molecules but also structures of the MHC molecules itself. Therefore, transplanted cells expressing foreign MHC molecules can immediately become targets of CTLs leading to an acute

immune rejection. As mentioned before MHC class I molecules are expressed on nearly every nucleated cell whereas MHC class II molecules are restricted to cells of the immune system. However, cytokine stimulation can induce MHC class II expression also on a variety of somatic cells. Whether ESCs could become targets of CTLs due to MHC mismatch is currently studied. Since neither mESCs nor hESCs express MHC class II complexes (Drukker et al, 2006; Grinnemo et al, 2006; Li et al, 2004; Tian et al, 1997), even after IFNγ stimulation, it is unlikely that these molecules elicit an immune rejection. However, for hESCs it is reported that small amounts of MHC class I molecules are expressed and several studies demonstrated their existence on mESCs (albeit beyond the detection limit of flow cytometry) (Abdullah et al, 2007; Dressel et al, 2009). Thus, ESC could indeed become targets of CTL-mediated cytotoxicity after transplantation. Moreover, transplanted ESCs could become targets of NK cells, since ESCs lack MHC class I molecules that act as inhibitory signal for NK cells (Dressel et al, 2010; Frenzel et al, 2009). In addition, transplanted pluripotent cells differentiate into a variety of somatic cells which exhibit a higher expression of MHC molecules at least in certain cell populations at specific time points of differentiation (Abdullah et al, 2007). Other PSC sources like iPSCs or maGSCs seem to be more suitable for transplantation, since these PSCs could be transplanted in an autologous setting, thereby avoiding a MHC mismatch.

1.5.2 The minor histocompatibility antigens

About one third of newly synthesized proteins in cells are rapidly degraded by the proteasome and the generated peptides can be presented on MHC class I molecules to CTLs (Schubert et al, 2000). Therefore, every expressed protein that differs from the host, e g. due to polymorphisms, could potentially elicit an immune response even when donor and recipient are identical at the MHC locus. Cells which express such mHC antigens are immunogenic, albeit less strongly than cells with MHC mismatch. In the context of PSC transplantation, mHC antigen expression could be critical. Even autologously transplanted PSCs might express mHC antigens e.g. in form of differentiation antigens or other gene products expressed only in early development or pluripotent cells, respectively. Since the immune system never encountered such gene products before, tolerance towards these antigens might lack. In humans it was already demonstrated that T cells exist, which were specific for the transcription Oct4, a key factor of pluripotency (Dhodapkar et al, 2010). However, whether the expression of mHC antigens render murine PSCs indeed immunogenic is currently insufficiently analyzed and a key question of this thesis.

1.5.3 The allorecognition pathways

The allorecognition pathways are mainly mediated by professional APCs and T cells and can be divided into the direct and the indirect allorecognition pathway. In the direct allorecognition pathway donor derived APCs, contained within the graft, move to near lymph nodes where they interact with host $CD4^+$ and $CD8^+$ T cells. Due to the expression of foreign MHC class II molecules resident $CD4^+$ and $CD8^+$ T cells become activated and elicit an immune response leading to acute graft rejection.

In the indirect allorecognition pathway professional APCs of the host capture antigens derived from transplanted cells which became necrotic or apoptotic. These mHC antigens, would subsequently been displayed to host $CD4^+$ and $CD8^+$ T cells in draining lymph nodes what induces the immune rejection of all somatic cells which display these antigens. In the context of murine PSC transplantation mainly the indirect pathway would be involved due to lacking MHC class I and MHC class II expression. However, since PSCs could theoretically differentiate into APCs, also the direct allorecognition pathway could be involved in the immune rejection of transplanted cells.

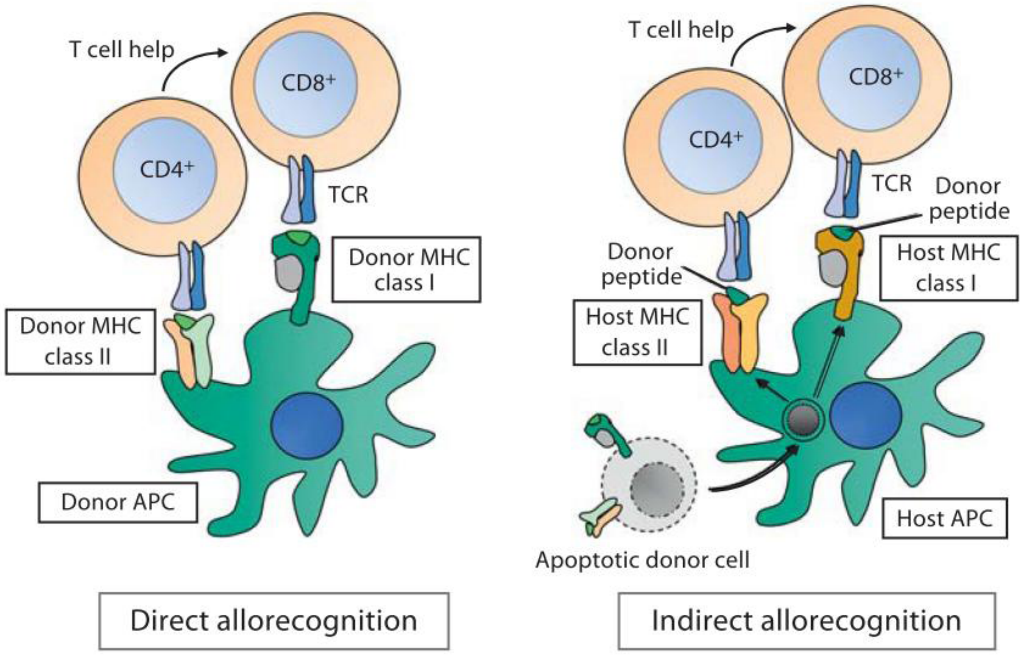

Figure 4: Allorecognition pathways
The illustration shows the direct and the indirect allorecognition pathway. The direct allorecognition pathway is mediated by donor derived APCs, which activate $CD4^+$ and $CD8^+$ T cells in draining lymph nodes due to MHC mismatch. The indirect allorecognition pathway is mediated by host derived APCs, which display mHC antigens, derived from proteins of apoptotic donor cells, to $CD4^+$ and $CD8^+$ T cells.
(Saric et al, 2008)

1.6 Aims of this thesis

The major goal of this thesis was to characterize the immunogenicity of PSCs and their derivatives. Therefore, the three different PSC types ESCs, maGSCs and iPSCs were analyzed and systematically compared. Several lines of each PSC type, derived from different mouse strains, were used in order to determine the extent of cell type and cell line specific variations.

1) Immunogenicity of PSCs which express a mHC antigen

Using endogenously expressed Ovalbumin (OVA) as a model for a mHC antigen, the ability of these PSCs to induce immune responses was analyzed *in vivo* and *in vitro*. It was tested, whether the OVA-expressing PSCs were able to activate naïve OVA-specific $CD4^+$ and $CD8^+$ T cells in co-culture assays. Moreover, the ability of syngeneic hosts to induce an OVA-specific immune response and to reject OVA-expressing cells was investigated. In these teratoma growth assays also the effect of the immune response against a mHC antigen on the tumorigenicity of iPSCs was assessed.

2) Capability of PSCs to process and present antigens

Recognition of mHC antigens requires antigen presentation by MHC class I molecules. Despite low MHC class I expression, PSCs can become targets of activated peptide-specific CTLs after pulsing with the appropriate peptide. However, it has remained unclear so far whether PSCs can process endogenous antigens. It is possible that defects in antigen presentation pathway are responsible for the low MHC class I expression on PSCs. Using the OVA-expressing PSC lines as model, the ability of different PSC types to process and present antigens was analyzed. Moreover, the expression of peptide loading complex related genes was determined.

3) Immune escape mechanisms

Several mechanisms conferring an immune privilege of ESCs in addition to low MHC class I expression have been described in the last years. In embryo-derived ESCs it might be evolutionary reasonable to exhibit immune escape mechanisms due to their semi-allogeneic nature in the maternal environment. However, iPSCs and maGSCs lack this fetal origin. Therefore, it was investigated whether these types of PSCs are also immune privileged. The expression of several molecules, potentially involved in immune escape mechanisms was analyzed and compared in different PSC lines.

2 Materials

2.1 Biological material

2.1.1 Bacterial strains

The chemo-competent *E. coli* strain One Shot® Top10F` from Invitrogen was used for cloning procedures and plasmid preparation. This bacterial strain had the following genotype: *F´ lacIq Tn10 (TetR) mcrA Δ(mrr-hsdRMS-mcrBC) Φ80lacZΔM15 ΔlacX74 recA1 araD139 Δ(ara-leu)7697 galU galK rpsL endA1 nupG.*

2.1.2 Cell lines

Table 1: Cell lines

Label	Origin	Description
ESC (BTL-1)	129/Sv mouse	blastocyst-derived embryonic stem cell
ESC (C57Bl/6)	C57Bl/6 mouse	blastocyst-derived embryonic stem cell
ESC (FVB)	FVB/N mouse	blastocyst-derived embryonic stem cell
ESC (MPI-II)	129/Sv mouse	blastocyst-derived embryonic stem cell
ESC (R1)	129/Sv mouse	blastocyst-derived embryonic stem cell
iPSC (129/Sv)	129/Sv mouse	iPSCs; clone 11.1; derived from MEFs
iPSC (C57Bl/6)	C57Bl/6 mouse	iPSCs; clone 6-5-120; derived from MEFs
TTF-iPSC	129/Sv mouse	iPSCs derived from tail tip fibroblasts
maGSC (129/Sv)	129/Sv mouse	multipotent adult germline stem cell
maGSC (C57Bl/6)	C57Bl/6 mouse	multipotent adult germline stem cell
maGSC (FVB)	FVB/N mouse	multipotent adult germline stem cell
maGSC (Stra8)	Stra8-eGFP/Rosa26 mouse	multipotent adult germline stem cell
F9	129/Sv mouse	teratocarcinoma cell line
J774	BALB/cN mouse	monocyte/macrophage cell line
RMA	C57Bl/6 mouse	T cell lymphoma cell line
YAC-1	A/Sn mouse	Lymphoma cell line

The TTF-iPSC line was provided by R. Jänisch, Whitehead Institute for Biomedical Research (Meissner et al, 2007). IPSC as well as maGSC lines were kindly provided by Kaomei Guan-Schmidt, Cardiology and Pneumology, University Medical Center Göttingen (Guan et al, 2006). The ESC line MPI-II was kindly provided by Ahmed Mansouri, Department of Molecular Cell Biology, Max-Planck-Institute for Biophysical Chemistry Göttingen and the remaining ESC lines by Wolfgang Engel, Department of Human Genetics, University Medical Center Göttingen.

2.1.3 Laboratory animals

All animals were bred in the central animal facility of the University Medical Center of the University of Göttingen and are listed in Table 2.

Table 2: Laboratory animals

Label	Organism	Description	Reference
OT-I	mouse	TCR transgenic for SIINFEKL/H2K^{b}	(Hogquist et al, 1994)
OT-II	mouse	TCR transgenic for ISQAVHAAHAEINEAGR/ H2A^{b}	(Barnden et al, 1998)
C57Bl/6	mouse	MHC haplotype: H2^{b}	
129/Sv	mouse	MHC haplotype: H2^{b}	
SCID/beige (CB-17)	mouse	severe combined immunodeficiency affecting B, T and NK cells	
RAG/2$^{-/-}$ cγ$^{-/-}$ (C57Bl/6)	mouse	severe combined immunodeficiency affecting B, T and NK cells	(Mombaerts et al, 1992)
LOU/c	rat	MHC haplotype: RT1^{u}	
BUF	rat	MHC haplotype: RT1^{b}	

2.1.4 Antibodies

Antibodies were used according to manufacturer's instructions and diluents as well as concentrations are listed in the corresponding method section.

Table 3: Primary antibodies

Label	Host	Isotype/clone	Supplier
anti-β Actin	mouse	IgG1/AC-15	Sigma
anti-CD3	rat	IgG1/CD3-12	AbD Serotec
anti-CD3 PE	rat	IgG2b/17A2	BioLegend
anti-CD4 PE	rat	IgG2b k/PJP6	Immunotools
anti-CD4 FITC	rat	IgG2a/RM4-5	Caltag
anti-CD4 TC	rat	IgG2a/RM4-5	Invitrogen
anti-CD8a	rat	IgG2a/53-6.7	Biolegend
anti-CD8 PE	rat	IgG2b/YTS 169.4	ImmunoTools
anti-CD8 FITC	rat	IgG2b/YTS 169.4	ImmunoTools

anti-CD15 (SSEA1)	mouse	IgM/MC-480	Biolegend
anti-CD45R	rat	IgG2a/RA3-6B2	Biolegend
anti-CD49b (DX5)	rat	IgM/DX5	Biolegend
anti-CD80	rat	IgG2a/1G10-B7	BD (Becton Dickinson)
anti-CD86	rat	IgG2a/GL1	BD
anti-CD276 LEAF	rat	IgG2a/MIH35	Biolegend
anti-CtsB	goat	IgG	R&D Systems
anti-F4/80	rat	IgG2b/A3-1	Biolegend
anti-H2D^{b} PE	mouse	IgG2b/KH95	Biolegend
anti-H2K^{b} PE	mouse	IgG2a/AF6-88.5	Biolegend
anti-IDO	rat	IgG2b/m-IDO48	Biolegend
anti-Ki-67	rat	IgG2a/TEC3	DAKO
anti-NKp46	rat	IgG2a/29A1.4	Biolegend
anti-Oct3/4	mouse	IgG1/40-Oct3	BD
anti-OVA ascites	mouse	IgG1/OVA-14	Sigma
anti-SIINFEKL/H2K^{b} APC	mouse	IgG1/25-D1.16	eBioscience
anti-TCR Vβ 5.1,5.2 FITC	mouse	IgG1/MR9-4	BD

Table 4: Secondary antibodies

Label	Host	Isotype/clone	Supplier
anti-mouse APC	goat	IgG/Poly4053	Biolegend
anti-mouse Cy3	donkey	IgG F(ab')2-Fragment	Jackson ImmunoResearch
anti-mouse FITC	goat	IgG/Poly4053	Biolegend
anti-mouse-IgG TC	goat	IgG1/M35006	Caltag
anti-mouse-IgG1	rat	IgG1/A85-1	BD
anti-mouse-IgG2a	rat	IgG1/R11-89	BD
anti-mouse-IgG2b	rat	IgG2a/R12-3	BD
anti-mouse-IgG3	rat	IgG1/R2-38	BD
anti-mouse-IgA	rat	IgG1/C10-1	BD
anti-mouse-IgM	rat	IgG2a/II-41	BD
anti-mouse-IgE	rat	IgG1/R35-72	BD
anti-rat TC	goat	IgG/ R40106	Caltag

Table 5: Isotype controls

Label	Supplier
mouse-IgG1 FITC	Caltag
mouse-IgG1 PE	Immunotools
mouse-IgG2a FITC	Pharmingen
mouse-IgG2a PE	Caltag

mouse-IgG2b PE	Caltag
mouse-IgM FITC	Caltag
rat-IgG1 FITC	Biolegend
rat-IgG2a FITC	Caltag
rat-IgG2b FITC	Caltag
rat-IgM FITC	Caltag

2.1.5 Enzymes

Table 6: Enzymes

Label	Supplier
Calf intestine phosphatase	NEB (New England Biolabs)
M-MLV Reverse Transcriptase	Promega
Pfu Polymerase	Fermentas
Phusion Polymerase	Finnzymes and NEB
Proteinase K	Merck
Restriction enzymes	NEB and Promega
RNase A	Roche Diagnostics
RNasin® Plus Ribonuclease Inhibitor	Promega
T4 DNA Ligase	Fermentas and NEB
Taq Polymerase	Genecraft and NEB

2.2 Chemicals and reagents

All chemicals and reagents, which are only listed in the corresponding method section, were purchased at Carl Roth or Sigma. Chemicals and reagents supplied by other companies are specified in Table 7.

Table 7: Chemicals and reagents

Chemical/Reagent	Supplier
Ammonium chloride (NH_4Cl)	Merck
Ammonium persulphate (APS)	Serva
Bromphenol Blue (Na^+-salt)	Merck
Bovine serum albumine (BSA)	PAA
Dimethylsulfoxide (DMSO)	Merck
dNTPs	Genecraft, NEB
Dulbecco's modified Eagle's medium (DMEM)	Gibco
ECL Western Blotting Substrate	Promega
ESGRO® (LIF)	Chemicon (Millipore)
Ethanol (analytical grade)	UMG Apotheke
Fetal calf serum (FCS)	PAA

FACSflow	Becton Dickinson
GeneRuler 1kb DNA ladder	Fermentas
Hexadimethrine Bromide (Polybrene)	Merck
Iscove's Modified Dulbecco's Medium (IMDM)	Gibco
Isoamylalcohol	Merck
Isopropanol	Merck
Magnesium chloride ($MgCl_2$)	Merck
Methanol	Merck
Mitomycin C	AppliChem
Natrium chromate ($Na_2{}^{51}CrO_4$)	Hartmann Analytic
Non-essential amino acids	PAA
Phosphate-buffered saline (PBS)	Biochrome
Pre-stained protein marker, Broad Range	NEB
Propidium iodide (PI)	AppliChem
Protease Inhibitor Cocktail (P2714)	Sigma
Pyruvat	Biochrom
Random primer	Promega
Recombinant mouse interleukin-2 (IL-2)	R & D Systems
Roswell Park Memorial Institute medium (RPMI)	Gibco
Scintillator Optiphase HiSafe 3	PerkinElmer
SIINFEKL (Ovalbumin amino acid (aa) 257–264)	Bachem AG
N,N,N,N-tetramethyl-ethane-1,2-diamine (TEMED)	AppliChem
TiterMax®	TiterMax
TRIzol®	Invitrogen
Trypsin	Biochrom
UltraPure™ Agarose	Invitrogen

2.3 Disposables

Table 8: Disposables

Label	Supplier
96 - well Wallac plates	PerkinElmer
Top seal for Wallac plates	PerkinElmer
96 - well plates for real-time PCR	Applied Biosystems
Top seal for real-time PCR plates	Applied Biosystems
Blotting paper GB 003	Whatman
Cell culture 96- and 24-well plates	Sarstedt
Cell culture flasks (250 ml)	Sarstedt
Cell culture plates (5 ml, 10 ml & 25 ml)	Greiner
Cell strainer	Becton Dickinson
Conical tubes (13 ml, 15 ml & 50 ml)	Greiner/Sarstedt
Cover slips	Sarstedt
Cryo tubes	Greiner
FACS tubes	BD/Sarstedt

Microscope slides	Menzel
Multipette® plus Combitips	Eppendorf
Parafilm®	Pechiney Plastic Packaging
Pasteur pipettes	Wilhelm Ulbrich Mainz
Pipette tips (10 µl, 200 µl & 1000 µl)	Greiner/Sarstedt
Reaction tubes (0,2 ml, 1 ml & 2 ml)	Greiner/Sarstedt
Sterile pipettes (1 ml, 2 ml, 5 ml, 10 ml & 25 ml)	Greiner
Sterile filters (pore size 0.2 µm & 0.45 µm)	Greiner
Syringes (2 ml, 5 ml, 10 ml & 20 ml)	Becton Dickinson
Transwell® cell culture inserts (0.4 µm)	Nunc
UVette	Eppendorf
Wheighing paper	Machery-Nagel

2.4 Devices

Table 9: Devices

Description	Label	Supplier
Agarose gel trays and chambers	Perfect Blue™ Gel System	Peglab
Aqua bidest. Supply	arium® pro	Sartorius
Autoclave	High pressure steam sterilisator FVS	Integra Biosciences
Biological Safety Cabinet	HERASave®	Thermo Fisher Scientific
Centrifuges	Multifuge 1 b Multifuge 3 S-R	Heraeus
	Mini Centrifuge MCF-2360	LMS Consult
	3K30	Sigma
	RC 3B Plus	Sorvall
Counting chamber	Neubauer improved	Krannich
Dispenser	Multipette® plus	Eppendorf
Electroporation	GenePulser & Cap. Extender	BioRad
Flow Cytometer	FACS Calibur	Becton Dickinson
Homogenizer	Tenbroeck	schuett-biotec
Imaging devices	Chemilux Blot Detection Imager UV workbench GelImager	Intas
Incubators	HERACell 150	Heraeus
Incubator shaker	Unitron-plus	Infors
Liquid Scintillation Counters	MicroBeta Trilux 1450 MicroBeta2 Plate Counter	PerkinElmer
Magnetic stirrer/heater	RH basic 2	IKA
Microscopes	Axiovert 35 LSM 510 Axioplan 2	Zeiss
pH-Meter	inoLab® pH Level 1	WTW
Pipettes	Research® & Reference®	Eppendorf
Power supply	EPS-301/-3501 XL	GE Heathcare

Scales	ACCULAB Vicon BP 61	Sartorius
SDS gel chambers	Hoefer SE600 Ruby	GE Heathcare
Spectrophotometer	BioPhotometer NanoDrop™ ND-1000	Eppendorf Thermo Fisher Scientific
Thermal Cycler	ABI 7500 Real-Time PCR System MasterCycler epgradient TPersonal 48	Applied Biosystems Eppendorf Biometra
Thermoblocks	Thermomixer comfort Stuart Block Heater SBH130	Eppendorf Bibby Scientific
Vortexer	MS1 Minishaker	IKA
Western blot device	Semiphor Transpher Unit	GE Heathcare

2.5 Buffers and solutions

The composition of buffers and solutions is listed in the corresponding method section. For sterilization the solutions were autoclaved at 125 °C for 30 min or filtrated with a 0,2 µm sterile filter. A consistently used buffer was PBS with the following composition:

PBS: 137 mM NaCl
12 mM Phosphate
2.7 mM KCl
pH 7.4

2.6 Oligonucleotides

All primers were synthesized by Metabion international AG or biomers.net GmbH, respectively. Restriction site sequences were introduced close to the 5' end of cloning primers to flank the resulting amplicons with new restriction sites if required (Kaufman & Evans, 1990).

The qPCR primers were designed using IDT's PrimerQuest that incorporates Primer3 software developed by the Whitehead Institute for Biomedical Research. The primer specificity was verified with the nucleotide BLAST web tool from NCBI. All qPCR primers were designed to span exon-exon junctions when it was feasible. In case of targets with two isoforms the primers were designed to target both transcripts. Some primer sequences were obtained from the RT primer database (www.rtprimerdb.org) and their DB-ID is listed in the RefSeq table column. All primer sequences are shown in table 10-12.

Table 10: Primers for qPCR

#	Label	Sequence 5'-3'	RefSeq
1	Arg1_F	ACC TGG CCT TTG TTG ATG TCC	NM_007482.3
2	Arg1_R	AGC ACC ACA CTG ACT CTT CCA TTC	
3	B2-M_F	CTC ACA CTG AAT TCA CCC CC	NM_009735.3
4	B2-M_R	CAG TAG ACG GTC TTG GGC TC	
5	B7-H3_F	TCA CGG CTC AGT CAC CAT CAC A	NM_133983.4
6	B7-H3_R	GCT TGA TCT TTC TCC AGC ACA CGA	
7	B7-H3_F_2	TCG TGT GCT GGA GAA AGA TCA AG	NM_133983.4
8	B7-H3_R_2	TTT CAG AGG GTT TCA GAG GCC GTA G	
9	B7-H4_F	GGA CAT CAA AGT GAC AGA TTC AGA GG	NM_178594.3
10	B7-H4_R	TCT TAG CAT CAG GCA ACA GGA GAG	
11	Calr_F	AGC TGT TTC CGA GTG GTT TG	NM_007591.3
12	Calr_R	GAT CAG CAC ATT CTT GCC CTT G	
13	Canx_F	TGA TCC TCT TCT GCT GTT CTG G	NM_007597.3
14	Canx_R	TTC ATC CTT CAC ATC TGG CTG G	
15	CD80_F	ATT GCT GCC TTG CCG TTA CAA CTC	NM_009855.2
16	CD80_R	GGT TCT TAT ACT CGG GCC ACA C	
17	CD86n_F	TCA GTA TCT CCA ACA GCC TCT CTC	NM_019388.3
18	CD86n_R	ACT CCG TTT CCA GAA CAC ACA C	
19	CD112_F	CGA GAG TCA CCC AGC ACA G	NM_008990.3
20	CD112_R	TGT TGT CGG CAG ATG AGG ATG	
21	CD155_F	AGC ACG AAC ACG GGT GAC TTT C	NM_027514.2
22	CD155_R	CTA GGG CAT TGG TGA CTT C	
23	eGFP_qRT_F	CAA GCA GAA GAA CGG CAT CAA GGT	U55761.1
24	eGFP_qRT_R	ACT GGG TGC TCA GGT AGT GGT T	
25	ERp57_F	TGA TAA AGA TGC CTC AGT GGT GGG	NM_007952.2
26	ERp57_R	TGT TGG TGT GTG CAA ATC GGT AG	
27	Gal-1_F	CAG GTC TCA GGA ATC TCT TCG CTT	NM_008495.2
28	Gal-1_R	GGC ACA GGT TGT TGC TGT CTT T	
29	GAPDH_F	TGT GTC CGT CGT GGA TCT GA	RTPrimerDB ID : 7880
30	GAPDH_R	TTG CTG TTG AAG TCG CAG GAG	
31	H2-D1_F	CCC TGT GAG CTT GGG TTC AG	NM_010380.3
32	H2-D1_R	ACA GGG CAG TGC AGG GAT AG	
33	H2-K_F	CCT GGA GTG GAC TTG GTG AC	NM_001001892.2
34	H2-K1_R	GGT GTA GAG GGG TGG ACT GG	
35	H60_F	GTG GCT TCT CCA GCA AAG GA	NM_198193.2
36	H60_R	GCC ACC ACT CTC ATG GGT TC	
37	HPRT1_F	GTC CTG TGG CCA TCT GCC TA	NM_013556.2
38	HPRT1_R	GGG ACG CAG CAA CTG ACA TT	
39	IdoI_F	CCA CAC TGA GCA CGG ACG G	NM_008324.1
40	IdoI_R	TGC GGG GCA GCA CCT TTC G	
41	LMP2_F	ATC TTC TGT GCC CTC TCA GGT TC	NM_013585.2
42	LMP2_R	AGA TGC GCT AAC AAG TCC TCA C	

43	LMP7_F	GCT TAT GCT ACC CAC AGA GAC AAC	NM_010724.2
44	LMP7_R	CAC TGA CAT CGG AAC TCT CCA C	
45	OVA_qRT_F	AGA GGT GGT AGG GTC AGC AGA GG	NM_205152.1
46	OVA_qRT_R	TGG TTG CGA TGT GCT TGA TAC AGA AG	
47	PD-L1_F	TTT GGA GAT CAC AGC CAG GGC AAA	NM_021893.3
48	PD-L1_R	ACC GTG GAC ACT ACA ATG AGG AAC	
49	PD-L2_F	TGT TGT CTC CTT CTG TCT CCC AAC	NM_021396.2
50	PD-L2_R	TGT GTC AAT ATC AGC ACC CAG CAC	
51	Qa_1b_F	GAT GTT GCT TTT TGC CCA C	NM_010398.3
52	Qa_1b_R	TAG CCG ACA ATG ATG AAC C	
53	Raet1_consF	CCA AGG AGA CGC CAG AGG AG	NM_020030.2
54	Raet1_consR	CAG GAC CTC TCC AAG AAC AGC A	
55	RCAS1_F	CGT GGG ATT GCG TAA CCA GAA A	NM_019480.4
56	RCAS1_R	CAC TGT TGC TAG GCA GGT ACA AA	
57	Sema3A_F	AGC TCC AGT TAC CAC ACC TTC CTT	NM_001243072.1
58	Sema3A_R	CCA GCC CAT TTG CAT TCA TCT CTC	
59	SPI9_Fnew	TGC AGA CAA AAC TTG TGA AGT CCT C	NM_011452.2
60	SPI9_Rnew	TGC CTG GAC ACC TCT GCT TC	
61	Tap1_F	CTG CTC TCC CTC TAC CCC TC	NM_001161730.1
62	Tap1_R	CTG AGT GGA GAG CAA GGA GTC	
63	Tap2_F	GCA GAC GAC TTC ATA GGG GA	NM_011530.3
64	Tap2_R	GTT GCT TCT GTC CCA CAG C	
65	Tapbp_F	ACT GGG AAT GGG ACC TTC TGG	NM_001025313.1
66	Tapbp_R	ACA CAA CGG GTG CTG GTG TTA G	
67	TGFb1_F	GCA ACA ATT CCT GGC GTT ACC TTG	NM_011577.1
68	TGFb1_R	AAG CCC TGT ATT CCG TCT CCT TG	
69	UBC_F	AGG TCA AAC AGG AAG ACA GAC GTA	RTPrimerDB ID : 42
70	UBC_R	TCA CAC CCA AGA ACA AGC ACA	

Table 11: Primers for cloning

#	Label	Sequence 5'-3'
1	OVA_PEGFP_HindIII_F	CTA AGC TTG CCA CCA TGG GCT CCA TCG GC
2	OVA_PEGFP_BamHI_R	CCG GAT CCA AAG GGG AAA CAC ATC TGC C
3	OVA_PEGFP_EcoRI_F	CTG AAT TCG CCA CCA TGG GCT CCA TCG GC

Table 12: Primers for sequencing

#	**Label**	**Sequence 5'-3'**
1	OVAeGFP_Seq_F1	TGT TGG TGC TGT TGC CTG ATG AAG TC
2	OVAeGFP_Seq_R1	CGG CCA TGA TAT AGA CGT TGT GGC TG
3	OVAeGFP_Seq_F2	CAA GGA GCT CAA AGT CCA CCA TGC C

4	OVAeGFP_Seq_R2	AGA CTT CAT CAG GCA ACA GCA CCA AC
5	PEGFP-1_Seq_F	GTA TTA CCG CCA TGC ATT AGT TAT TAC
6	PEGFP-1_Seq_R-neu	GAA CTT GTG GCC GTT TAC GTC G
7	T7_Seq_F	TAA TAC GAC TCA CTA TAG GG

2.7 Vectors

Table 13: Vectors

Label	Supplier
pBluescript II SK	Stratagene
PEGFP-1	Clontech
pTriEx™-1.1	Novagen

2.8 Commercial kits

Table 14: Commercial kits

Label	Supplier
ABsolute™ Blue QPCR SYBR® Green Low ROX Mix	Thermo Fisher
EndoFree Plasmid Maxi Kit	QIAGEN
CloneJET™ PCR Cloning Kit GeneJET™ Plasmid Miniprep Kit	Fermentas
High Pure RNA Isolation Kit	Roche Diagnostics
Invitrogen TA Cloning® Kit (with pCR®2.1 vector)	Invitrogen
Power SYBR® Green PCR Master Mix	Applied Biosystems
Promega PureYield™ Plasmid Midiprep System Promega Wizard® SV Gel and PCR Clean-Up System	Promega
TransIT®-293 Transfection Reagent	Mirus Bio LLC
Zymoclean™ Gel DNA Recovery Kit	Zymo Research

2.9 Software and databases

7000 System SDS Software	Applied Biosystems
Bio Edit	Ibis Biosciences
CellQuest Pro	Becton Dickinson
Cyflogic	Perttu Terho & CyFlo Ltd
Endnote X1.0.1	Thomson Reuters
GENtle	Magnus Manske - University of Cologne
LSM Image Browser	Zeiss
MicroBeta Workstation	PerkinElmer
NCBI database	National Center for Biotechnology Information (NCBI)
NEB-Cutter	New England Biolabs
Oligo Analyzer	Integrated DNA Technologies (IDT)
Primer Quest	Integrated DNA Technologies (IDT)
qPCR primer database	RTprimerDB.org
Works 2007	Microsoft
WinSTAT	Robert Fitch

3 Methods

3.1 Microbiological Methods

3.1.1 Culture and storage of *E. coli*

E. coli was cultured overnight at 37 °C and aerobic conditions in an incubator shaker at 222 rpm. For small volumes (3 ml) conical 13 ml tubes were used, for large volumes (100 ml) Erlenmeyer flasks. LB medium or LB agar plates supplemented with antibiotics according to the resistance gene of the *E. coli* strain were used for the cultures. For long-term storage, 800 µl of an *E.coli* o/n culture was vigorously mixed with 200 µl 100 % glycerin and stored at -80 °C.

LB medium:	0.5 % (w/v)	Yeast extract
	0.5 % (w/v)	NaCl
	1 % (w/v)	Tryptone
	dissolved in	dH_2O

LB agar plates: 1.5 % (w/v) agar in LB-Medium

Antibiotic concentrations:

Ampicillin:	100 µg/ml
Kanamycin:	50 µg/ml

3.1.2 Transformation of *E. coli*

Plasmid DNA was introduced into competent *E. coli* using the heat shock method. Therefore, *E. coli* were thawed on ice and mixed with 20 – 100 ng plasmid DNA or 10 – 15 µl of a ligation mixture. After 30 min incubation on ice the transformation mixture was heated to 42 °C for 1 min. After a brief cooling on ice, 500 µl SOC medium was added and the transformation mixture was incubated in a thermoblock at 37 °C and 700 rpm for 60 min. Subsequently the mixture was plated on LB agar plates and cultured o/n at 37 °C.

SOC medium:	2 % (w/v)	Tryptone
	0.5 % (w/v)	Yeast extract
	10 mM	$MgCl_2$
	10 mM	$MgSO_4$
	10 mM	NaCl
	2.5 mM	KCl
	20 mM	Glucose

3.2 Molecular biological methods

3.2.1 Purification of nucleic acids

3.2.1.1 Extraction of nucleic acids from agarose gels

DNA fragments were extracted and purified from agarose gels using the Zymoclean™ Gel DNA Recovery Kit or the Promega Wizard® SV Gel and PCR Clean-Up System according to manufacturer's instructions.

3.2.1.2 Precipitation of nucleic acids

Nucleic acids were precipitated from aqueous solution by adding 1/10 volume of 3 M sodium acetate, pH 4.8 stock, (0.3 M final) and one volume isopropanol or 2.5 volumes pure ethanol, respectively. Sodium acetate was exchanged by 1/3 volume of 7.5 M ammonium acetate (2.5 M final) when short oligonucleotides should not be co-precipitated. Samples were centrifuged and the resulting DNA pellet was solubilized in an appropriate volume of dH_2O.

3.2.1.3 Phenol chloroform extraction

Nucleic acid solutions were purified from proteins and other contaminants using phenol chloroform extraction. Therefore, 1 volume of a nucleic acid containing solution was thoroughly mixed with 1 volume phenol chloroform isoamylalcohol (15:24:1) solution. The solution was centrifuged and the aqueous phase was transferred into a new reaction tube. In order to remove phenol remains the nucleic acid containing solution was mixed with 1 volume chloroform. Following centrifugation the aqueous phase was again transferred into a new reaction tube and the nucleic acids were recovered by alcohol precipitation (see 3.2.1.2).

3.2.2 Isolation of nucleic acids

3.2.2.1 Plasmid DNA preparation

Plasmid DNA was isolated from an *E. coli* overnight culture, grown in LB-medium supplemented with the appropriate antibiotic, either from 1.5 ml for plasmid mini preparation or from 100 ml for plasmid midi preparation according to manufacturer's instructions using kits listed in Table 14: Commercial kits. For isolation of non-analytical grade plasmid DNA, *E. coli* were treated with

buffers for alkaline lysis according to standard protocol (Birnboim & Doly, 1979). Subsequently, DNA was precipitated by addition of 80 % isopropanol to this mixture (see 3.2.1.2). DNA was dissolved in dH_2O and stored at -20 °C.

3.2.2.2 RNA and genomic DNA preparation

RNA and genomic DNA, respectively, was isolated from $1x10^6$ to $5x10^6$ cells or 100 mg tissue using TriZol reagent according to the manufacturer's instructions. Genomic DNA was dissolved in 8 mM NaOH and stored at 4 °C. RNA was dissolved in dH_2o and stored at -80 °C. RNA quality was assured by visualization of the integrity of 18S and 28S RNA loaded on a 1 % agarose gel. All DNA and RNA samples were quantified with a spectrophotometer at a wavelength of 260 nm. Sample purity was assessed by calculating the ratio of the 260 nm to 280 nm values. A ratio of ≥ 1.8 indicated pure DNA, a ratio ≥ 2 pure RNA.

3.2.3 Amplification of nucleic acids

3.2.3.1 Polymerase chain reaction (PCR)

PCR allowed the rapid amplification of DNA fragments specified by a sense and an antisense primer in vitro.

For analytical proposes Taq polymerase was used and a reaction was set up as follows:

2.5 µl	10 x Taq PCR buffer
0.5 µl	dNTP-Mix (10 mM)
5 pmol	sense primer
5 pmol	antisense primer
100 ng	template DNA
5 U	Taq polymerase
add to 25 µl	dH_2O

For preparative proposes (cloning procedures etc.) Phusion polymerase was used, since this enzyme has proof reading activity. A reaction was set up as follows:

10 µl	5 x Phusion PCR buffer
1 µl	dNTP-Mix (10 mM each)
10 pmol	sense primer
10 pmol	antisense primer
100 ng	template DNA
2 U	Phusion polymerase
add to 50 µl	dH_2O

The PCR cycler program was adapted with respect to temperature and time for denaturation, annealing and elongation steps. Denaturation and elongation times were associated with the polymerase specifications and were set according to manufacturer's instructions. Annealing temperatures were set according to the specific melting temperatures of the primers that were used.

3.2.3.2 cDNA synthesis

RNA samples needed to by completely transcribed into cDNA for qPCR. Therefore, random hexamers were used to prime the RNA and M-MLV reverse transcriptase was used for transcription into cDNA.

In the beginning 2 µg RNA were mixed with 2 µl random hexamers and filled up with dH_2O to a final volume of 15 µl. This mixture was incubated at 70 °C for 10 min to break up secondary structures of the RNA. Following incubation, the sample was cooled on ice to prevent reforming of secondary structures. Subsequently, the following master mix was added to the sample:

5 µl	5× reverse transcriptase buffer
2 µl	dNTP mix (10 mM)
1 µl	DTT (0.1 M)
1 µl	RNasin plus RNase inhibitor (40 U/µl)
1 µl	MMLV-reverse transcriptase (200 U/µl)

The complete reverse transcription approach was incubated for 1 h at 37 °C for cDNA synthesis and afterwards stored at -20 °C.

3.2.3.3 Quantitative real-time PCR (qPCR)

Quantitative real-time PCR was performed in 96 well plates using the ABI 7500 Real-Time PCR System. All genes were analyzed in triplicates to obtain more valid results. The cDNA was diluted 1:40 with dH_2O prior to reaction, which was set up as follows:

10 µl	ABsolute™ Blue QPCR SYBR® Green Mix
5 pmol	sense primer
5 pmol	antisense primer
1 µl	template cDNA
add to 20 µl	dH_2O

The ABsolute™ Blue QPCR SYBR® Green Mix comprised polymerase buffer, dNTPs, a hot start polymerase and SYBR green dye to amplify and detect DNA. The following cycler program was used:

1.	50 °C	2 min	
2.	95 °C	10 min	
3.	95 °C	15 sec	} 40 cycles
4.	60 °C	60 sec	
5.	60 °C to 90 °C	+ 1 °C per min	

The stepwise increase in temperature during the 5th step (dissociation stage) was used to verify product specificity. Since SYBR green dye intercalates non-specifically into DNA, unintended products like primer dimers, contaminations and mispriming artifacts can cause a false positive fluorescence signals. Since the melting temperatures of intended products were known, their specificity was assured by comparison with the temperature peak of the according dissociation curve. No quantitative real-time PCR data were calculated, if the ct-values were above 33 since this late amplification was considered to be unspecific.

Efficiency of primer pairs

Primer efficiencies were estimated by a dilution series of pooled cDNA samples and calculating a linear regression based on the obtained Ct values. Subsequently the efficiency was inferred from the slope of the line. The following formula was used for efficiency calculation:

$$efficiency = 10^{\frac{-1}{slope}}$$

Relative quantification with Pfaffl

The Pfaffl method is an efficiency correlated quantification model (Pfaffl, 2001). Thereby differences in the expression of genes are normalized to the efficiency of target gene and reference gene amplification. The ratio of the target to the reference gene was calculated according to the following formula:

$$ratio = \frac{E_{(target\ gene)}^{\Delta Ct_{(target\ gene)}(control-treatment)}}{E_{(reference\ gene)}^{\Delta Ct_{(reference\ gene)}(control-treatment)}}$$

Estimating the most accurate reference gene

In order to ensure the stability of the reference (housekeeping) gene expression between different samples, three different reference genes were amplified in all samples. The reference gene should not be differentially regulated between different cell lines and therefore only the most accurate one was used for normalization. The following formulae were used for the calculation of the reference gene stability (M) as described (Vandesompele et al, 2002).

For every combination of two reference genes (j and k) an array (A_{jk}) of m elements was calculated:

$$A_{jk} = \left\{ log_2 \frac{a_{1j}}{a_{1k}}, log_2 \frac{a_{2j}}{a_{2k}}, \dots, log_2 \frac{a_{mj}}{a_{mk}} \right\} = \left\{ log_2 \frac{a_{ij}}{a_{ik}} \right\}_{i=1 \to m}$$

Subsequently, the pairwise variation (V_{jk}) for two reference genes (j and k) was defined as the standard deviation of the A_{jk} elements:

$$V_{jk} = st.dev(A_{jk})$$

Finally, the gene stability measure (M_j) for the reference gene (j) was calculated by the arithmetic mean of all pairwise variations (V_{jk}):

$$\mathrm{M}_j = \frac{\sum_{k=1}^{n} \mathrm{V}_{jk}}{n-1}$$

3.2.4 Molecular cloning

3.2.4.1 Restriction endonuclease digestion of nucleic acids

Nucleic acids were digested in a reaction volume of 20 µl according to the specific reaction conditions of the different type II restriction enzymes as described by the manufacturer. For the linearization of large amounts of plasmid DNA reaction time and volume was modified to assure complete digestion.

3.2.4.2 Dephosphorylation of nucleic acids

To avoid unintended re-ligation of vector DNA, especially in case of blunt ended DNA fragments, phosphate residues were removed using calf intestine phosphatase (CIP). Typically, 10 U of CIP enzyme were added directly to a restriction digestion and incubated for 15 to 30 min at 37 °C. Otherwise CIP was used according to the manufacturer's instructions.

3.2.4.3 Ligation of DNA fragments

DNA fragments and vector DNA were fused using T4 DNA Ligase. Typically 1 µl (5 U) of the enzyme in a total reaction volume of 20 µl was prepared and incubated at RT for 1 hr or overnight at 4 °C. The corresponding amounts of insert and vector DNA were calculated according to the following formula:

$$amount\ of\ insert\ (ng) = \frac{10 \text{ x amount of vector (ng)} x\ insert\ lenght\ (bp)}{\text{vector length (bp)}}$$

3.2.4.4 TA cloning

Invitrogen's TA cloning kit was used for direct ligation of DNA fragments ampfilified with Taq polymerase. DNA amounts and reaction volumes were set up according to manufacturer's instructions. For the direct ligation of blunt ended DNA fragments Fermentas' CloneJET PCR Cloning Kit was used according to the manufacturer's instructions.

2.2.5 Agarose gel electrophoresis

DNA fragments were identified and separated using the Perfect Blue™ Gel System. The agarose concentration varied from 0.7 % to 2 % according to the length of DNA fragments. TAE buffer was used as chamber run buffer and for agarose solutions (dissolved at 100 °C). In addition, ethidium bromide was added in concentrations of 0.1 % (v/v) to identify DNA fragments when exposed to UV light. DNA samples were supplemented with 6 x loading dye to aid the loading procedure and to visualize the progression. An electric field of 90 – 120 V and 220 mA was applied for 30 – 60 min according to the fragment length.

6 x loading dye:	34 % (w/v)	sucrose
	0.02 % (w/v)	cresol red dye
	dissolved in	dH_2O

1 x TAE buffer:	40 mM	Tris-acetate pH 8,0
	1 mM	EDTA
	dissolved in	dH_2O

3.3 Biochemical methods

3.3.1 SDS-PAGE

Discontinuous SDS-PAGE was used for the molecular weight depending separation of proteins. Protein samples were supplemented with 1/4 volume 4 x protein sample buffer and incubated for 5 min at 90 °C in order to denature the proteins. Subsequently, protein samples were loaded and concentrated in the stacking gel at 20 mA, following separation in the resolving gel at 50 mA. The concentration of acrylamide in the resolving gel varied between 8 % and 12.5 % according to the molecular weight of the protein that was investigated. Proteins were identified by comparison to a pre-stained protein marker.

Protein sample buffer:	100 mM	Tris-HCl pH 8.0
	4 % (w/v)	SDS
	0.2 % (w/v)	Bromphenol blue
	20 % (v/v)	Glycerol

Stacking gel buffer (pH 6.8):	0,5 M	Tris-HCl
	0,4 % (w/v)	SDS

Stacking gel:	16 % (v/v)	Acrylamid-Bis (30 %)
	25 % (v/v)	Stacking gel buffer
	59 % (v/v)	dH_2O
	0.01 % (v/v)	TEMED
	0.1 % (v/v)	APS (10 %)

Resolving gel buffer (pH 8.8):	1.5 M	Tris-HCl
	0.4 % (w/v)	SDS

Resolving gel (10 %):	33 % (v/v)	Acrylamid-Bis (30 %)
	22 % (v/v)	Resolving gel buffer
	45 % (v/v)	dH_2O
	0.01 % (v/v)	TEMED
	0.1 % (v/v)	APS (10 %)

SDS-Running Buffer:	25 mM	Tris-HCl
	192 mM	Glycine
	0.1 % (w/v)	SDS

3.3.2 Coomassie blue staining

Proteins in SDS gels were non-specifically stained using Coomassie blue staining solution. The Coomassie blue dye bound to basic side chains of amino acids. After 20 min incubation at RT the stained SDS gel was washed with dH_2O several times until the background color in the SDS gel was removed.

Coomassie blue staining solution:	0.25 % (w/v)	Coomassie Brilliant Blue R250
	45 % (v/v)	MeOH
	10 % (v/v)	acetic acid

3.3.3 Western Blot

Western blotting was used to transfer proteins from a SDS gel onto a nitrocellulose membrane for subsequent immunostaining. During this study, the semi-dry blotting technique was used. Therefore, the SDS gel was placed on a nitrocellulose membrane and this assembly was enclosed by Whattman paper moistened with blotting buffer. This stack was placed in the blotting chamber and an electric current of 1 mA/cm^2 was applied for 1 hr to transfer the proteins onto the membrane.

Blotting buffer:	48 mM	Tris-HCl
	39 mM	Glycine
	0.0375 % (v/v)	SDS
	20 % (v/v)	MeOH
	dissolved in	dH_2O

3.3.4 Immunostaining

For the staining of specific proteins on a nitrocellulose membrane, unspecific binding of epitopes by the applied antibody was inhibited by incubating the membranes in blocking solution for 1 hr. The specific antibody was diluted in antibody solution according to the manufacturer's instructions and incubated o/n at 4°C with the membrane. Following 3 washing steps with TBST for 10 min at RT, the second antibody was supplied for 1 hr at RT in antibody solution with a concentration of 1:5000. Subsequently, the nitrocellulose membrane was washed 3 times at RT for 10 min and the proteins visualized by 1:1 ECL A and B solutions in a LAS-4000 reader.

Blocking/antibody solution: 5 % (w/v) milk in TBST

3.4 Cell culture methods

3.4.1 Culture of cells

The culture of all cell lines was carried out in a 5 % CO2-humidified atmosphere at 37°C. The culture media composition with all additives is shown in table 15. FCS was inactivated at 56 °C for 30 min. Media additives sterility was assured by manufacturers or achieved by sterile filtration if possible. Genecitin (G418) was added to the media for selection of transgenic cell lines. The minimal working concentration for different cell lines was estimated in kill curve assays and is shown in Table 15.

Table 15: Cell culture media

Media type	Media composition
SC media	DMEM + Glutamax + 10 % (v/v) FCS + 1 % (v/v) 100 x NEAA + 50 µM 2-mercaptoethanol + 1000 U/ml LIF + 50 U/mL Penicillin + 50 µg/mL Streptomycin (+ 300 ng/ml G418)
MEF media	DMEM + Glutamax + 10 % (v/v) FCS + 1 % (v/v) 100 x NEAA

media for cells of lymphatic origin	RPMI + Glutamax + 10 % (v/v) FCS + 50 µM 2-mercaptoethanol + 50 U/mL Penicillin + 50 µg/mL Streptomycin (+ 1000 ng/ml G418)

3.4.2 Freezing and thawing cells

Cells were harvested from cell culture dishes depending on their specific growth conditions. Subsequently cells were centrifuged for 5 min at 1000 rpm and resuspended in an adequate volume of cell specific medium. 500 µl of the cell suspension was transferred into cryo tubes and 500 µl cell specific 2 x freezing medium was added. Cryo tubes were slowly frozen in a closed styrofoam box at -80 °C. After 24 hrs cryo tubes were transferred to -140 °C for long-term storage. For thawing cells cryo tubes were briefly incubated in a water bath at 37 °C. Thawed cells were diluted in 10 ml MEF medium and centrifuged for 5 min at 1000 rpm. Subsequently, cells were resuspended in their specific growth medium and plated in an appropriate cell culture vessel.

2 x freezing media:	20 % (v/v)	DMSO
	20 % (v/v)	FCS
	60 % (v/v)	cell specific culture medium

3.4.3 Transfection

DNA fragments and plasmids were introduced into cells using electroporation. For stable integration the plasmid DNA was linearized prior to transfection. Only endotoxin free and highly purified plasmid DNA was used in order to increase the transfection success rate. In the beginning 1 x 10^7 cells were collected and diluted in 800 µl PBS. Subsequently, 40 µg DNA was added. The whole mixture was transferred into an electroporation cuvette and pulsed with the following cell type specific conditions:

stem cell lines: 250 mV, 500 µF

other cell lines: 250 mV, 960 µF

After a short incubation for 5 min at RT, cells were diluted in 20 ml pre-warmed complete growth medium and seeded in a 15 cm cell culture dish. Selection procedure started at earliest 24 hrs after electroporation.

3.4.4 Stem cell culture

3.4.4.1 Preparation of MEFs

The uterus of a pregnant mouse was dissected on day 13.5 and transferred into a cell culture dish with 10 ml pre-warmed PBS. Subsequently the embryos were removed from the uterus and transferred into a new cell culture dish with 10 ml pre-warmed PBS. Heads, extremities, tail and organs were removed. The remaining parts were picked to fine pieces using forceps and transferred into an Erlenmeyer flask prepared with sterile ballotinis and 5 ml trypsin. This mixture was incubated at 37 °C on a magnetic stirrer for 20 min. The reaction was stopped and simultaneously washed by addition of 10 ml MEF medium. After centrifugation for 5 min at 1000 rpm the pellet was resuspended in 25 ml MEF medium and plated on a 15 cm cell culture dish. Following 3 days of culture, cells were frozen (see 3.4.2) and stored at -140 °C.

MEF-trypsin: 0.25 % (w/v) Trypsin
0.02 % (w/v) EDTA
dissolved in PBS

3.4.4.2 Expansion and inactivation of MEFs

One vial of primary MEFs was thawed and expanded up to passage 4 in 15 cm cell culture dishes. After expansion, when they reached nearly confluence, cells were inactivated with Mitomycin C or by gamma irradiation in the Department of Transfusion Medicine, University Medical Center, Göttingen. For inactivation with Mitomycin C culture medium was exchanged with 10 ml inactivation medium and the cells were incubated for 2.5 hrs in a cell incubator. Subsequently cells were washed 2 times with PBS and harvested by trypsinization. For inactivation by gamma irradiation cells were harvested by trypsinization and subsequently transferred into a 50 ml conical tube with pre-warmed MEF medium. Cells were irradiated for a total of 30 Gy. Following inactivation procedure cells were counted and 2 x 10^6 cells were frozen (see 3.4.2) or cells were plated directly for later usage.

Mitomycin C stock solution: 2 mg Mitomycin C dissolved in 2 ml PBS
Inactivation medium: 1 % (v/v) Mitomycin C stock solution in MEF medium

3.4.4.3 Passaging of stem cells

Stem cells were cultured on a monolayer of inactivated mouse embryonic fibroblasts (MEFs) (see 3.4.4.2). One day before passaging the stem cells, MEFs were seeded on cell culture vessels treated with 0.1 % (w/v) gelatine for 15 min at RT. Stem cells were washed once with PBS and subsequently incubated with 1 volume SC-trypsin at 37 °C until dissociation of stem cell colonies occurred. Single cell suspension was prepared by diluting cells in 10 volumes SC medium and gently pipetting up and down. About 1/10 volume of this cells suspension was transferred into a new cell culture vessel prepared with MEFs for further culture.

SC-trypsin: 0.1 % (w/v) Glucose
0.3 % (w/v) Tris-HCl
0.25 % (w/v) Trypsin
0.02 % (w/v) EDTA
dissolved in PBS

3.4.4.4 Stem cell differentiation in Embryoid Bodies (EBs)

Stem cells were harvested and a single cell suspension was prepared. Cells were subsequently pre-plated into a gelatinized dish. After 1 hr of incubation at 37 °C stem cells were collected from the supernatant. Since remaining MEFs adhere much faster to the culture dish surface than stem cells, both cell types were separated. Pure stem cells were collected from supernatant, counted and diluted with EB-medium to a concentration of 2.5×10^5 cells/ml (500 cells per drop). Now, the inner side of a bacterial (ultra-low-attachment) culture dish cover was seeded with drops of the cell suspension. The dish cover was placed on top of a bacterial culture dish filled with 10 ml PBS to avoid dehydration of the hanging drops. After 2 days of culture, hanging drops were collected from the dish cover, diluted in 10 ml of fresh EB medium and incubated in suspension for additional 1-2 days. The EBs were collected from suspension culture and seeded into gelatinized (high- attachment) cell culture dishes which allows the EBs to adhere and further differentiate until the desired time points were reached.

EB medium: IMDM + Glutamax
+ 20 % (v/v) FCS
+ 1 % (v/v) 100 x NEAA
+ 0.3 % (v/v) MTG stock solution

MTG stock solution: IMDM + Glutamax
+ 1.3 % (v/v) MTG

3.5 Immunological methods

3.5.1 Immunocytology

3.5.1.1 Cell fixation

Adherent cells were cultured on cover slips until the desired density was reached. Suspension cells were incubated on Starfrost microscope slides for 15 min at RT. Subsequently, cells were washed with PBS and covered with chilled Methanol. After 7 min of incubation at -20 °C cells were air dried. For fixation with paraformaldehyde, cells were washed 2 times with PBS and covered with 3.7 % paraformaldehyde. After 20 min of incubation at RT, cells were washed 5 times with PBS. Fixated cells were directly used for immunofluorescence staining or were covered with PBS and subsequently stored at 4°C.

3.5.1.2 Immunofluorescence staining

Cellular organelles and proteins were detected using specific antibodies and dyes. Prior to antibody incubation cells were blocked and permeabilized with PBS supplemented with 1 % (w/v) BSA and 0.2 % (v/v) Triton X for 1 hr at RT. Primary antibodies were diluted in PBS according to manufacturer's instructions and incubated for 1 hr at RT. After 3 times washing with PBS, primary antibodies were detected by secondary antibodies coupled to a fluorescent dye. Therefore, secondary antibodies were diluted in PBS according to manufacturer's instructions and incubated for 1 hr with the cover slips at RT in dark. Simultaneously, Hoechst 33342 dye (1 µM final) was used to stain the nuclei of cells. After 4 washing steps with PBS cells were covered with DAKO mounting media to sustain fluorescence signal. Finally, cover slips were fixed on microscope slides with nail polish to avoid dehydration.

3.5.2 Flow cytometry

Flow cytometry allowed rapid counting of cells and detection of different characteristics of a single cell suspension. Endogenous fluorescence signals such as GFP and antibodies coupled to a fluorescent dye were detected, as well as size and granularity. Single cells were collected from suspension cell culture or by trypsinization for adherent cells (see 3.4.4.3) and washed with PBS. For staining of cell surface molecules fluorescence conjugated antibodies or a primary antibody followed by a secondary fluorescence conjugated antibody was diluted in 100 µl PBS according to manufacturer's instructions and incubated with the cells for 30 min at 4 °C. After washing with

PBS cells were resuspended in an appropriate volume of PBS for measurement. Propidium iodid (PI) was added to the sample (10 µM final) in order to assess the viability of the cells.

3.5.3 Cytoxicity assay

3.5.3.1 Preparation of Concanavalin A supernatant from rat spleens

Rat spleens were dissected and homogenized. Splenocytes were subsequently resuspended in 40 ml DMEM supplemented with 5 % FCS and 200 µl Concanavalin A and incubated 4 hrs at 37 °C. Following this stimulation, splenocytes were collected and washed with DMEM before they were further cultured in 20 ml DMEM supplemented with 10 % FCS for 24 hrs in a cell incubator. During that incubation time stimulated lymphocytes secreted various cytokines. The cytokine conditioned supernatant was collected after centrifugation for 10 min at 1100 x g, aliquoted and stored at -20 °C.

3.5.3.2 Generation of MHC $H2K^b$/SIINFEKL-specific CTLs from OT-I mice

Spleens from OT-I mice were dissected and subsequently homogenized in 10 ml Hepes-buffered DMEM using a Tenbroeck homogenizer or a cell strainer, respectively. The spleen cells were incubated for 1 min in 5 ml erythrocyte-lysis buffer. Following incubation, spleen cells were washed two times with Hepes-buffered DMEM and subsequently taken up in 20 ml DMEM supplemented with 10 % FCS, 20 % Con A supernatant, 20 µg/ml recombinant murine IL-2 and 10 µg/ml SIINFEKL peptide to stimulate antigen-specific CTLs. This splenocyte suspension was plated in a 96-well plate and incubated for 4 days in a cell incubator.

3.5.3.3 ^{51}Chromium release assay

^{51}Chromium release assays were performed to assess the susceptibility of different target cells to cytotoxic immune effector cells. A single cell suspension of 1 x 10^6 target cells was incubated in 300 µl Hepes-buffered DMEM containing 100 µl FCS and 50 µCi $Na_2{}^{51}CrO_4$ at 37 °C for 1 hr. In between, a serial dilution of splenocytes from OT-I mice in DMEM with 10 % FCS was prepared in a 96-well plate to achieve different effector target ratios ranging from 10:1 to 0.16:1. After washing the target cells three times with Hepes-buffered DMEM, 1 x 10^4 labeled target cells per well were added to the splenocytes, followed by an incubation at 37 °C for 4 hrs in a final volume of 200 µl. The target cells either expressed the Ovalbumin protein endogenously or 0.25 µg/ml

SIINFEKL peptide (Ovalbumin aa 257–264) was added before the final incubation step was performed. After incubation the probes were centrifuged and 50 µl supernatant and 50 µl of the sediment part were separated into two 96-well Wallac plates. The sediment part had been treated with 10 µl 10 % Triton-X before, to destroy remaining cell membranes and set all ^{51}Chromium isotopes free. All probes were mixed with 200 µl Scintillator and sealed before measurement in the MicroBeta2 Plate Counter. The lysis was calculated according to the following formula:

$$[\%]\ \text{lysis} = \frac{4 \times \text{cpm supernatant} \times 100}{3 \times \text{cpm sediment} + 1 \times \text{cpm supernatant}}$$

The specific lysis was calculated by subtracting the values of the spontaneous release (^{51}Chromium release in the absence of effector cells) from the determined lysis values. Thereby, the cytotoxic activity of the splenocytes was assessed. Furthermore, the relative lysis compared to SIINFEKL-pulsed RMA cells, which served as positive control in these assays, was calculated to normalize individual experiments.

3.5.4 CFSE proliferation assay

The influence of stem cells on the activation or proliferation of $CD4^+$ and $CD8^+$ T cells was analyzed using a co-culture approach of stem cells (or stem cell supernatant) and CFSE-labeled splenocytes. 5 x 10^4 cells from different stem cell lines were seeded on a 24 well plate on day 1. On day 2 splenocytes from OT-I and OT-II mice were isolated and erythrocytes were lysed (see 3.5.3.2). After washing the cells with Hepes-buffered DMEM two times, a small part of the splenocytes was saved and cultured as non-stained control. The remaining splenocytes were diluted in 4 ml PBS supplemented with 1 % (w/v) BSA and 20 µl CFSE stock solution and incubated for 5 min at 37 °C. Following two washing steps with Hepes-buffered DMEM 5 x 10^5 splenocytes were seeded onto stem cells or controls, respectively. The culture media were supplemented with mouse IL-2 (1000 U/ml) and with or without Ovalbumin as antigen. The final Ovalbumin concentration was 1 µM for stimulation of $CD8^+$ T cells from OT-I mice and 100 µM for $CD4^+$ T cells from OT-II mice. The splenocytes had either direct contact to the stem cells or were separated by a 0.4 µm permeable membrane (Transwell). A typical experimental set up is shown in Figure 5 .

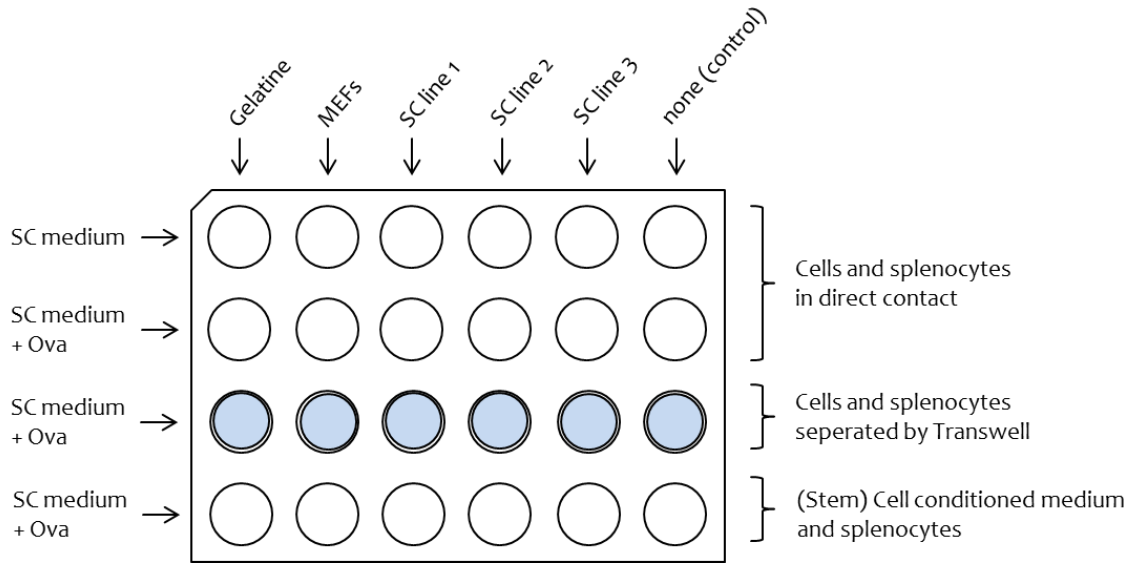

Figure 5: Experimental set up of a CFSE proliferation assay

After 4 days of co-culture splenocytes from OT-I mice and after 5 days splenocytes of OT-II mice were collected and stained either with a PE coupled CD8- or CD4-specific antibody. The proliferation of CD4/CD8 positive splenocytes was analyzed using flow cytometry. In assays in which anti-B7-H3 blocking antibody was used, the final concentration of the antibody in the culture medium was 5 µg/ml as described previously (Prasad et al, 2004).

CFSE stock solution: 5 mM CFSE dissolved in DMSO

3.5.5 Teratoma assay

In order to proof the retention or loss of pluripotency, stem cells were inoculated subcutaneously into immunodeficient mice. Furthermore, either wild type stem cells or transgenic stem cells, expressing OVA as minor histocompatibility antigen, were inoculated into syngeneic, immunocompetent mice in order to analyze their immunogenicity and tumorigenicity. Stem cells were harvested from cell culture and washed in pre-warmed PBS. Following resuspension of the cells in pre-warmed PBS, 1 x 10^6 cells in 100 µl PBS were inoculated subcutaneously into the flank of the animals. Tumor growth was monitored for 100 days and regularly observed by palpation. Animals were early sacrificed when they showed signs of pain, when they lost more than 20 % of their body weight or when the tumor reached a volume of approximately 1 cm^3. The tumor size was determined using linear calipers and the volume was calculated by the formula $V=\pi abc/2$ (a,b

and c were the orthogonal diameters). All animals underwent autopsy and tumors, spleens as well as blood samples were kept for subsequent analysis.

3.5.6 ELISA

The presence of OVA-specific antibodies in the serum of animals, that received OVA-expressing stem cell transplants, was analyzed using ELISA. The 96-well plates were coated with 1 µg OVA per well diluted in 50 µl carbonate buffer at 4 °C o/n. Subsequently, the 96-well plate was incubated with 150 µl of 1 % (w/v) gelatine dissolved in PBS at 37 °C for 1 hr in order to block unspecific binding sites. The serum of the animals was diluted in PBS/Tween and 100 µl thereof was incubated for 2 hrs at 37 °C in the prepared 96-well plate. Subsequently, plates were washed 3 times with H_2O. The peroxidase conjugated goat anti mouse IgG was diluted 1:5000 in PBS/Tween, 100 µl per well was added to the plate and incubated for 1 hr at 37 °C. In addition, isotype-specific secondary antibodies were used in order to differentiate the Ig isotypes in the serum of the animals. These were in turn detected with a peroxidase conjugated goat anti rat antibody. Following 5-fold washing with H_2O, 100 µl substrate solution was added per well and incubated for 5 min at RT. The maximum absorbance at 405 nm was then detected in an ELISA reader.

Carbonate buffer:	85 ml Na_2CO_3 (0.2 M) 40 ml $NaHCO_3$ (0.2 M) 375 ml dH_2O
PBS/Tween:	PBS + 0.05 % (v/v) Tween
Substrate buffer:	0.1 M $C_2H_3NaO_2$ 0.05 M NaH_2PO_4 pH 4.0
Substrate solution:	10 ml substrate buffer 500µl ABTS (40mM) 10µl H_2O_2 (30 %)

3.5.7 Immunohistochemistry

Paraffin sections (2 µm) were stained with H&E for histological overview and with antibodies to detect specific proteins. Therefore, tissue sections were deparaffinized using Xylol (3 x 5 min) and rehydrated in a graded alcohol series (EtOH 100%, 96%, 75% and 60% for 5 min each step) and washed with dH_2O for 5-10 min. After rehydration, the antigen retrieval was performed by boiling the samples in citrate buffer (10 mM, pH 6.0) for 3 x 5 min. The samples were cooled down in a cold water bath to RT and subsequently incubated with 0.1 % Triton X in PBS for 30 min at RT. Subsequently, the samples were incubated for 1 hr at RT in IHC blocking solution. The primary antibody was diluted in IHC blocking solution according to manufacturer's instructions and incubated o/n at 4 °C with the samples in a humidified atmosphere. The samples were washed three times for 5 min with PBS before the secondary Biotin-conjugated antibody, diluted according to manufacturer's instructions, was applied (1hr at RT in a humidified atmosphere). Following washing with PBS (3 x 5 min), the samples were incubated with HRP-streptavidin diluted according to manufacturer's instructions in PBS for 20 min at RT. For Hematoxylin counterstaining, the samples were incubated in Hematoxylin for 2 min, rinsed with dH_2O for 5-10 min. After washing with H_2O for 5-10 min, stained sections were dehydrated (rising EtOH-series 60% 1 min, 75% 1 min, 96% 5 min and 100% 5 min and Xylol 3 x 5 min) and mounted with Roti-Histokitt for imaging.

IHC blocking solution: 4 % BSA in PBS

4 Results

4.1 Expression of MHC class I genes in pluripotent stem cells

Pluripotent stem cells (PSCs) are promising tools for new transplantation therapies due to their ability to differentiate in all adult tissues. Currently, problems of this concept including teratoma formation and immune rejection are not solved and investigations systematically comparing various PSCs are rare. In the context of transplantations it is important to determine the presence of MHC molecules on PSCs. Murine PSCs are negative for MHC class I molecules in flow cytometry but can nonetheless become targets of peptide-specific CTL, indicating that trace amounts of these molecules must be present (Dressel et al, 2009). Therefore, gene expression of *H2D*, *H2K* and β2-microglobulin (*β2m*) was analyzed and compared between the different types of PSCs by qPCR. Three different housekeeping genes (*Gapdh*, *Ubc* and *Hprt*) were analyzed in all cell lines and their gene expression stability was calculated. *Hprt* was the most stabile housekeeping gene between all cell types and therefore chosen for normalization of RNA amounts. The gene expression was considered to be negative, if no amplification before cycle 33 occurs, since such a late amplification was most likely unspecific. Moreover, specificity of products was confirmed by evaluation of the amplification product melting temperature in dissociation curves. RMA lymphoma cells, highly susceptible targets for CTL-mediated lysis, were chosen as reference cell line and the mRNA expression in this cell line was set to 1. Amounts of *H2D, H2K* and *β2m* mRNAs in PSCs were quantified relative to RMA cells using the Pfaffl method (see 3.2.3.3) (Pfaffl, 2001). This quantification method takes the different efficiencies of the primer pairs into account. In addition, the pluripotent teratocarcinoma cell line F9 and mouse embryonic fibroblasts (MEFs), from which the induced pluripotent stem cells (iPSCs) were derived, were analyzed for comparison. ESCs and maGSCs, obtained from different mouse strains, as well as a iPSC line was analyzed to depict cell line and strain specific variations.

Despite their negativity for MHC class I expression in flow cytometry (Figure 9), mRNA of *H2D*, *H2K* and *β2m* was detected in all analyzed stem cell lines. However, mRNA amounts were low compared to the RMA control cells. The amount of *H2D* and *H2K* mRNA in PSCs was between 4 % and 22 % compared to RMA reference cells, whereas MEFs and F9 teratocarcinoma cells comprised similar amounts to reference cells. The *β2m* mRNA level in PSCs varied from 4 % up to 43 % compared to RMA cells while MEFs and F9 teratocarcinoma cells had even 5-fold higher amounts of *β2m* mRNA.

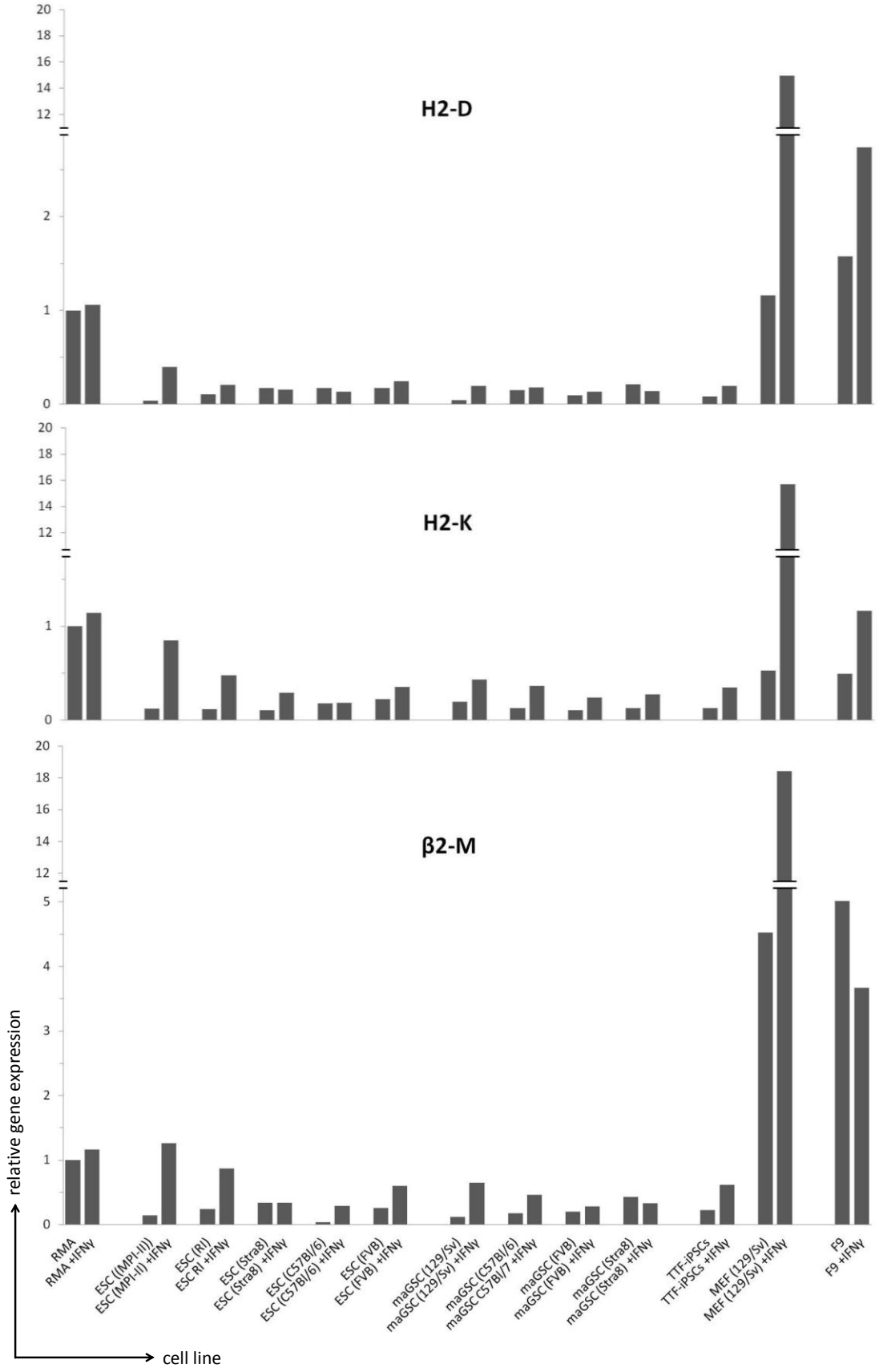

Figure 6: Relative gene expression of the MHC class I genes *H2D*, *H2K* and *β2m*.
Diagrams represent the mRNA amounts in PSCs relative to RMA reference cells under normal conditions and after IFNγ treatment (48 hrs; 1000 U/ml). Expression values were calculated from mean of technical triplicates after normalization to the housekeeping gene *Hprt*.

The expression of these genes is usually induced in somatic cells by the cytokine IFNγ. However, conflicting data regarding the response of ESCs to IFNγ were published while data for iPSCs and maGSCs are rare or missing (Abdullah et al, 2007; Bonde & Zavazava, 2006; Nussbaum et al, 2007). Therefore, the impact of IFNγ treatment on the expression of the MHC class I genes was analyzed. Cell lines were cultured in the presence of 1000 U/ml IFNγ for 48 hrs before RNA isolation. In the majority of all tested PSCs *H2D, H2K* and *β2m* mRNA amounts increased upon IFNγ stimulation. However, the majority of these PSCs, which responded to the IFNγ treatment, showed only low increase in mRNA expression compared to their non-treated counterparts. In contrast, some PSC lines exhibited well detectable changes of *H2D, H2K* and *β2m* mRNA amounts e.g. an at least 10-fold increase in the ESC line MPI-II. Other PSC lines did not respond to IFNγ: The amount of *H2D* mRNA was not changed in ESC lines Stra8, C57Bl/6 and the maGSC line Stra8. *H2K* mRNA was not increased in the ESC line C57Bl/6. The *β2m* mRNAs were unaffected in IFNγ treated ESC Stra8 and maGSC Stra8 cells. In contrast, *H2D* mRNA increased 15-fold and *H2K* mRNA 30-fold in the MEF positive control compared to their non-treated counterparts (Figure 6). Thus, PSCs differed in their response to IFNγ treatment, some responded weakly and others failed to induce MHC class I gene expression.

4.2. Antigen presentation in pluripotent stem cells

4.2.1 Expression analysis of the model antigen Ovalbumin (OVA)

In order to investigate the ability of murine PSCs to process and present antigens an Ovalbumin (OVA) expression construct was introduced into different PSC lines and as control in RMA cells. The Ovalbumin cDNA was therefore fused to eGFP to monitor transgene expression. Transgene expression was controlled by the ubiquitously active hEF1α promoter. In other iPSC lines the same construct controlled by the CAG promoter was used. Both promoters allow similar expression rates but the CAG promoter conferred more stable transgene expression in long-term culture (Liew et al, 2007). A schematic view of the expression construct is depicted in Figure 7A. PSCs were transfected by electroporation and clones with stable transgene integration were selected by Neomycin resistance. Expression of the OVA-eGFP fusion protein was verified by western blot analysis, flow cytometric analysis of eGFP expression, qPCR and immunocytology (Figure 7 C). The tested clones expressed various amounts of OVA. The mean fluorescence intensity (MFI) of eGFP (Figure 10) largely correlated with the intensity of western blot bands and the amount of OVA mRNAs (Figure 7 E). Moreover, the presentation of the SIINFEKL peptide on MHC class I $H2K^b$ molecules was verified by flow cytometry using an antibody specific for these complexes (Figure 7

B). In contrast to RMA transfectants, PSCs expressed only trace amounts of MHC class I H2K^b molecules that were beyond the detection limit.

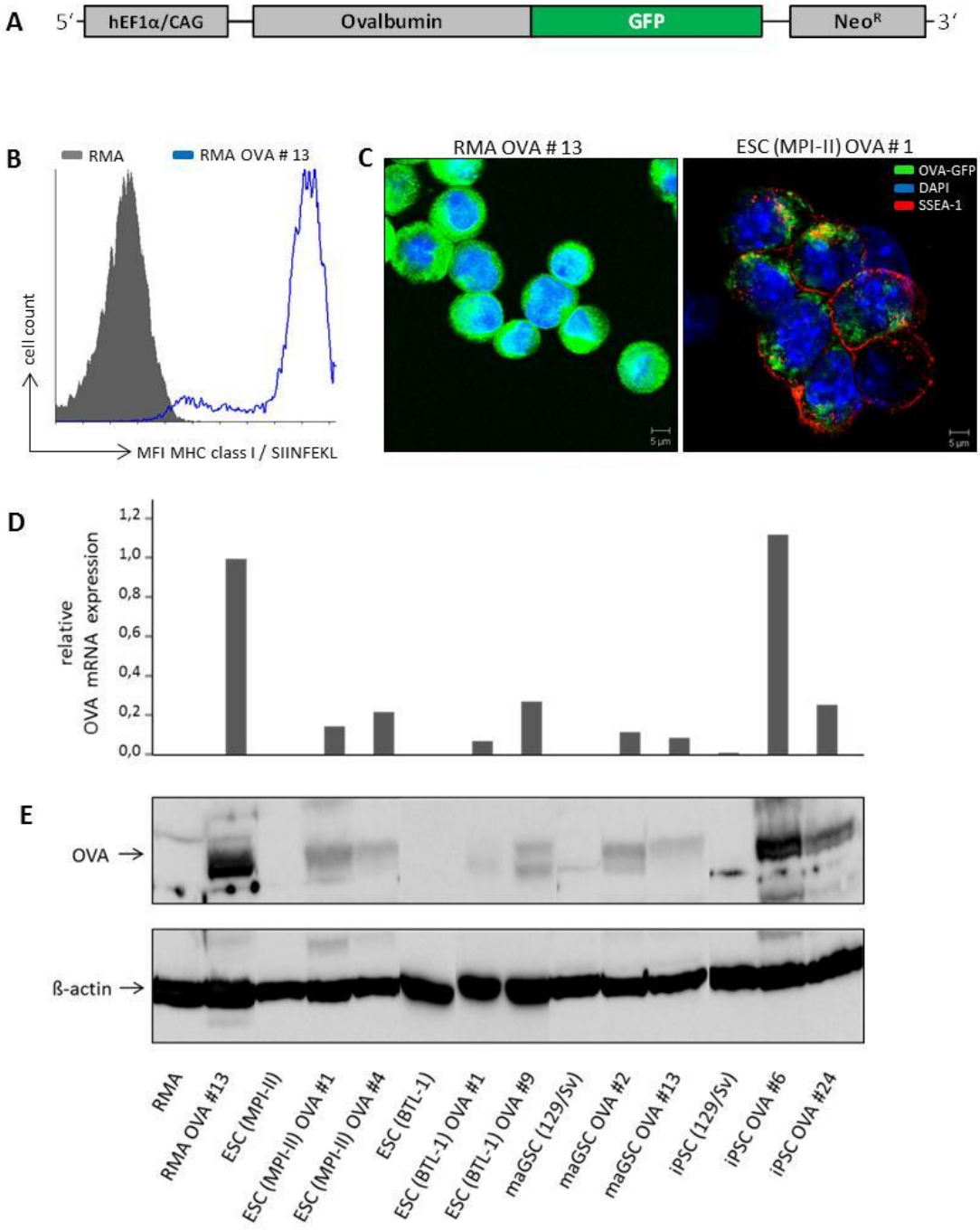

Figure 7: Expression of the model antigen OVA
(A) Schematic view of the OVA-expression construct used to generate OVA-transgenic cell lines. **(B)** Flow cytometric histogram depicting MHC class I H2K^b/SIINFEKL expression on wt RMA and RMA OVA #13 cells. **(C)** Confocal laser scanning microscopy of RMA cells and ESCs (MPI-II) expressing OVA-eGFP (green). Nuclei were stained with DAPI (blue). ESCs (MPI-II) were counterstained with the pluripotency marker SSEA-1 (red) to distinguish ESCs from feeder cells. **(D)** Diagram shows relative OVA mRNA amounts of OVA-expressing PSCs compared to OVA-expressing RMA cells. The results were calculated as mean from technical triplicates and normalized to the housekeeping gene HPRT. **(E)** Western Blot analysis of OVA expression in different wt cell lines and OVA-expressing clones.

4.2.2 Ability of OVA-expressing PSCs to present antigens

The ability of OVA-expressing PSCs to process endogenous expressed antigens was assessed using them as target cells for peptide specific cytotoxic T cells (CTLs). These CTLs derived from transgenic OT-I mice express a T cell receptor (TCR) specific for the OVA derived SIINFEKL peptide in context of MHC class I $H2K^b$ molecules.

PSCs of the $H2K^b$ haplotype are susceptible to OT-I CTL mediated killing when artificially loaded with SIINFEKL peptide (Dressel et al, 2009). Therefore, OVA-expressing PSCs of this haplotype, if able to process and present antigens, are expected to be lysed in similar extend without additional incubation with the SIINFEKL peptide. At least two different clones of each cell line were analyzed and similar results were obtained for all tested clones independently of their OVA-expression intensity. Wt RMA cells pulsed with the SIINFEKL peptide served as standard positive control in these assays (Figure 8). The relative lysis compared to SIINFEKL-pulsed wt RMA cells was calculated for the other analyzed cell lines in order to compare results obtained in different experiments.

The OVA-expressing MPI-II ESCs (clones #1 and #4) were unable to present antigen since the relative lysis was similar to that of wt MPI-II ESCs. After addition of SIINFEKL, however, OVA-expressing MPI-II ESCs were lysed to a similar extend as SIINFEKL-pulsed wt MPI-II ESCs (Figure 8 B). In contrast, OVA-expressing RMA cells, used as positive controls in order to proof the functionality of this construct, were efficiently killed by CTLs from OT-I mice (Figure 8 A). RMA OVA cells were even more efficiently killed than wt RMA cells pulsed with the SIINFEKL peptide and additional incubation of RMA OVA cells with SIINFEKL did not further enhance the lysis of these cells (data not shown). A second ESC line was analyzed in order to validate this result. Like MPI-II ESCs the BTL-1 ESCs (clones #1, #4 and #9) were unable to present antigen. OVA-expressing BTL-1 ESCs were killed to similar extend as their wt counterparts. Incubation with SIINFEKL resulted in moderate killing of the OVA-expressing ESCs similar to wt BTL-1 ESCs (Figure 8 E). Only the clone ESC (BTL-1) OVA #9 was slightly killed in the absence of the SIINFEKL peptide. However, it turned out later that this clone had lost, at least in part, its pluripotency as indicated by western blot analysis of Oct4 expression (Figure 12 B). That particular clone only expressed the Oct4B isoform that is known to be unable to sustain ES cell self renewal (Lee et al, 2006). Furthermore, in light microscopy the ESC OVA #9 clone exhibited an atypical morphology and it failed to give rise to teratomas in immunodeficient mice (data not shown).

When the iPSCs (129/Sv) were analyzed for their antigen presenting capability similar results as for ESC lines were obtained. The OVA-expressing iPSCs (clones #6 and #24) were not killed by antigen-specific CTLs, just like wt iPSCs. Both, wt iPSCs as well as OVA-expressing iPSCs were moderately killed after incubation with the SIINFEKL peptide (Figure 8 F).

OVA-expressing maGSCs (129/Sv) exhibited a slightly increased lysis compared to wt maGSCs without additional SIINFEKL incubation in all tested clones. The lysis of OVA-expressing maGSCs was still lower than the lysis of SIINFEKL-pulsed maGSCs. Following SIINFEKL incubation the relative lysis of OVA-expressing maGSCs was similar to SIINFEKL-pulsed wt maGSCs (Figure 8 D).

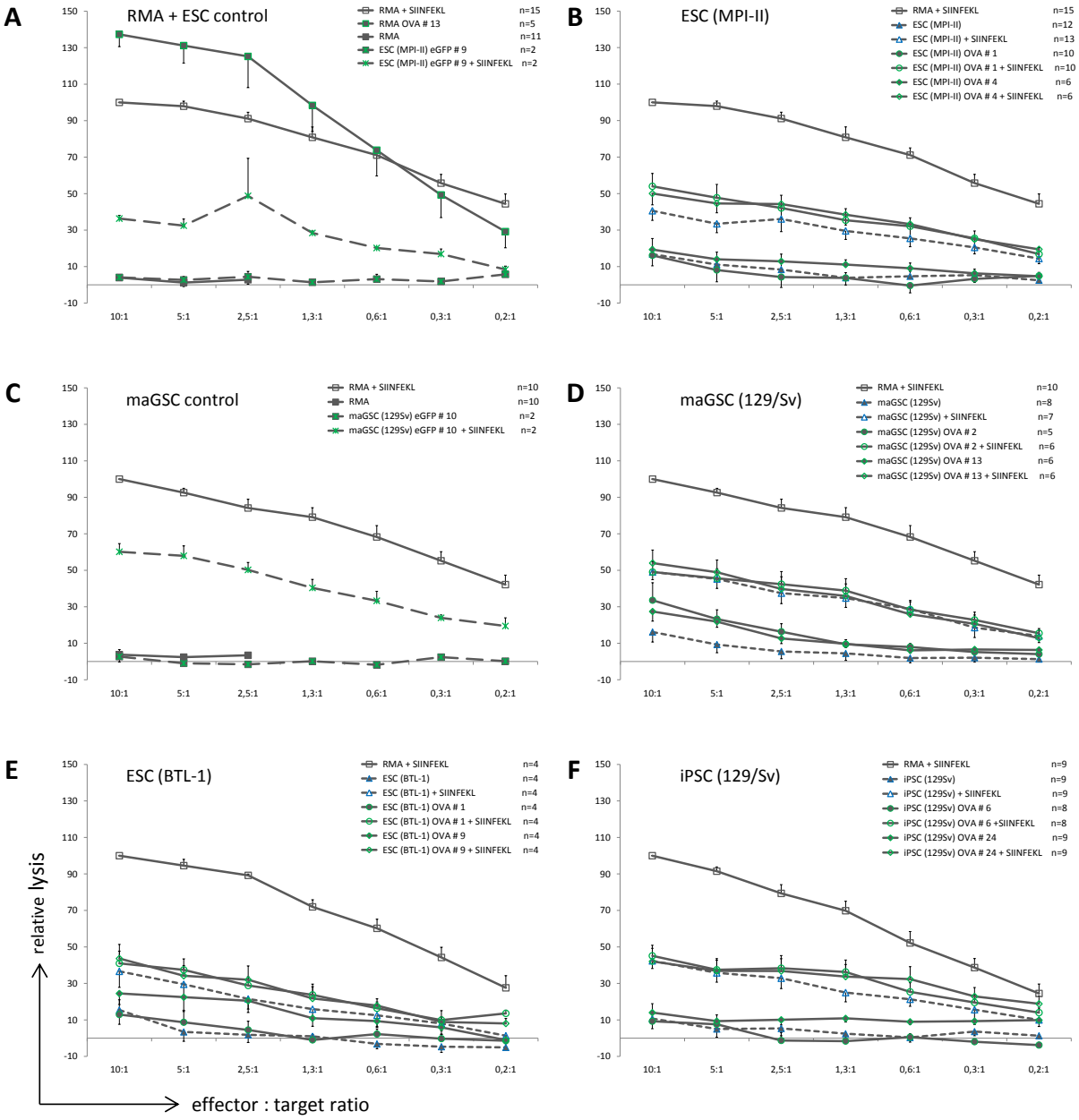

Figure 8: Susceptibility of OVA-expressing PSCs to peptide specific CTLs
Diagrams show the mean relative lysis and SEM of the different cell lines mediated by OT-I CTLs at different effector to target ratios. The lysis of SIINFEKL-pulsed RMA cells (0.5 µg/ml SIINFEKL peptide) at the highest effector to target ratio was adjusted to 100 % in each test and relative lysis of the different target cell lines was calculated.

RMA cells, ESCs (MPI-II) and maGSCs (129/Sv) were transfected with an eGFP expression construct as negative control. These eGFP-expressing cells were not killed by OT-I CTL without SIINFEKL incubation, demonstrating the peptide dependency of cell lysis for the RMA cells and PSCs. In addition, wt cells were not killed without SIINFEKL incubation (Figure 8 A, C).

In order to assess, whether the results could have been influenced by NK cell-mediated killing, YAC-1 lymphoma cells were used as control cell line, since they are high susceptible targets for NK cells but unsusceptible to CTLs. Tests in which the specific lysis of YAC-1 cells exceeded 10 %, results were excluded from final analysis since NK cells could have contributed to the killing of PSCs in these assays.

4.2.3 MHC class I and OVA-eGFP expression in target cell lines

Target cell lines were routinely tested in parallel to ^{51}chromium release assays for expression of MHC class I molecules by flow cytometry. A summary of these results is shown in Figure 9. RMA cells consistently expressed high levels of $H2K^b$ and $H2D^b$ and the OVA-expressing RMA cells express comparable levels to wt RMA cells. In PSC lines no MHC class I expression was detectable by flow cytometry. After prolonged time in culture, the clones partially lost their transgene expression. Therefore, the OVA-eGFP transgene expression was routinely observed by flow cytometry, in order to ensure sufficient OVA expression for the functional analyses in ^{51}chromium release assays (Figure 10). To this end, early passages of all clones were stored at -140 °C and thawed if less than 90 % of the clones in culture expressed OVA-eGFP.

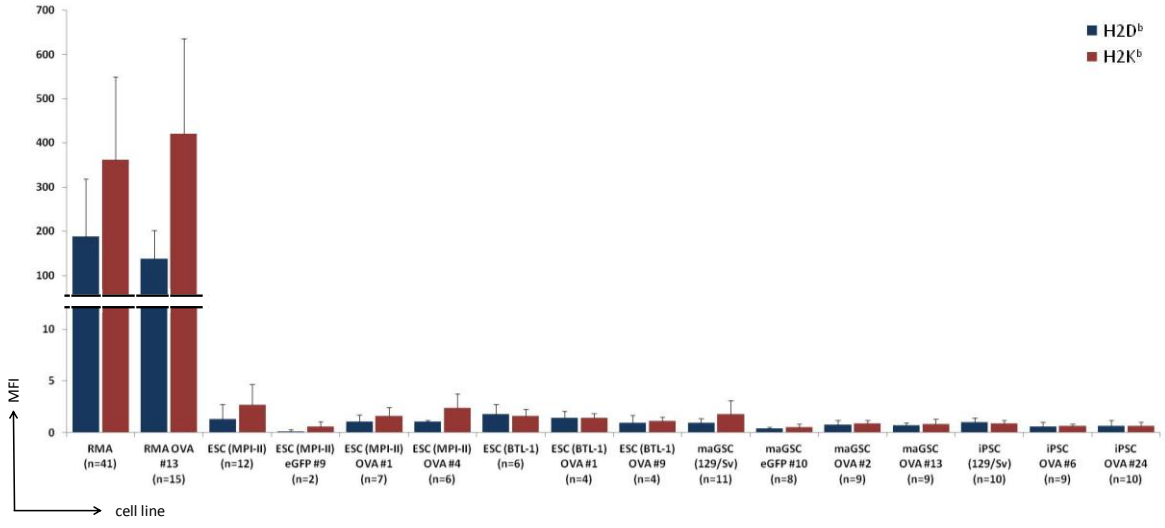

Figure 9: MHC class I expression in target cell lines
Expression of MHC class I molecules in target cell lines were analyzed using $H2D^b$ and $H2K^b$ specific antibodies in flow cytometry in parallel to ^{51}chromium release assays. Data represent specific MFI (fluorescence of specific reagent minus fluorescence of isotype control) and SD.

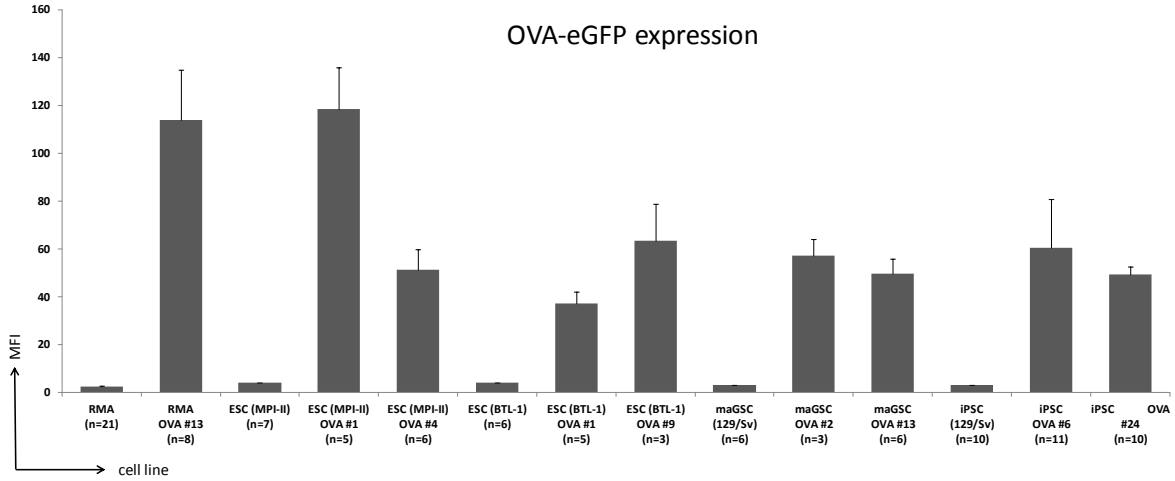

Figure 10: OVA-eGFP transgene expression in target cell lines
The OVA-eGFP transgene expression was routinely observed by flow cytometry in parallel to ^{51}chromium release assays. The diagram shows the MFI of eGFP in wt and OVA-expressing target cells and SEM.

4.2.4 Ability of OVA-expressing iPSCs to present antigens after IFNγ treatment

Since iPSCs might have the highest therapeutical potential for future transplantations, due to ethical reasons and easy accessibility of autologous cells, their immunological properties were analyzed in more detail. After transplantation, iPSCs or iPSC-derived cells are exposed to an environment in which pro-inflammatory cytokines might be present. Therefore, the effect of IFNγ stimulation on the ability of iPSCs and their corresponding OVA-expressing clones to present antigens to peptide specific CTLs was assessed using ^{51}chromium release assays. Target cells were stimulated with 1000 U/ml IFNγ for 48 hrs prior to the assay. Again the relative lysis compared to SIINFEKL-pulsed RMA control cells at different effector to target ratios was calculated.

The IFNγ treatment had no effect on the antigen processing capability of iPSCs. Neither the lysis of OVA-expressing clones compared to wt iPSCs nor the lysis of SIINFEKL-pulsed iPSCs increased after IFNγ stimulation (Figure 11 A). The lysis of IFNγ-treated OVA-expressing iPSCs was similar to IFNγ treated wt iPSC when both where pulsed with the SIINFEKL peptide. While flow cytometric analysis revealed that MHC class I expression was notably raised in IFNγ treated RMA control cells, no increased expression of $H2K^b$ and $H2D^b$ was detectable in iPSCs and their OVA-expressing counterparts (Figure 11 B).

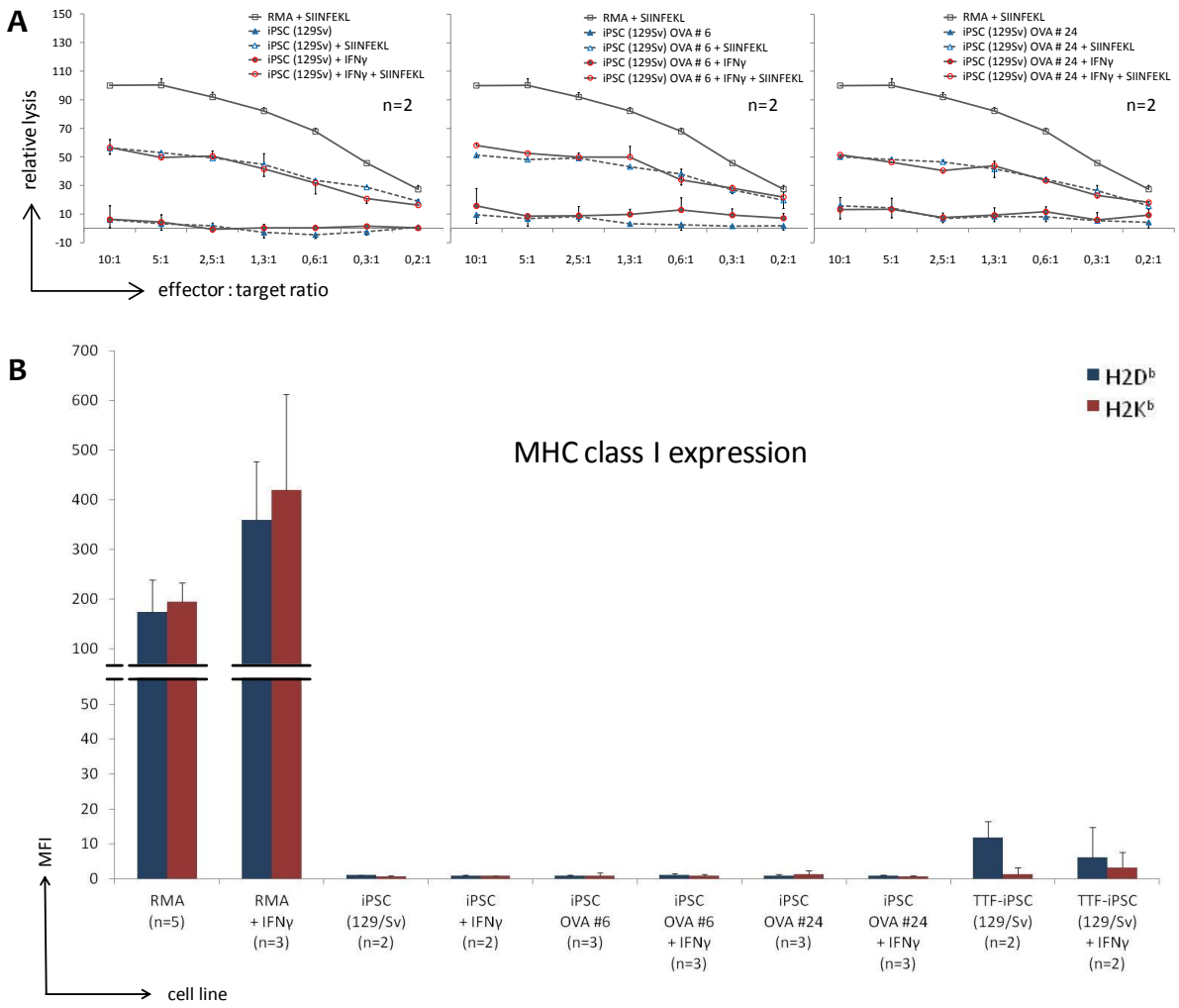

Figure 11: Susceptibility of OVA expressing iPSC to peptide specific CTLs after IFNγ treatment
(A) Diagrams represent the mean relative lysis and SEM of iPSCs relative to RMA control cells at different effector to target ratios. Lysis of iPSCs with and w/o IFNγ treatment (1000 U/ml for 48 hrs) as well as with and w/o SIINFEKL pulsing is shown.
(B) Following IFNγ treatment (1000 U/ml for 48 hrs) $H2D^b$ and $H2K^b$ specific antibodies were used to detect MHC class I molecules in flow cytometry. Diagram represents the mean specific MFI and SD.

4.2.5 Ability of OVA-expressing PSCs to present antigens after differentiation

We were interested to determine, whether PSC-derived cells acquire the ability to process and present antigens upon differentiation. Therefore, OVA-expressing PSCs were differentiated for 14 days in an undirected manner using embryoid body (EB) formation. The effect of differentiation on the ability of PSCs to present antigens should be determined using OVA-expressing EB cells as targets for peptide specific CTLs. Following the differentiation period potential target cells were analyzed for their OVA-eGFP transgene expression and expression of pluripotency markers using flow cytometry and western blot. The differentiation of PSCs was confirmed by flow cytometry using the pluripotency marker SSEA-1. The majority of EB-derived cells were negative for SSEA-1

(data not shown). In addition, differentiation was confirmed for OVA-expressing ESC BTL-1 cells by western blot. Oct4-expression, crucial for pluripotency of PSCs, got completely lost in differentiated ESCs (Figure 12 B). Functional tests *in vitro*, such as ^{51}chromium release assays were not performed successfully, since in all tested OVA-expressing PSC clones lost transgene expression after the differentiation period. This was shown by lost or greatly reduced eGFP expression in flow cytometry (Figure 12 A). In addition, OVA expression in EBs derived from different ESC OVA clones was not detected in western blot, while undifferentiated ESC OVA clones expressed OVA (Figure 12 B). Differentiation of OVA-expressing ESCs, maGSCs and iPSCs was repeated several times but transgene expression in the differentiated cells was not sustained in any attempt.

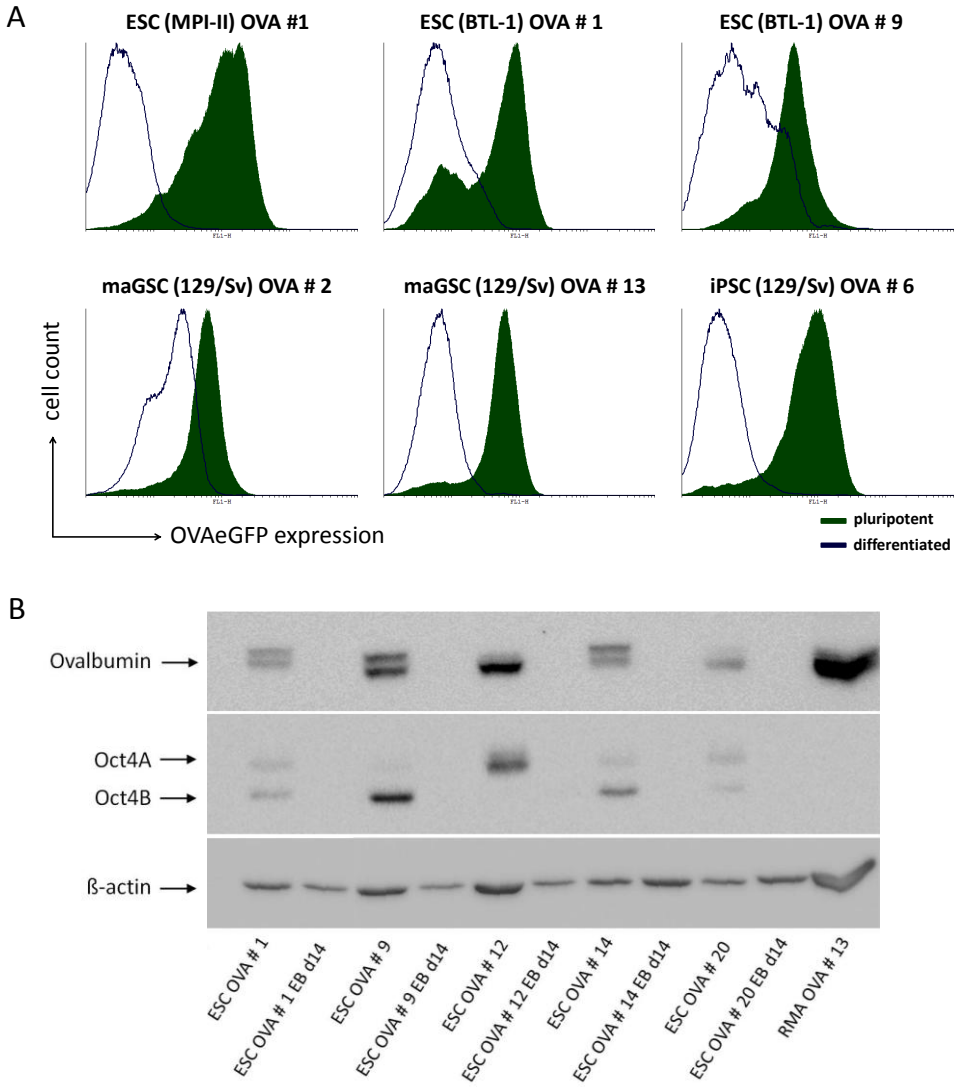

Figure 12: OVA-expression in differentiated SCs
(A) Representative histograms showing OVA-eGFP expression as determined in flow cytometry. The different OVA-expressing PSC lines before (green) and following differentiation for 14 d using embryoid body formation (blue line) are shown. **(B)** Western blot showing OVA- and Oct4-expression in the ESC line BTL-1 and their OVA-expressing clones before and following differentiation. β-actin staining was used as loading control.

4.2.6 Peptide loading complex gene expression analysis

To determine why PSCs failed to process and present antigens, the major components of the antigen processing machinery were analyzed in all functionally tested PSC lines and their corresponding OVA-expressing clones, as well as in RMA control cells by qPCR. The gene expression was analyzed in technical triplicates and mRNA amounts in different cell lines were normalized using the housekeeping gene *Hprt*. Subsequently, mRNA amounts were calculated relative to RMA cells which comprised high amounts of peptide loading complex associated gene transcripts. The transcript amount in RMA cells was set to 1 and relative amounts of PSCs derived transcripts were calculated using the Pfaffl method (Pfaffl, 2001). RMA cells were again chosen as reference cell line for peptide loading complex gene expression, since RMA OVA cells had proven the ability to present antigens of endogenous expressed proteins in ^{51}chromium release assays (Figure 8 A).

The transporter associated with antigen processing (TAP) is responsible for the active transport of peptides generated in the cytoplasm into the lumen of the endoplasmatic reticulum (ER). TAP is a heterodimer consisting of TAP1 and TAP2 proteins. The according mRNA amounts quantified in PSCs were low. Compared to RMA reference cells the mRNA amount of *Tap1* was only 7 % to 25 % in PSCs. In general, only minor differences in mRNA amounts between wt cells and their OVA expressing counterparts were detectable. However, the ESC line MPI-II and the corresponding OVA clones as well as RMA and RMA OVA cells exhibited differences, most likely due to clonal effects. *Tap2* mRNA was not or only in trace amounts detectable in all PSCs. The mRNA amounts were similar between wt and OVA-expressing cells.

The TAP binding protein (TAPBP) or Tapasin is crucial for the interaction of newly synthesized MHC class I molecules and TAP. *Tapbp* mRNA was found in all tested PSCs in well detectable amounts. At least 30 % of *Tapbp* mRNA compared to RMA reference cells was detected. Again clonal variations between wt ESC (MPI-II) and ESC (MPI-II) OVA #1 and between RMA and RMA OVA cells were detected, whereas the mRNA amounts between wt cell and OVA-expressing cells in other PSC lines was similar.

Calnexin (*Canx*) and Calreticulin (*Calr*) are chaperone molecules assisting protein folding and stabilization of MHC class I molecules in the ER. Transcripts of both genes were detectable in similar amounts in the majority of PSC lines and OVA clones and the expression was never below 50 % compared to RMA reference cells. Only in the ESC (MPI-II) OVA #1 clone the gene expression was again lower but still well detectable. In this clone *Canx* mRNA amounts were about 50 % and *Calr* mRNA amounts about 40 % of RMA reference.

ERp57 is a co-factor assisting in the establishment of disulfide bonds. The mRNA amounts varied slightly between different clones and cell lines but were usually not below 40 % compared to RMA control.

In contrast, mRNA of the immunoproteasome subunit *LMP 2* was only expressed in trace amounts and *LMP 7* mRNA was generally not detectable in the PSCs (Figure 13).

In summary, the majority of genes involved in antigen presentation were expressed in PSCs. However, only low amounts of *Tap1* and no *Tap2* mRNA was detectable in the majority of PSCs. Furthermore, no or only trace amounts, respectively, of the immunoproteasomal subunit mRNAs were found in PSCs.

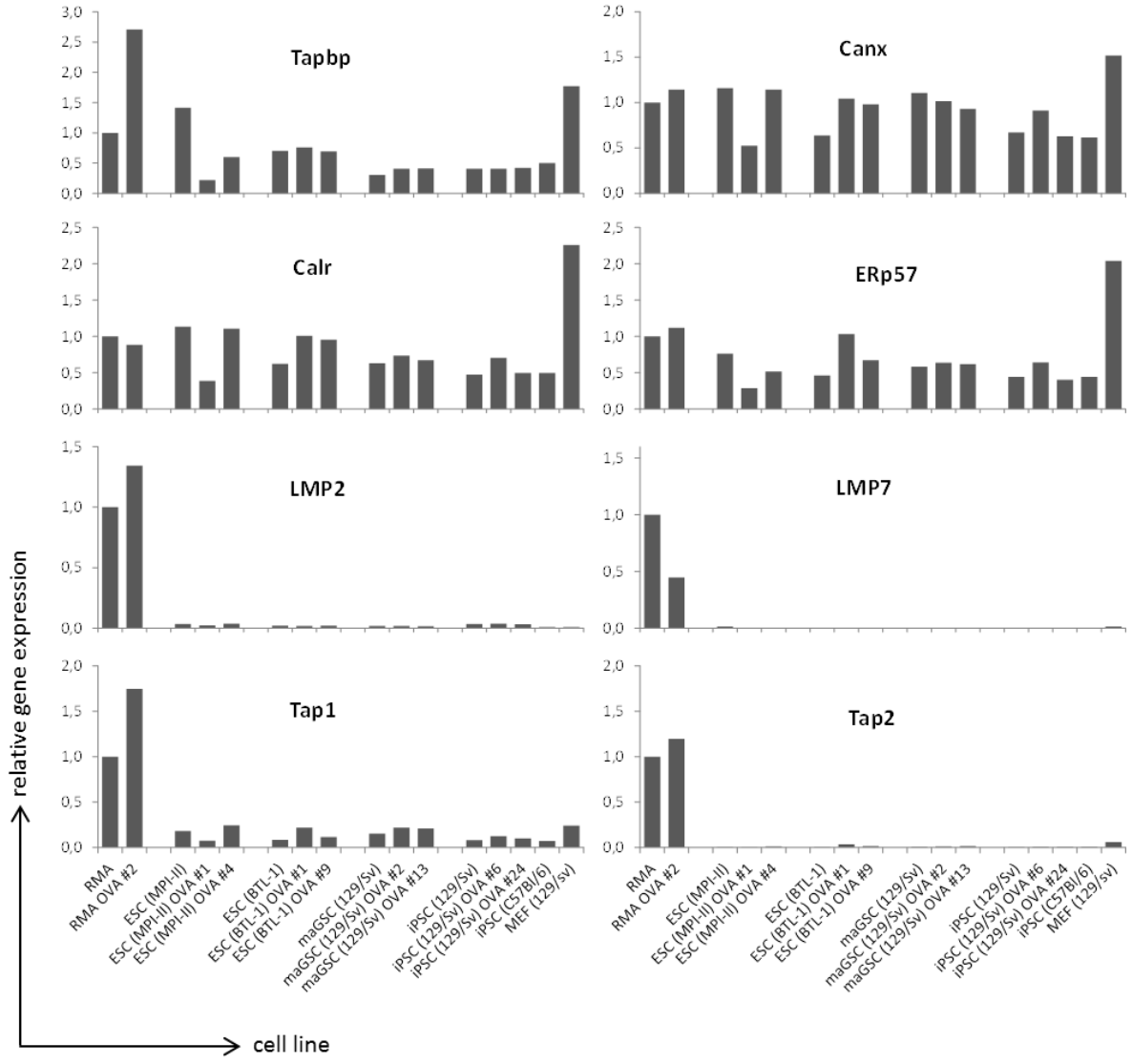

Figure 13: Expression analysis of peptide loading complex related genes
Diagrams depict relative mRNA amounts of peptide loading complex genes in different PSCs. The mRNA amounts in wt RMA cells were used as reference and set to 1. Results represent mean values of technical triplicates after normalization to the housekeeping gene HPRT.

4.3 Analysis of immune escape mechanisms in PSCs

Several mechanisms have been reported, by which PSCs (or tumor cells) inhibit CTL mediated cytotoxicity. This might be highly relevant for the survival of PSCs and PSC-derived cells after transplantation. Western blot analysis as well as qPCRs were performed to assess whether these escape mechanisms might have contributed to the results of the cytotoxicity assays. Therefore, the expression of Cathepsin B (CtsB) and Serine protease inhibitor 6 (SPI-6), known to inhibit CTL-mediated cytotoxicity, was determined in different PSCs and suitable controls (Figure 14).

Furthermore, the transcript levels of the amino acid depleting enzymes Indoleamine 2,3-dioxygenase (IDO) and Arginase 1 (Arg1) were analyzed in PSCs. It was reported, that Arg1 inhibits T cell function by depletion of L-arginine from the cell microenvironment (see 1.3). The Arg1 isoform is primarily located in the cytoplasm of the liver (Iyer et al, 1998). Therefore, *Arg1* gene expression in PSCs was determined by qPCR and quantified relative to liver RNA. In none of the analyzed PSC lines was any expression of this gene detectable. Since the *Arg1* gene was not expressed in PSCs no additional western blot analysis was performed.

Similar results were obtained for the expression of IDO. On mRNA level only trace amounts of *Ido* were detected in all tested cell lines, with a maximum of 3 % expression compared to placenta RNA in maGSCs from C57Bl/6 mice and MEF control cells from 129/Sv mice. On protein level also only very low amounts of IDO were detectable with slightly higher amounts in RMA cells than in PSCs. Thus, IDO expression did not correlate with the functional data obtained from ^{51}chromium release assays.

SPI-6 is a specific inhibitor of granzyme B, the serine protease that enables cytotoxic cells to kill target cells. It was shown that dendritic cells (DCs) protect themselves from CTL-mediated lysis by expression of SPI-6 (Medema et al, 2001b). Therefore, spleen RNA was used for the relative quantification of the analyzed RNA. SPI-6 mRNA was found in various but low amounts in all tested PSC lines. In maGSC derived from C57Bl/6 mice with 9 % relative to spleen mRNA the highest amount of SPI-6 mRNA was detected. Moderate mRNA amounts compared to spleen were detected in RMA and MEF cells, which were included as further controls. The relative expression of RMA cells was about 15 % compared to spleen mRNA demonstrating that the SPI-6 expression did not correlate with the susceptibility to CTLs. This confirms previous results obtained in western blot analyses (Dressel et al, 2009; Dressel et al, 2010).

CtsB gene expression was detectable in all PSC lines, ranging from 12 % in the ESC line MPI-II to 31 % in the iPSC line derived from 129/Sv mice compared to spleen RNA used as control. However, again a similar *CtsB* gene expression level was detectable in RMA control cells. This result was

validated by western blot, where mature CTSB protein was detected in all cell lines albeit in less amounts than in spleen (Figure 14 B).

In summary, albeit CTSB and SPI-6 as well as small amounts of IDO mRNA and protein were detectable in PSCs, a contribution of these molecules to CTL resistance is unlikely, since similar expression levels were detected in CTL-susceptible RMA cells.

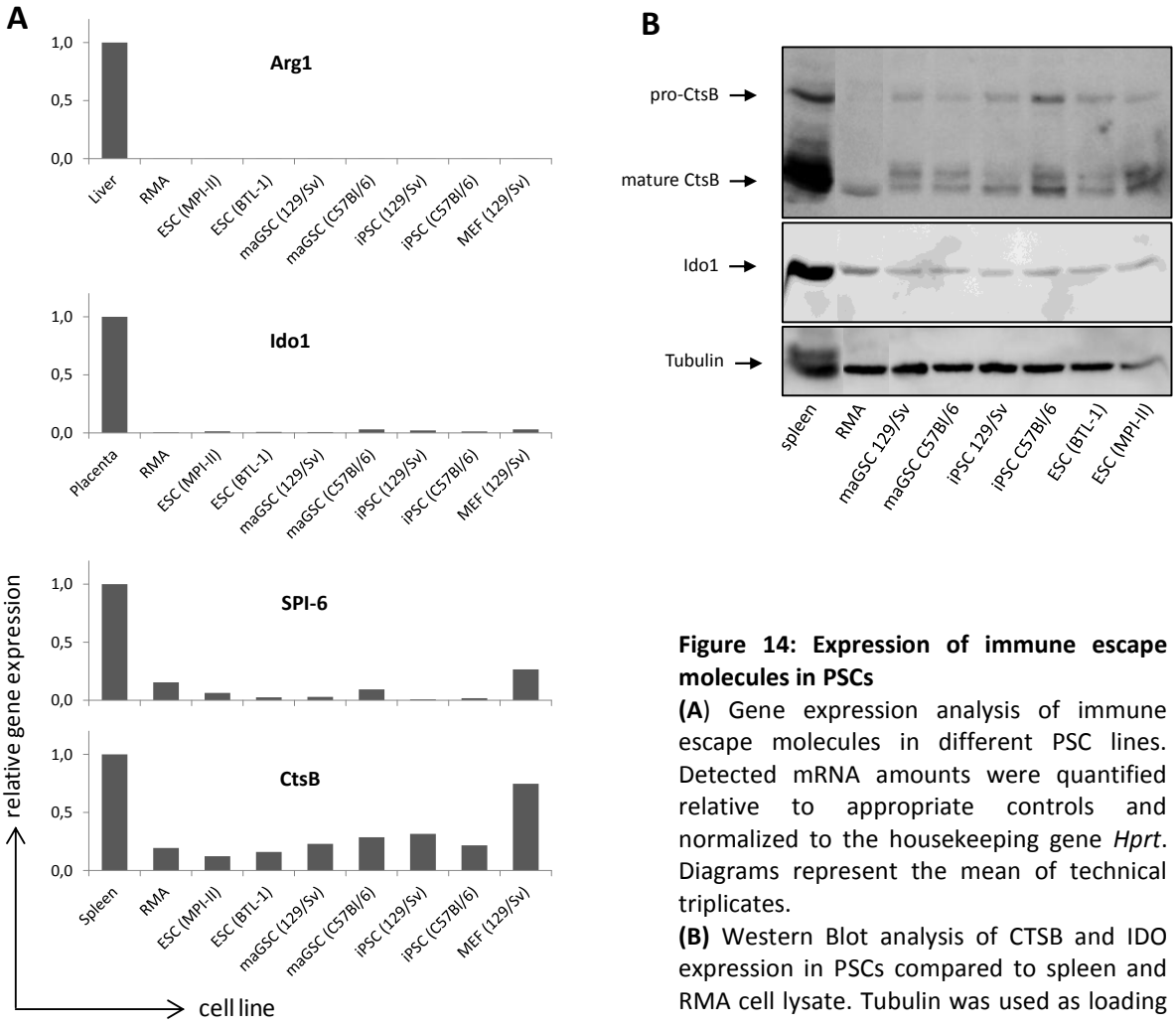

Figure 14: Expression of immune escape molecules in PSCs

(A) Gene expression analysis of immune escape molecules in different PSC lines. Detected mRNA amounts were quantified relative to appropriate controls and normalized to the housekeeping gene *Hprt*. Diagrams represent the mean of technical triplicates.

(B) Western Blot analysis of CTSB and IDO expression in PSCs compared to spleen and RMA cell lysate. Tubulin was used as loading

4.4 Analysis of the immunogenicity of PSCs

PSCs were impaired in their ability to present antigens. Nonetheless, PSCs were killed by activated CTLs, if the appropriate peptide was added to the assays. Next the ability of OVA-expressing PSCs to activate naive peptide-specific $CD8^+$ T cells was investigated. Therefore, 5 x 10^5 splenocytes derived from OT-I mice were stained with CFSE and co-cultured with 5 x 10^4 OVA-expressing PSCs and RMA OVA cells as control for 4 days. In addition, the activation of peptide-specific $CD4^+$ T cells

was analyzed. The $CD4^+$ T cells were derived from transgenic OT-II mice and express T cell receptors (TCR) specific for the OVA derived ISQAVHAAHAEINEAGR peptide in context of MHC class II $H2A^b$ molecules. The OT-II splenocytes were cultured for 5 days together with OVA-expressing PSCs in equal cell numbers. Therefore, the cultures contained in addition to the peptide-specific T cells, professional antigen presenting cells from the TCR transgenic mice. The culture medium was furthermore supplemented with 1000 U/ml IL-2. Splenocytes from OT-I mice, supplemented with 1000 U/ml IL-2 and 1 µM OVA protein, and splenocytes from OT-II mice supplemented with 1000 U/ml IL-2 and 100 µM OVA protein were used as positive control. Splenocytes alone and splenocytes co-cultured with MEFs without OVA protein were used as negative controls to assess the base-line proliferation in absence of antigen. Following co-culture, the activation of naive $CD8^+$ and $CD4^+$ T cells was determined by flow cytometric analysis of their proliferation frequency. To assess the specific proliferation, splenocytes were gated for viable lymphocytes and for $CD4^+$ or $CD8^+$ cells, respectively (Figure 15). The proliferation frequency was determined by percentage calculation of cells that divided at least once.

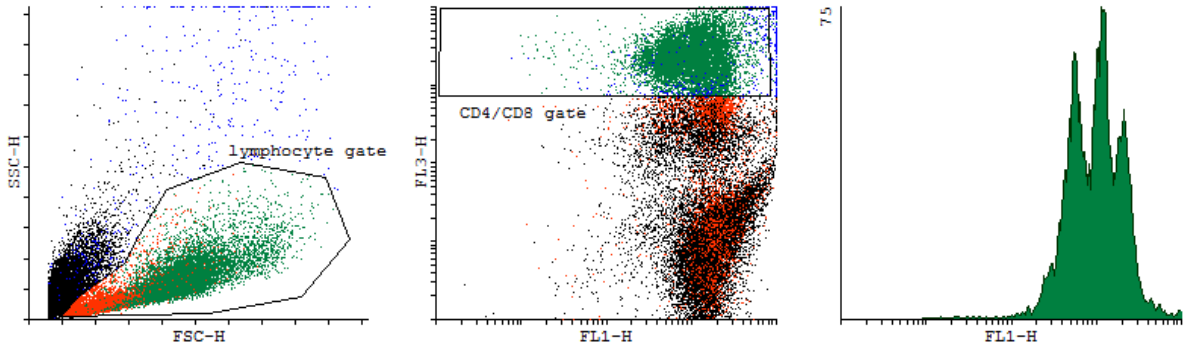

Figure 15: Gating strategy to access $CD4^+$ and $CD8^+$ specific proliferation of viable lymphocytes
Viable lymphocytes were identified according to their size and granularity (lymphocyte gate: red staining). In addition, $CD4^+$ and $CD8^+$ T cells were identified using antibody staining (CD4/CD8 gate: blue staining). Proliferation of cells, detectable in the combination of these gates was determined (green staining).

PSCs expressing OVA completely failed to induce proliferation of OT-I-derived $CD8^+$ T cells specific for SIINFEKL/$H2K^b$. The proportion of proliferating $CD8^+$ T cells co-cultured with wt or OVA-expressing PSCs was even lower than the base-line proliferation in negative and MEF control. In contrast, about 80 % of $CD8^+$ T cells proliferated following co-culture with OVA-expressing RMA cells. This proliferation frequency was even 20 % higher than in positive control. However, in co-culture with wt RMA cells the proliferation frequency of $CD8^+$ T cells was also about 20 % higher compared to negative control. Therefore, RMA cells itself possessed the ability to enhance T cell proliferation (Figure 16 A).

OVA-expressing PSCs were also unable to induce proliferation of peptide-specific, OT-II-derived $CD4^+$ T cells. The proliferation frequency was similar to peptide-specific $CD4^+$ T cells cultured with wt PSCs. Moreover, in general the proliferation frequency was lower than in negative controls once $CD4^+$ T cells were co-cultured with either OVA-expressing or wt PSCs. The proliferation frequency of $CD4^+$ T cells co-cultured with wt RMA control cells was again slightly elevated compared to the base-line proliferation in standard and MEF control without antigen supplementation. However, OVA-expressing RMA cells completely failed to elicit proliferation of $CD4^+$ T cells, in contrast to $CD8^+$ T cells (Figure 16 B). In summary, the results of these assays demonstrated that PSCs were unable to activate antigen-specific naive $CD8^+$-and $CD4^+$ T cells directly.

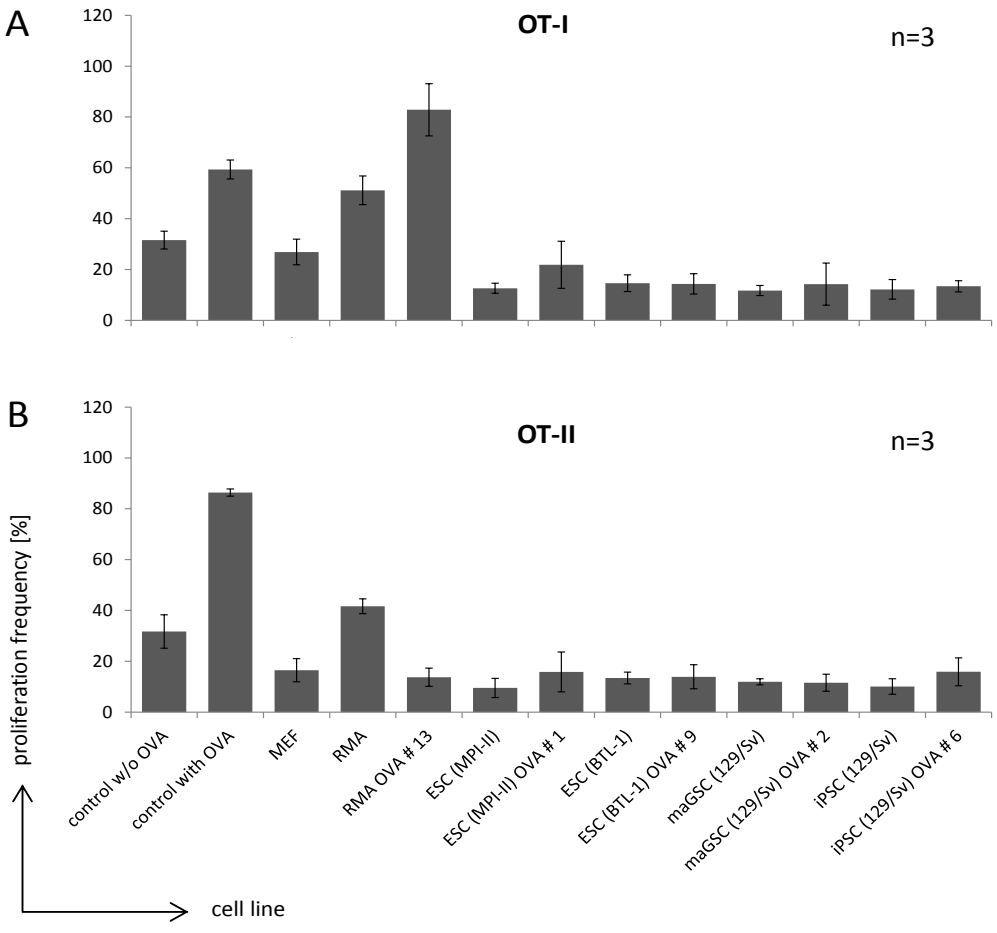

Figure 16: Proliferation frequency of OVA-specific $CD8^+$ and $CD4^+$ T cells
Splenocytes derived from OT-I mice **(A)** or OT-II mice **(B)** were stained with CFSE and cultured together with wt and OVA-expressing PSCs as well as control cell lines. Diagrams represent mean proliferation frequencies and SEM of $CD8^+$ and $CD4^+$ T cells as detected in flow cytometry. The proliferation was considered to be positive, when the T cells divided at least once.

Several mechanisms have been reported, by which ESCs suppress T cell activation or induce apoptosis in T cells. Since all OVA-expressing PSCs were apparently unable to stimulate T cells directly, the following assays focused on the analysis whether PSCs used such mechanisms to inhibit T cell activation. Therefore, co-cultures of wt PSCs and OVA-specific T cells were supplemented with defined amounts of OVA protein to stimulate T cell proliferation. PSCs co-cultured with OT-I derived $CD8^+$ T cells were supplemented with 1 µM OVA and PSCs co-cultured with OT-II derived $CD4^+$ T cells with 100 µM OVA protein. Furthermore, the cytokine IL-2 (1000 U/ml) was added to support T cell proliferation.

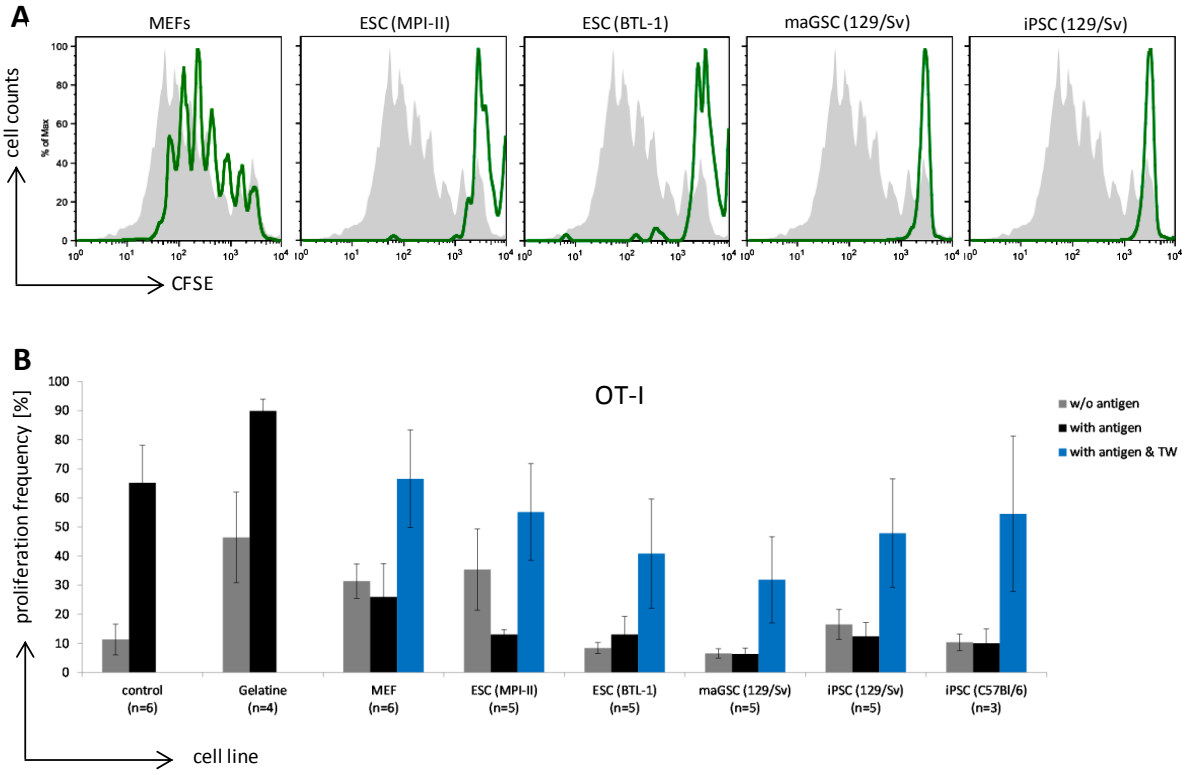

Figure 17: Proliferation of $CD8^+$ T cells co-cultured with PSCs
(A) Representative histograms show the proliferation of CFSE-stained, $CD8^+$ T cells ($5x10^5$ splenocytes) in presence of antigen (1µM OVA) and IL-2 (1000 U/ml) after 4 days of co-culture with $5x10^4$ cells of the different PSC lines. Proliferation of $CD8^+$ T cells in positive control is depicted in grey in the histograms.
(B) Diagram represents the mean proliferation frequencies and SEM of $CD8^+$ T cells co-cultured with PSC lines. $CD8^+$ T cells were cultured with and w/o antigen as well as with antigen (1µM OVA) separated from PSCs by a membrane (Transwell (TW)). The cells were considered to proliferate, when the $CD8^+$ T cells divided at least once.

PSCs were separated from MEFs and plated on gelatine-coated dishes, since preliminary studies (data not shown) revealed that MEFs themselves, at least partially, suppress T cell proliferation. Therefore, T cells were also co-cultured with MEFs, with and without OVA supplementation as further control. Again T cells cultured alone (without OVA protein as antigen) were used as negative control to assess the base-line proliferation and T cells cultured in presence of OVA were

used as positive control. In addition, the proliferation of T cells, cultured on gelatine coated dishes (with and without OVA), was analyzed as further control. In order to assess whether the suppressive effect of PSCs on T cell proliferation resulted from cell-to-cell contact or rather by release of soluble substances, PSCs and splenocytes were separated by a membrane (Transwell (TW), with a pore size of 0.4 µm).

The proportion of proliferating $CD8^+$ T cells in positive controls was above 65 %, whereas the proliferation frequency of $CD8^+$ T cells co-cultured with PSCs was only about 10 %. This proliferation frequency was similar to that, observed in absence of antigen in the negative control. In contrast, proliferation of $CD8^+$ T cells, which were separated from PSCs by a membrane, was largely restored (40 to 60 %) (Figure 17). Moreover, in accordance with higher proliferation of CFSE-stained $CD8^+$ or $CD4^+$ T cells, also their cell number was higher when separated from PSCs by a membrane. Therefore, it is possible that the T cells did not proliferate when cultured directly on pluripotent cells but also that PSCs might induced apoptosis in T cells.

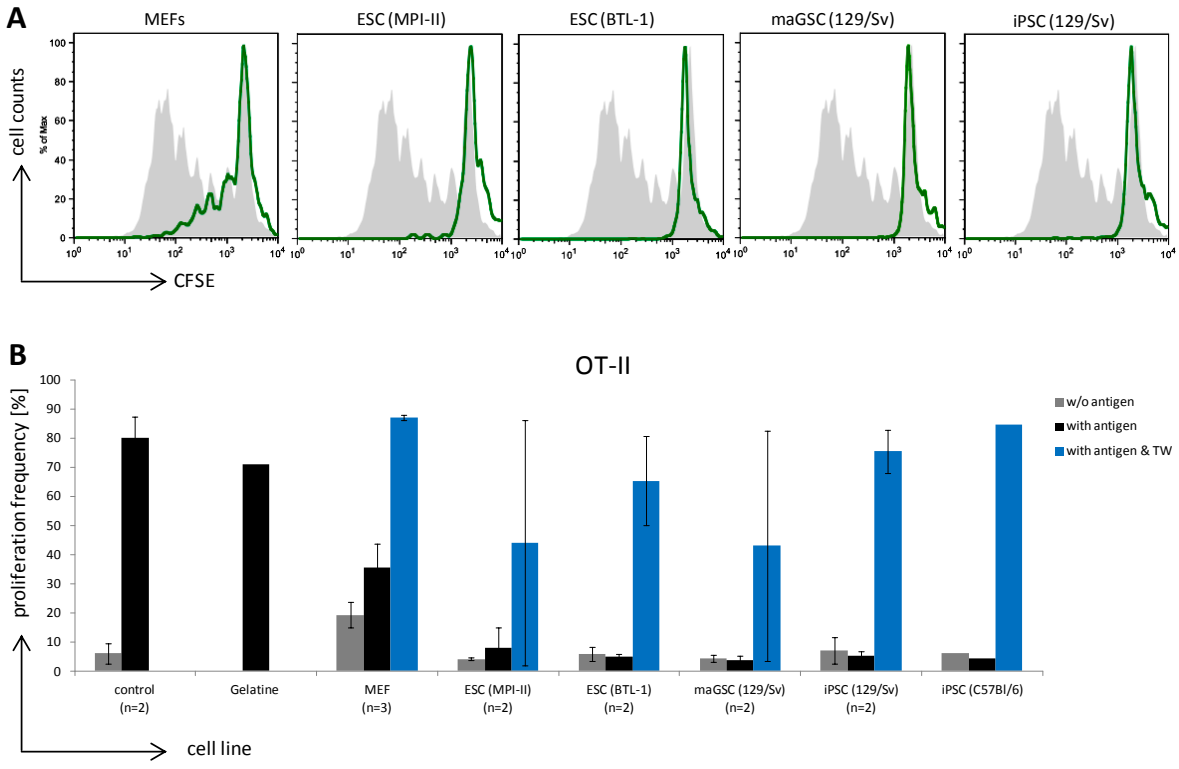

Figure 18: Proliferation of $CD4^+$ T cells co-cultured with PSCs

(A) Representative histograms show proliferation of CFSE stained, $CD4^+$ T cells derived from OT-II mice ($5x10^5$ splenocytes) in presence of antigen (100µM OVA) and IL-2 (1000 U/ml) after 5 days of co-culture with $5x10^4$ cells of different PSC lines. Proliferation of $CD4^+$ T cells in positive control is depicted in grey in the histograms.

(B) Diagram represents the mean proliferation frequencies and SEM of $CD4^+$ T cells co-cultured with PSC lines. $CD4^+$ T cells were cultured with and w/o antigen as well as with antigen (100µM OVA) but separated from PSCs by a membrane (Transwell (TW)). The cells were considered to proliferate, when the $CD4^+$ T cells divided at least once.

Similar results were obtained for proliferation frequencies of $CD4^+$ T cells. Only 5 to 10 % of $CD4^+$ T cells proliferated when cultured together with different PSC lines in presence of antigen (100 µM OVA) and IL-2 (1000 U/ml). These proliferation frequencies were equivalent to that in negative control, where no antigen was added. In contrast, in positive controls 70 to 80 % of $CD4^+$ T cells proliferated. Separation of PSCs and $CD4^+$ T cells by a membrane completely recovered proliferation frequencies of $CD4^+$ T cells. However, in single experiments the membrane separation failed to recover proliferation frequencies of $CD4^+$ T cells, what most likely resulted from technical failures and explain the high variations of the according results (Figure 18).

The impact of soluble substances, released by PSCs, on the proliferation of $CD8^+$ and $CD4^+$ T cells was further analyzed using PSC-conditioned medium. After 24 hrs, PSC culture medium was collected and separated from possible cell contaminations by filtration with a 0.45 µm filter. Splenocytes from OT-I mice were cultured 4 days, splenocytes from OT-II mice for 5 days in the PSC-conditioned media supplemented with IL-2 (1000 U/ml) and OVA (OT-I: 1 µM, OT-II: 100 µM) as antigen. The medium conditioned by the ESC line MPI-II as well as the medium conditioned by the maGSC line from 129/Sv mice had no suppressive effect on proliferation frequencies of $CD8^+$ and $CD4^+$ T cells. The proliferation frequencies of $CD8^+$ T cells ranged from 80 to 90 % and were comparable to the positive control and MEF control. The base-line proliferation frequencies without antigen in all media were also comparable, ranging from 10 to 15 %. About 70 to 80 % of $CD4^+$ T cells proliferated in media conditioned by PSCs, again corresponding to proliferation frequencies in controls. The basic proliferation of $CD4^+$ T cells cultured in MEF and PSC-conditioned media was approximately 35 % and slightly elevated compared to the negative control (Figure 19).

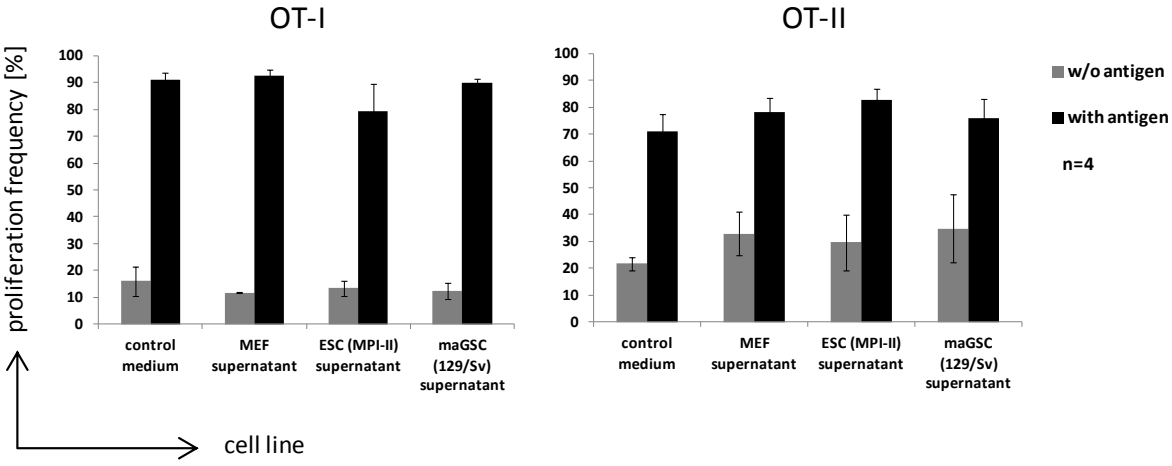

Figure 19: Proliferation of $CD8^+$ and $CD4^+$ T cells cultured in PSC-conditioned media
Splenocytes were isolated from OT-I and OT-II mice, respectively, stained with CFSE and subsequently cultured in media conditioned by different PSC lines for 4 to 5 days in presence of IL-2 (1000 U/ml) and antigen (OVA: OT-I: 1 µM, OT-II: 100 µM). Diagrams represent the mean proliferation frequencies and SEM of $CD8^+$ and $CD4^+$ T cells as detected in flow cytometry. The proliferation was considered to be positive, when the $CD4^+$ or $CD8^+$ T cells divided at least once.

In summary, the data demonstrates that $CD4^+$ as well as $CD8^+$ T cells were unable to proliferate in presence of PSCs. Thus, even in presence of their specific antigen and the cytokine IL-2 that supports T cell proliferation, PSCs efficiently inhibited T cell activation. Furthermore, the PSC-mediated inhibition of T cell proliferation was abrogated upon separation by a membrane, suggesting that this effect was not mediated by the release of soluble substances but rather by cell-cell contact.

4.4.1 Expression of co-stimulatory molecules and FasL in PSCs

Since OVA-expressing PSCs were apparently unable to activate antigen-specific T cells, PSCs were analyzed for their expression of CD80 and CD86 in order to assess their ability to provide co-stimulatory signals to antigen-specific T cells. Gene expression was analyzed by qPCR and the expression on the cell surface using CD80- or CD86-specific antibodies in flow cytometry.

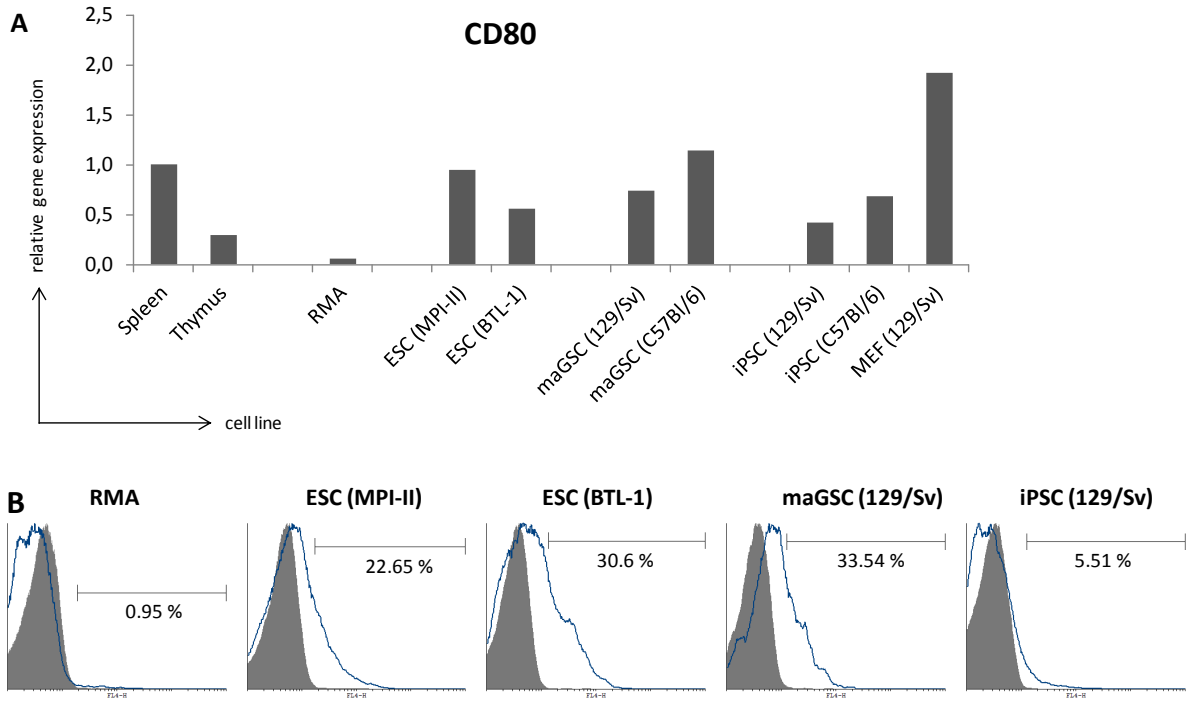

Figure 20: Expression analysis of the co-stimulatory molecule CD80 in different PSCs
(A) Diagram represents the fold change of PSC-derived CD80 mRNA amount relative to spleen mRNA. Values represent mean of technical triplicates normalized to the expression of the housekeeping gene *Hprt*.
(B) Representative histograms show cells positive for CD80 as detected in flow cytometry using a CD80-specific antibody. Unspecific staining is depicted in grey using staining with the secondary antibody only. Specific percentages (cells positive for CD80 minus cells positive by staining with secondary antibody) of cells positive for CD80 are shown.

The transcripts of co-stimulatory molecule CD80 were found in the ESC lines and the maGSC lines at comparable levels to the spleen control RNA used as reference. The CD80 transcript level was less prominent in the iPSC lines compared to other PSC lines but still about 40 % to 70 % compared to spleen reference and higher as in thymus used as additional control. In RMA cells only minor amounts of CD80 transcripts were detectable (Figure 20 A). These results were confirmed by flow cytometry. CD80 surface expression was detectable in all tested PSC lines. In the ESC lines and the maGSC line 22 % to 34 % cells were positive for CD80, whereas 6 % of iPSC cells were positive for CD80 (Figure 20 B).

In contrast, mRNA of the co-stimulatory molecule CD86 was not detectable in the different PSC lines. In addition to spleen and thymus positive controls, only in RMA and MEF control cells minor amounts of CD86 transcripts were found (Figure 21 A). These observations were confirmed by flow cytometry. Only in RMA cell 5 % of the cells were positive for CD86, whereas both analyzed ESC lines as well as the tested maGSC and iPSC line were completely negative for CD86 expression (Figure 21 B).

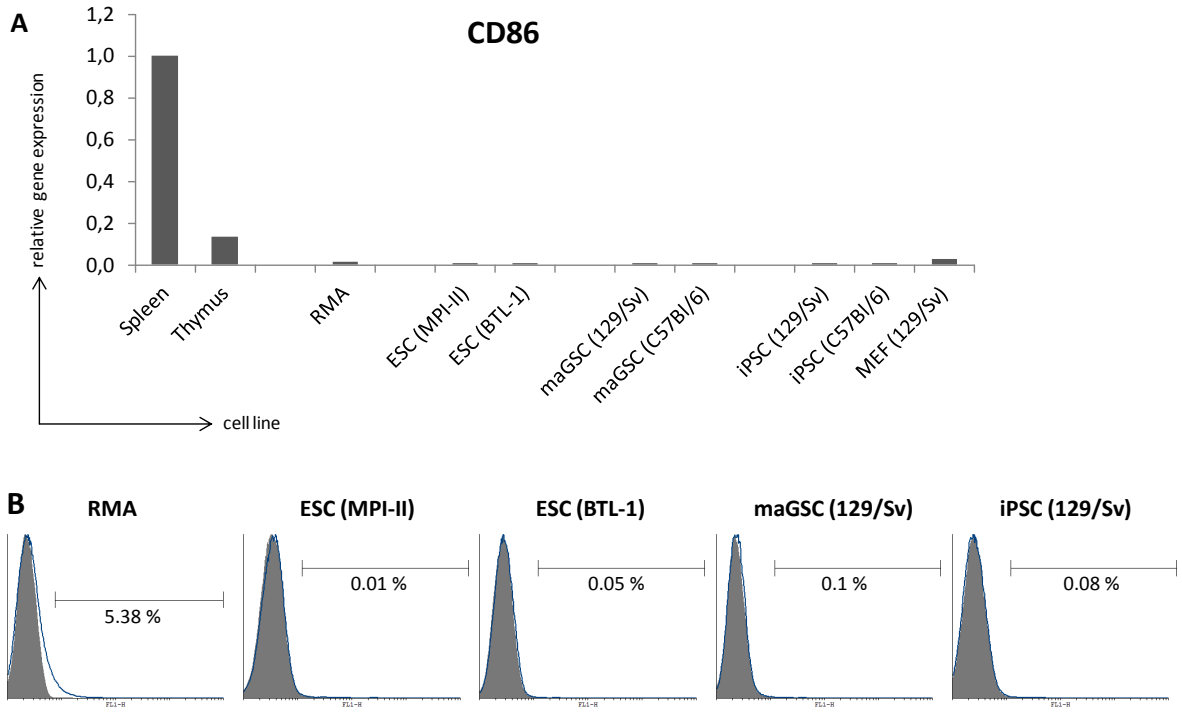

Figure 21: Expression analysis of the co-stimulatory molecule CD86 in different PSCs
(A) Diagram represents the fold change of PSC-derived CD86 mRNA amount relative to spleen mRNA. Values represent mean of technical triplicates normalized to the expression of the housekeeping gene *Hprt*.
(B) Histograms show cells positive for CD86 as detected in flow cytometry using a CD86-specific antibody. Unspecific staining is depicted in grey color using the secondary antibody only. Specific percentages of CD86-positive cells are shown.

In order to analyze, whether expression of the Fas ligand (FasL) on PSCs could have induced apoptosis in T cells in co-culture experiments, PSC lines were stained with a FasL specific antibody and analyzed by flow cytometry. FasL cell surface expression was undetectable in all tested PSC lines as well as in RMA lymphoma cells (Figure 22). Therefore, the Fas ligand/receptor interaction is unlikely responsible for the low cell numbers and the missing proliferation of naive antigen-specific T cells, observed in co-culture experiments with PSCs.

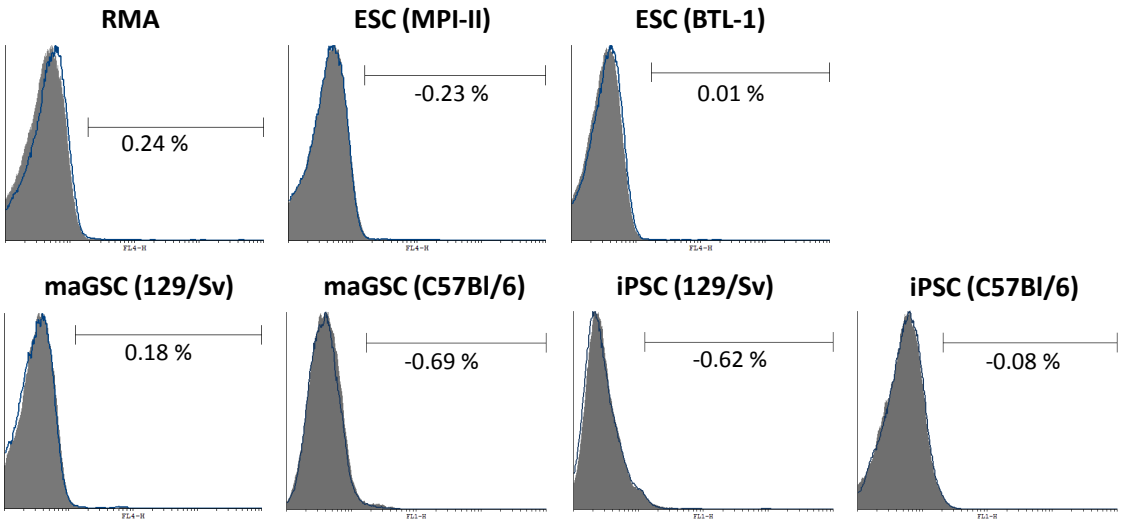

Figure 22: Expression analysis of the Fas Ligand on PSCs
Histograms show cells positive for FasL as detected in flow cytometry using a FasL specific antibody. Unspecific staining is depicted as grey background using secondary antibody staining only. Specific percentages of cells positive for FasL are shown.

4.4.2 Expression analysis of putative T cell activation inhibitors

Several proteins have been reported to inhibit T cell function. To examine the role of these proteins in PSC-mediated immune inhibition their gene expression in PSCs was analyzed by qPCR. Except for TGFβ, until now none of these proteins was reported to contribute to PSC-mediated T cell inhibition (see 1.3). Nevertheless, it was analyzed whether these proteins might contributed to T cell inhibition observed in co-culture experiments, since the contribution of previous reported mechanisms such as Arg1, SPI-6, CtsB, IDO and FasL expression could be excluded (see 1.3 and 4.4.1). The transcript amount of RMA cells was chosen as reference, since these cells did not possess an inhibitory effect on T cell activation in co-culture experiments. In addition, spleen and thymus RNA as well as MEF RNA were included as further controls (Figure 23).

Galectin-1 (Gal-1) is as a cytokine-like molecule involved in immune-escape of tumors by regulation of T cell activity. It was shown that *Gal-1* expression can induce T cell apoptosis and

reduce numbers of infiltrating T cells in tumor tissues (Cooper et al, 2010; Kovacs-Solyom et al, 2010; Le et al, 2005). In both ESC lines high amounts of *Gal-1* transcripts were found. The mRNA amounts were comparable to thymus reference RNA that also comprised high amounts of *Gal-1* transcripts. In maGSCs as well as iPSCs the expression was even higher (about 160 % to 420 % compared to thymus reference RNA). However, in RMA control cells the expression of *Gal-1* mRNA was about 700 % of thymus what suggests that *Gal-1* expression was not responsible for the observed T cell inhibition.

Semaphorin-3A (Sema-3A) is a protein with an immunoglobulin-like domain that is expressed in a variety of human tumor cell lines. In mixed lymphocyte culture, recombinant Sema-3A inhibited the activation of cytotoxic activity against K-562 cells. Furthermore, it inhibited T cell proliferation as well as cytokine production of primary human T cells stimulated with anti-CD3 and anti-CD28 (Catalano et al, 2006). *Sema-3A* transcripts were detectable in various amounts in all analyzed PSCs. Thereby, the mRNA amounts were similar to spleen reference, except for the maGSC line C57Bl/6 in which nearly a 5-fold mRNA amount was detected. However, the *Sema-3A* transcript level in RMA cells was even 9-fold higher that in spleen reference and consistently higher than in PSCs, suggesting that Sema-3A expression did not confer T cell inhibiting activity to PSCs.

It was reported, that TGFβ expression confers immune suppressive properties to ESCs (see 1.3). Indeed, moderate levels of *TGFβ* transcripts were detectable in PSCs. The transcript amount varied slightly between the different PSC lines and origins. However, again the *TGFβ* transcript amount detected in RMA cells was very high and at least more than 2-fold higher as in PSC-derived RNAs. The high expression of *TGFβ* in RMA cells, which lacked T cell inhibiting activity, in addition to the finding that the inhibitory activity of PSCs was rather not mediated by a soluble substance (see 4.4), suggests that TGFβ expression did not contributed to PSC-mediated T cell inhibition.

The receptor-binding cancer antigen expressed on Siso cells (RCAS1) induces apoptosis or cell cycle arrest in RCAS1 receptor expressing immune cells. It was demonstrated that soluble RCAS1-induced apoptosis of lymphocytes following co-culture of IL-2 activated peripheral blood lymphocytes with a human oral squamous cell carcinoma cell line (KB cells) (Fukuda et al, 2004). *RCAS1* mRNA amounts were generally low in all analyzed samples, including references. The according Ct values were consistently about 30 and above in PSCs. Nonetheless, *RCAS1* transcripts were still detectable but very variable in amount in different PSC lines. In iPSCs and maGSCs derived from C57Bl/6 mice the amounts of *RCAS1* mRNA were at least 2-fold higher than in their counterparts derived from 129/Sv mice. However, also in the ESC line MPI-II and the ESC line BTL-1, both derived from 129/Sv mice the *RCAS1* gene was rather differently expressed. Whereas the *RCAS1* transcript level was comparable to thymus and spleen control in MPI-II cells, the transcript

level in BTL-1 cells was only about 40 % compared to spleen control. The highest *RCAS1* gene expression was detectable in RMA cells, nearly 4-fold higher than in spleen and thymus control RNA. Therefore, and due to the very low *RCAS1* transcript amounts in general, RCAS1 was unlikely responsible for PSC-mediated T cell inhibition.

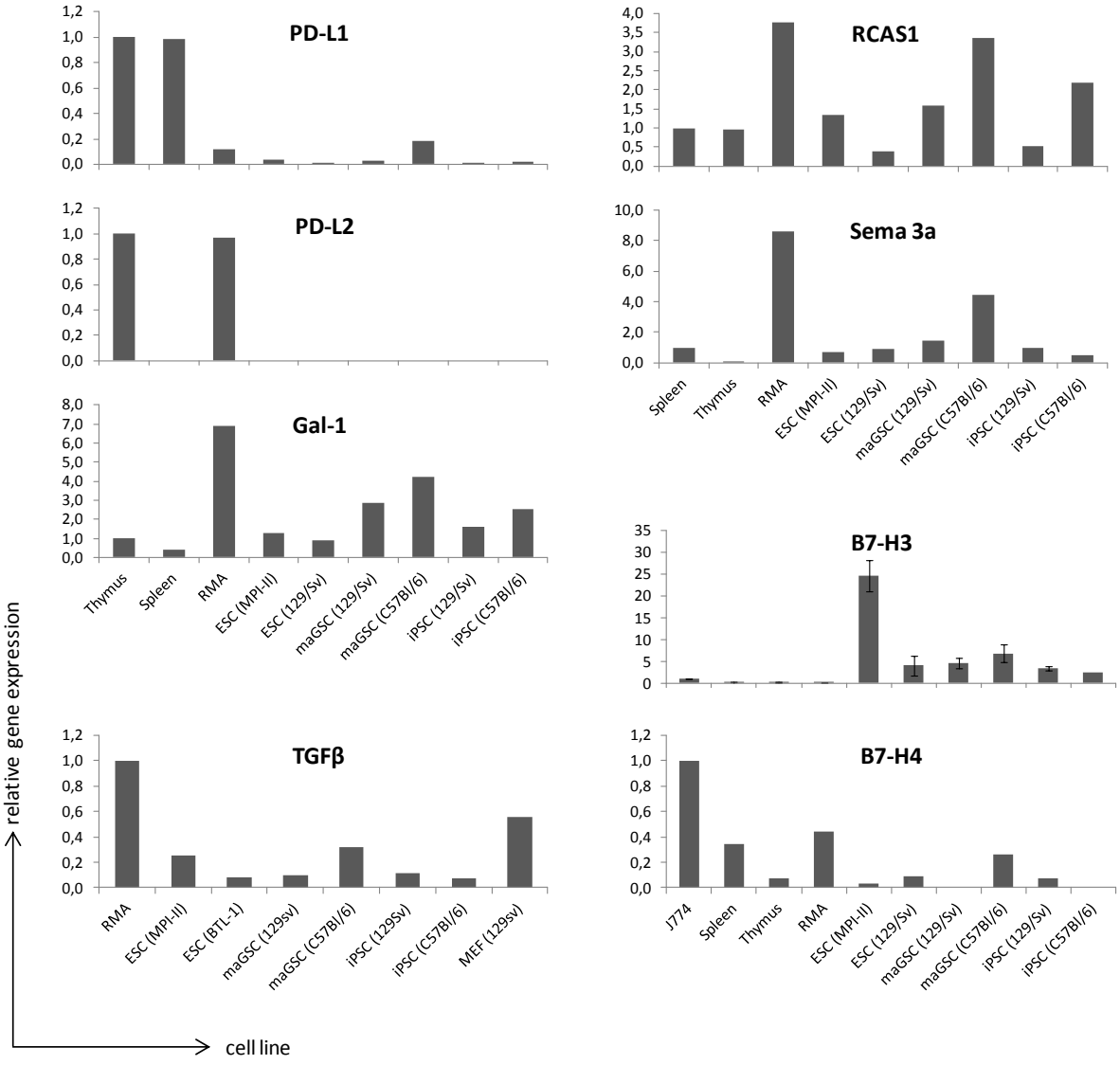

Figure 23: Expression analysis of genes involved in inhibition of T cell activity
Diagrams represent the fold change in gene expression relative to appropriate reference control RNAs. Values are efficiency correlated calculated (Pfaffl calculated) as mean of technical triplicates normalized to the housekeeping gene *Hprt*.

The programmed death ligands (PD-L1 and PD-L2), part of the B7 family, bind to the programmed death receptor (PD-1) expressed by T cells and negatively regulate T cell activation (Dong et al, 1999). It was reported, that up-regulation of PD-L1 leads to increased number of PD-1$^+$ CD8$^+$ T cells in tumor tissues and that these CD8$^+$ T cells are impaired in cytotoxic granule and cytokine

production (Matsuzaki et al, 2010; Sfanos et al, 2009; Shi et al, 2011; Wu et al, 2009; Zhang et al, 2010). Only very low amounts of *PD-L1* mRNA were detectable in spleen and thymus control and in the majority of PSCs nearly no *PD-L1* mRNA was detectable. Only in the maGSC line from C57Bl/6 mice, but also in RMA cells trace amounts of *PD-L1* transcripts were detectable, albeit only 12 % to 19 % of thymus reference. Due to the relative quantification method and low expression in the reference cells the depiction of true gene expression in the diagram is deceptive. The according Ct values in PSCs were consistently about 30 and above. Therefore, *PD-L1* transcripts could be considered to be absent in PSCs, except maGSC (C57Bl/6).

PD-L2 transcripts were generally not detectable in PSCs and in the spleen. Also in thymus reference probes and RMA control only very low amounts of *PD-L2* mRNA was detectable. The according Ct values were about 29 in both samples. Therefore, the expression of the PD-L1 and PD-L2 in PSCs is unlikely the reason for the inhibitory activity of PSCs observed in co-culture assays. B7-H3 and B7-H4, further members of the B7 family are also reported to have an inhibitory effect on proliferation, differentiation and cytotoxicity of T cells. Prasad et al. reported that the murine B7-H3 protein inhibited T cell activation and effector cytokine production and the addition of an antagonistic antibody to B7-H3 enhanced T cell proliferation *in vitro* (Prasad et al, 2004). Furthermore, over-expression of B7 family members is associated with immune modulating properties of a variety of tumors (for review see (Du & Wang, 2011)). However, while most data published so far reported B7-H3-mediated inhibition of T cell function also contradicting data was published. Hashiguchi et al. identified TREML2 as receptor for B7-H3 and reported that this interaction co-stimulates the activation of T cells (Hashiguchi et al, 2008).

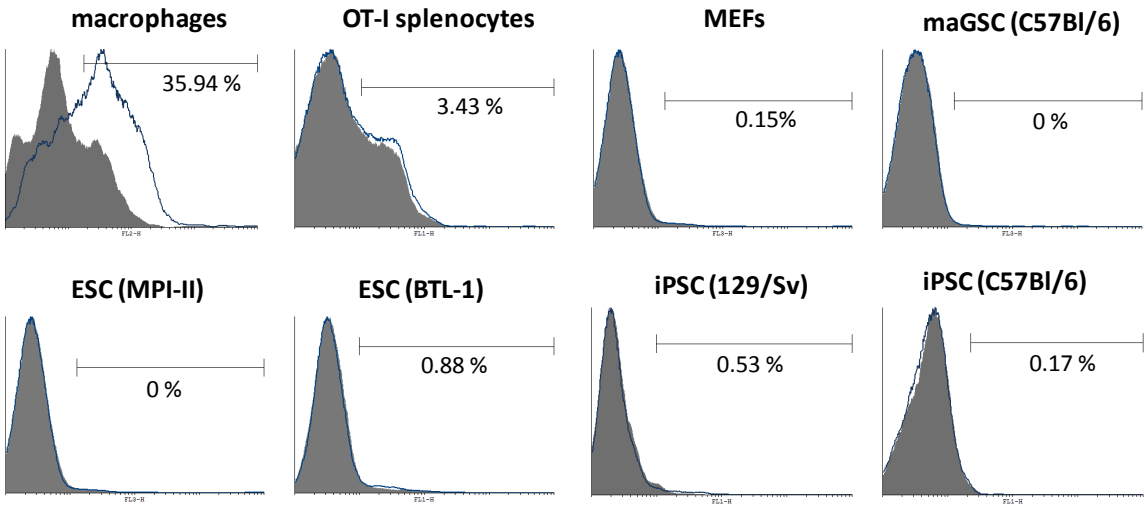

Figure 24: Cell surface expression of B7-H3
Representative histograms show the cell surface expression of B7-H3 as detected by flow cytometry. The specific percentages of cells, (B7-H3 positive cells minus cells positive for isotype control) positive for B7-H3 are shown.

The B7-H3 and B7-H4 ligands are known to be expressed on monocytes or macrophages, respectively. Therefore, RNA of the macrophage cell line J774 was included as reference. Only trace amounts of *B7-H4* mRNA was detectable in some tested PSC lines. In addition, the B7-H4 mRNA amount in J774 reference RNA was low. Therefore, PSCs could be considered to be negative for *B7-H4* expression. Only in maGSC (C57Bl/6) cells minor *B7-H4* transcript levels were detectable. In contrast, the amount of detectable B7-H3 mRNA was very high in all PSC lines, about 3-fold up to 8-fold higher compared to J774 positive control cells that also comprised well detectable levels of *B7-H3* transcripts. The gene expression in the ESC line MPI-II was even 25-fold higher compared to J774 reference. Interestingly, *B7-H3* transcripts were not detectable in RMA cells. The result was confirmed by an independently performed assay, using another set of primers specific for *B7-H3*. The mean of both assays was calculated and the relative expression is shown in Figure 23. Since *B7-H3* transcript levels were undetectable in RMA cells but high in PSCs, B7-H3 was chosen for further investigations.

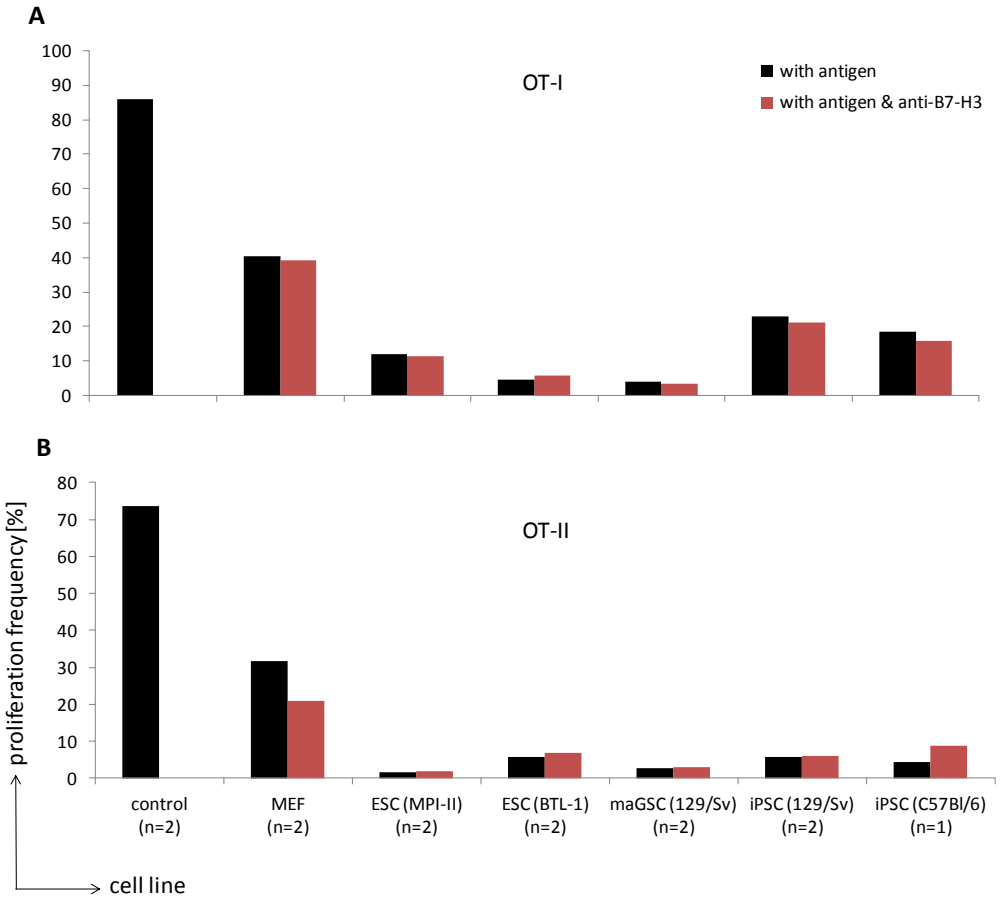

Figure 25: Proliferation frequencies of $CD8^+$ and $CD4^+$ T cells after co-culture with PSCs in presence of a B7-H3 blocking antibody
(A) Diagram represents the mean proliferation of $CD8^+$ T cells derived from OT-I mice after 4 days of co-culture with PSCs. **(B)** Diagram shows the mean proliferation of $CD4^+$ T cells derived from OT-II mice after 5 days of co-culture with different PSC lines. All cells were supplemented with IL-2 and OVA as antigen. In addition, a B7-H3 blocking antibody in a final concentration of 5 µg/ml was added in order to block B7-H3-mediated interactions.

The surface expression of B7-H3 was analyzed by flow cytometry. PSCs as well as MEF control were negative for B7-H3 expression. Only on primary macrophages, which were isolated from femurs of a C57Bl/6 mouse, cells positive for B7-H3 were found. To induce differentiation towards the macrophage lineage, these cells were stimulated with different cytokines gained from the supernatant of L929 cells and 10 ng/ml IFNγ prior to flow cytometric analysis (Figure 24) (Coligan, 2005).

Since the B7-H3 expression on PSCs could have been induced following co-culture with splenocytes, the role of the B7-H3 ligand in modulating T cell activation was further analyzed in co-culture assays with CFSE-stained, antigen-specific T cells. Therefore, a specific antibody against B7-H3 was added (5 µg/ml) in order to block possible interactions between PSCs and T cells.

Co-culture with PSCs again significantly suppressed proliferation of $CD8^+$ as well as of $CD4^+$ T cells. In addition co-culture with MEFs also suppressed T cell proliferation albeit less extensively than PSCs. The supplementation with a B7-H3 blocking antibody had no effect on T cell proliferation, neither on $CD8^+$ nor on $CD4^+$ T cells (Figure 25). In accordance with the finding, that the B7-H3 ligand is absent on the cell surface of PSCs, the co-culture data suggests that B7-H3 did not contribute to PSC-mediated inhibition of T cell proliferation since B7-H3 was not expressed on protein level. Thus, it remains unclear by which mechanism PSCs block T cell proliferation in a contact dependent manner.

4.5 Immunogenicity of OVA-expressing iPSCs *in vivo*

4.5.1 Tumor formation in syngeneic hosts

Since iPSCs might provide the most interesting PSC type for future medical therapies, this cell type was chosen for *in vivo* studies. The effect of OVA-expression as a model for a minor histocompatibility antigen on successful engraftment in otherwise syngeneic hosts was studied using wt iPSCs and their OVA-expressing counterparts for transplantation. Therefore, 1×10^6 cells were injected subcutaneously into the flank of syngeneic 129/Sv mice. In addition, wt RMA cells as well as OVA-expressing RMA cells were injected into syngeneic C57Bl/6 mice as control. Tumor growth was regularly controlled by palpation. Furthermore, iPSCs were injected into immunodeficient mice to confirm their ability to form teratomas. The iPSCs possessed a male genotype and 88.9 % (10/12) of wt iPSCs successfully engrafted and formed teratomas in syngeneic mice, independently of host gender.

In contrast, only 50 % (5/10) of the OVA-expressing iPSC clone #6 and only 20 % (2/10) of clone #24 were able to form teratomas, preferentially in male syngeneic hosts. Thus, whereas a different gender of wt iPSCs alone was not sufficient to induce an immune rejection, the OVA-expressing iPSCs were only rejected in female hosts.

Table 16: Tumor formation of OVA-expressing cells in syngeneic hosts

cell line	syngeneic hosts			immunodeficient hosts	gender (syngeneic hosts)	
	tumor frequency	mean tumor size [mm^3]	mean tumor weight [mg]	tumor frequency	engraftment	rejection
RMA (C57Bl/6)	100 % (4/4)	1515	793,25			
RMA OVA #13	50 % (2/4)	418,5	218,5			
iPSC (129/Sv)	88.9 % (10/12)	2150,8	1126,2	100 % (3/3)	7 x ♂ / 3 x ♀	1 x ♂ / 1 x ♀
iPSC OVA #6	50 % (5/10)	549,8	287,8	100 % (3/3)	5 x ♂	5 x ♀
iPSC OVA #24	20 % (2/10)	1116,0	584,0	100 % (3/3)	2 x ♂	8 x ♀

Wt RMA cells formed tumors in 100 % (4/4) of the host animals whereas OVA-expressing RMA cells were rejected in 50 % (2/4) from syngeneic hosts. A summary of these results is shown in Table 16. Although OVA-expressing cells were not rejected from all syngeneic hosts, the formed tumors remained significantly smaller in size and weight. The mean transplantation interval of wt iPSCs was 34 days and that of OVA-expressing iPSCs 52 days, before the host animals had to be sacrificed for ethical reasons (see 3.5.5). Therefore, the smaller tumor size and weight of iPSC OVA derived tumors did not result from a shorter growth interval. The findings rather suggest that the tumor growth rates were affected by the hosts immune system, due to the expression of the mHC antigen OVA. This conclusion is supported by the findings made in immunodeficient hosts since the tumor volume and size of wt iPSC and iPSC OVA derived tumors was similar in these animals (Figure 26). Moreover, the engraftment or rejection, respectively, did not depend on the OVA expression level of the iPSC clones, since the iPSC OVA clone #6, which expressed much higher levels of OVA, was not rejected more frequently.

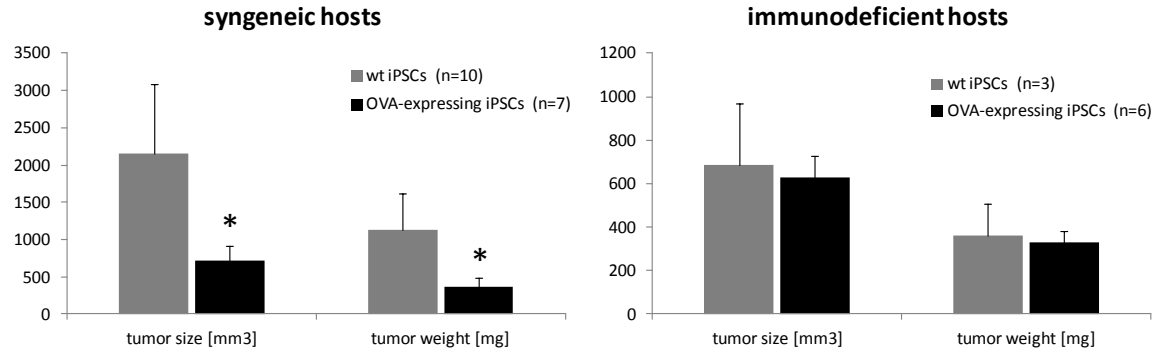

Figure 26: Size and weight of wt iPSC and iPSC OVA derived tumors
The diagrams show the mean size and weight of tumors derived from wt iPSCs and OVA-expressing iPSCs formed in syngeneic or immunodeficient hosts. Tumors were dissected and subsequently measured using linear calipers and micro scales. Tumors, formed by iPSC OVA cells remained significantly smaller in syngeneic hosts compared to wt iPSC derived tumors. Significances were calculated using the Mann-Whitney (U-) test.

4.5.2 Analysis of iPSC-derived teratomas

All teratomas, which had formed after injection of iPSCs and their OVA-expressing counterparts into syngeneic hosts, were dissected and subsequently analyzed regarding viability and leukocyte infiltration. Similar results were obtained for all teratomas which were analyzed by immunohistochemistry. All teratomas contained cells positive for the pluripotency marker Oct4 and the proliferation marker Ki67. Thus, even after at least 34 days following transplantation, viable cells exist within the teratomas which did not differentiate. Moreover, tumors were infiltrated with different leukocyte populations. These included moderate amounts of $CD3^+$ T cells and high amounts of F4/80-positive macrophages. Furthermore, tumors contained cells positive for CD45R, a marker for B cells, albeit only in minor amounts (Figure 27). Differences in leukocyte infiltration between iPSC and iPSC OVA-derived tumors were not observable.

In addition to immunohistochemistry, infiltration of leukocytes was quantified by flow cytometry after digestion of some dissected tumors to single cells. Prior to final analysis the detected cells were gated for viable cells as detected in forward and side scatter. In all tumors, formed by inoculation of OVA-expressing iPSCs and RMA cells, cells positive for different leukocyte markers were detected. The proportion of $CD8^+$ and $CD4^+$ T cells was 1.5 % to 2.5 % in tumors formed by OVA-expressing iPSCs, slightly lower compared to tumors formed by RMA OVA #13 cells. However, RMA cells were inoculated in C57Bl/6 mice and iPSCs in 129/Sv mice. Therefore, differences between the host specific immune response could have contributed to observed differences between RMA and iPSC derived tumors. Cells positive for the B cell marker B220 accounted for 1.3 % to 2 % in all analyzed tumors. In addition to T and B cells, also NK cells and macrophages were detected. Tumors formed by RMA OVA #13 and iPSC OVA #24 clones

comprised about 3 % NK cells and about 4.5 % macrophages. In comparison, tumors formed by iPSC OVA #6 clones comprised lowered cell numbers positive for NKp46 and F4/80 (Figure 28).

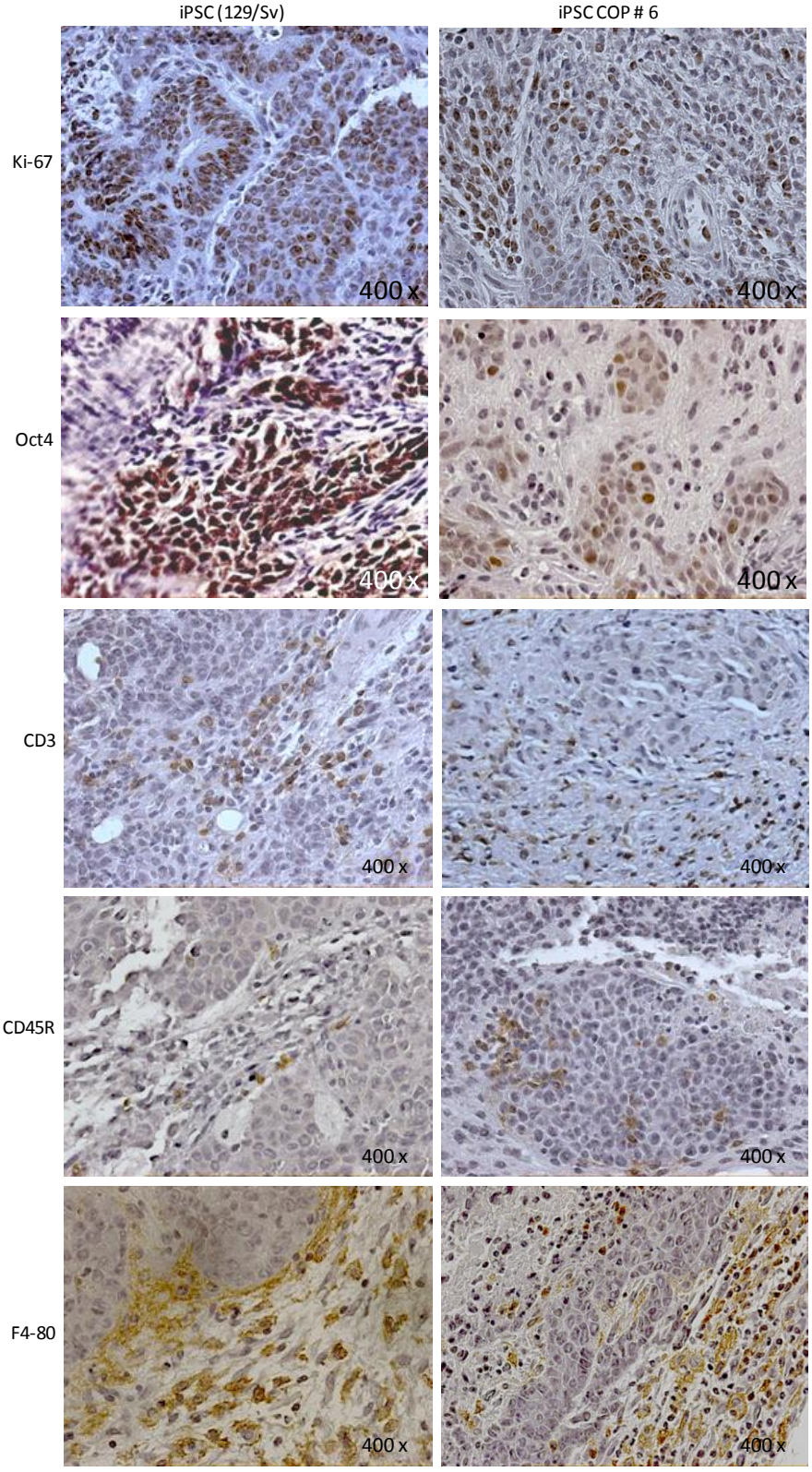

Figure 27: Immunohistology of teratomas formed after injection of iPSCs
In immunohistochemical stainings the analyzed tumor tissue was positive for Ki67 and Oct4, demonstrating that tumor cells proliferated and remained partially pluripotent. In addition, tumor tissue was infiltrated by leukocytes, shown by staining of T cells (CD3), B cells (CD45R) and macrophages (F4/80).

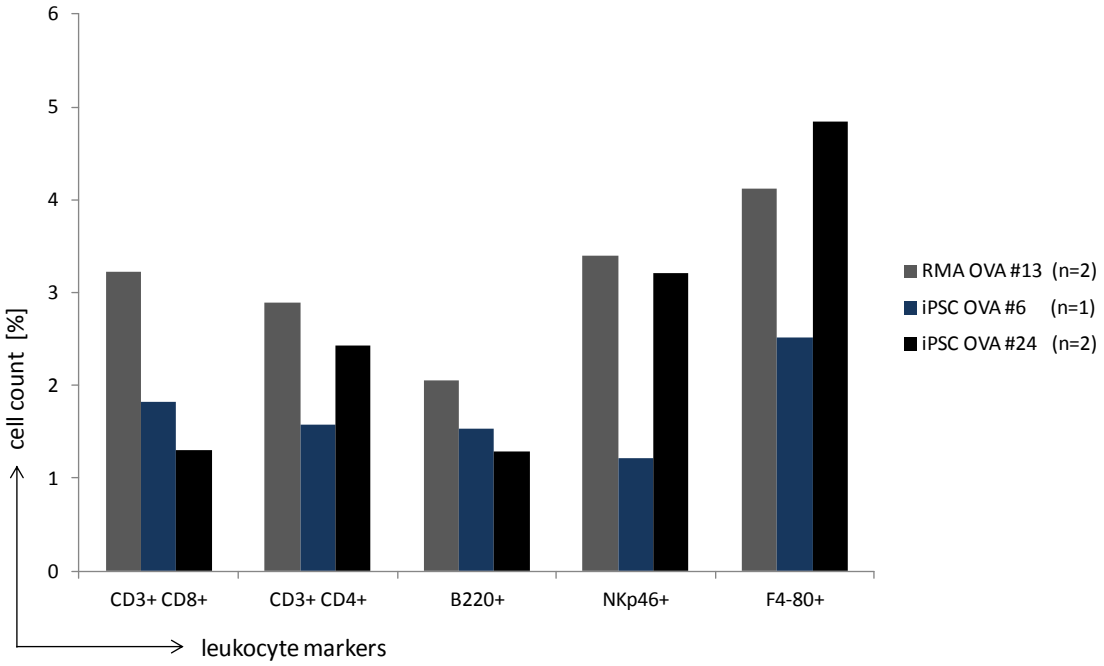

Figure 28: Analysis of tumor infiltrating leukocytes
Diagram represents mean leukocyte numbers found in tumors formed by inoculated OVA-expressing iPSCs (129/Sv) and RMA cells (C57Bl/6) into syngeneic hosts. Tumors were digested into single cell suspensions and analyzed in flow cytometry using leukocyte marker specific antibodies. For final analysis the cells were gated for viability using the according size and granularity specificities.

4.5.3 Generation of OVA-specific CTLs in syngeneic hosts

To evaluate, whether OVA-specific T cells arose in host animals after injection of OVA-expressing stem cells, spleens of these animals were dissected on the day of sacrification and the splenocytes were re-stimulated with OVA and subsequently used as effector cells in ^{51}chromium release assays against wt and OVA-expressing RMA target cells (Figure 29).

When OVA-expressing RMA cells were injected as control cell line into syngeneic C57Bl/6 mice OVA-specific CTLs arose independently of engraftment or rejection of injected cells. In contrast, preferentially in animals that successfully rejected OVA-expressing iPSCs, OVA-specific CTLs were induced, shown by increased lysis of RMA OVA cells compared to wt RMA cells.

CTLs, isolated from animals in which tumors formed, were unable to kill OVA-expressing target cells. Since the maximum number of isolated splenocytes differed between the animals also the effector to target ratios in single ^{51}chromium release assays differed. Due to this fact the killing ratio of RMA OVA to wt RMA cells at the highest effector to target ratio was calculated in order to summarize all assays.

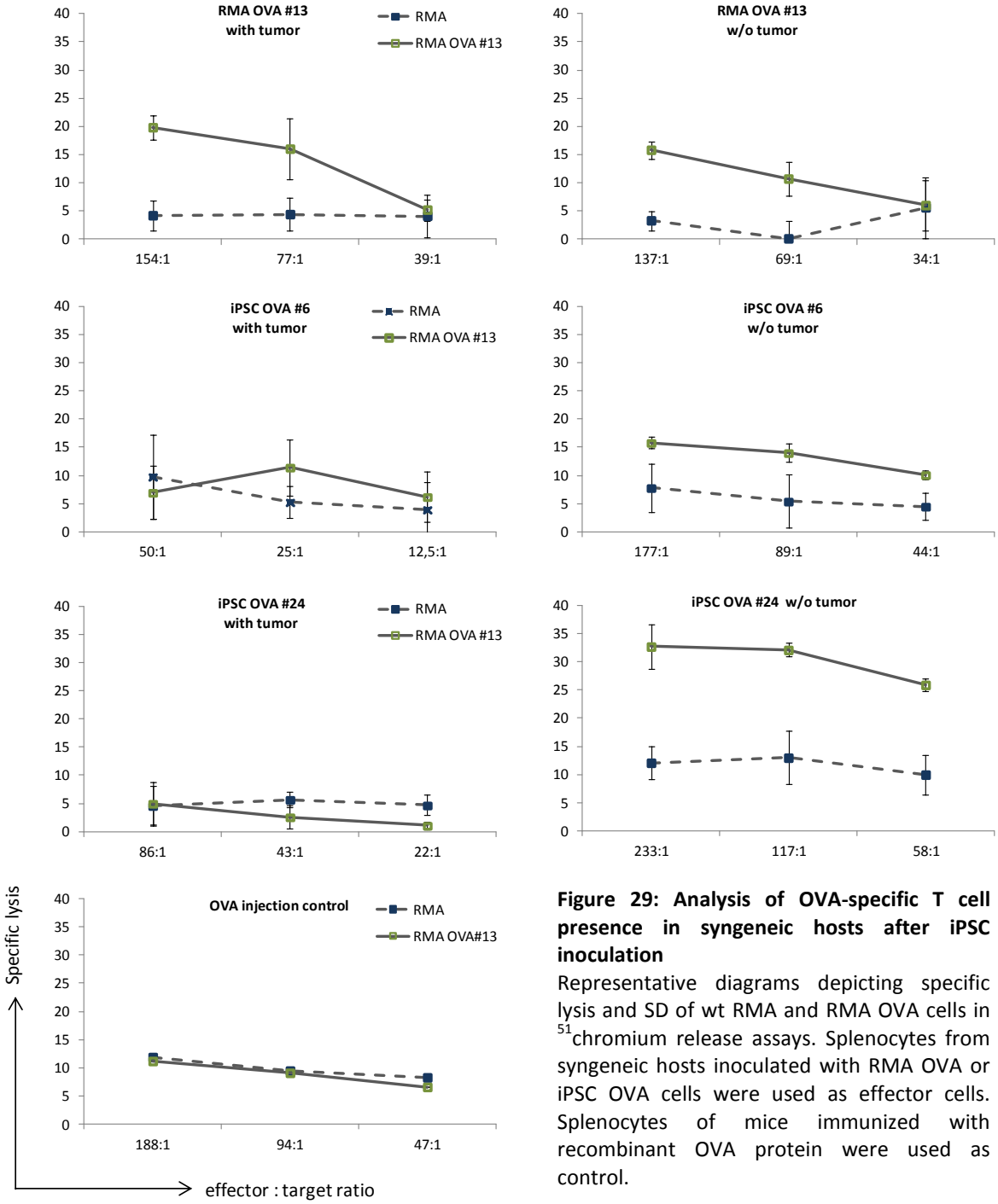

Figure 29: Analysis of OVA-specific T cell presence in syngeneic hosts after iPSC inoculation

Representative diagrams depicting specific lysis and SD of wt RMA and RMA OVA cells in ^{51}chromium release assays. Splenocytes from syngeneic hosts inoculated with RMA OVA or iPSC OVA cells were used as effector cells. Splenocytes of mice immunized with recombinant OVA protein were used as control.

Splenocytes derived from animals that either were inoculated with wt RMA and wt iPSC cells served as control as well as splenocytes from animals immunized with OVA protein. The killing ratio of RMA OVA to wt RMA cells exposed to these splenocytes was therefore nearly 1. Similar results were obtained with splenocytes derived from animals in which iPSC OVA #24 cells successfully engrafted. In contrast, splenocytes derived from animals that rejected iPSC OVA #6 and iPSC OVA #24 cells exhibited a higher cytotoxicity against OVA-expressing target cells (Figure 30).

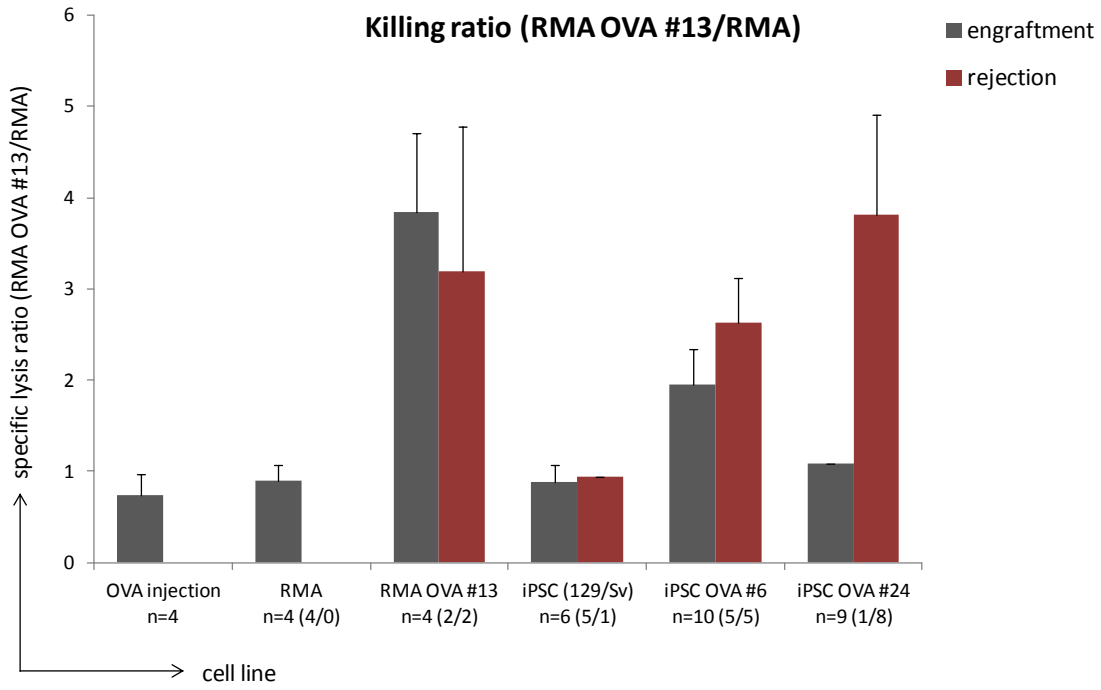

Figure 30: Specific lysis ratio of RMA/RMA OVA cells to OVA-specific CTLs arose in syngeneic hosts
Diagram depicts the killing ratio and SD of RMA OVA to RMA target cells. Splenocytes, derived from hosts after inoculation of syngeneic iPS (129/Sv) or RMA cells (C57Bl/6) that either did or did not express OVA, were used as effector cells. Splenocytes of mice immunized with recombinant OVA protein were used as reference. In braces the partition of the total numbers regarding engraftment/rejection are shown.

To compare the cellular composition of host splenocytes, flow cytometric analysis of lymphocyte populations was performed. About 40 % of analyzed splenocytes were T cells, positive for CD3 and CD4. Moreover, about 25 % of the splenocytes were T cells positive for CD3 and CD8. Only splenocytes derived from hosts that were inoculated with iPSC OVA #6 cells comprised lower numbers of $CD8^+$ T cells. No differences between the splenocyte composition in hosts that rejected iPSC OVA cells to hosts in which iPSC OVA cells engrafted were found (data not shown). Less than 5 % of the analyzed cells represented NK cells (Figure 31).

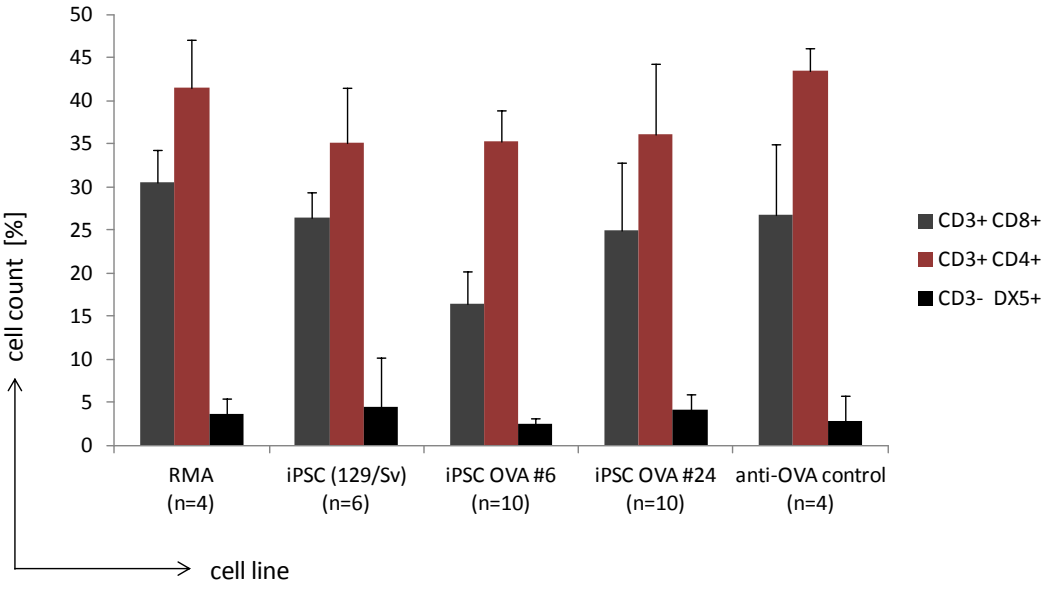

Figure 31: Lymphocyte composition of host splenocytes
Diagram represents mean percentages and SD of lymphocytes collected from spleens of syngeneic hosts after iPSC transplantation. Splenocytes of 129/Sv mice immunized with recombinant OVA protein were used as reference.

4.5.4 OVA-specific antibody generation in syngeneic hosts

To analyze whether iPSC OVA cells elicited an antibody response in syngeneic hosts and to evaluate whether antibodies against OVA had an impact of on the outcome of iPSC OVA engraftment was analyzed using ELISA. Sera of animals, inoculated with OVA-expressing cells, were collected and the ODs (405 nm) at eight different serum dilutions were measured (Figure 32 A). Four 129/Sv mice were initially immunized with recombinant OVA protein and TiterMax adjuvants, followed by at least 3 more injections of OVA protein for boosting. The serum of these animals was used as reference control. Normal sera of four untreated 129/Sv mice as well as sera collected from animals inoculated with wt iPSCs were used as negative control.

In order to summarize these experiments the relative anti-OVA titer was calculated. Therefore, the mean ODs derived of the sera of the immunized animals at the highest concentrated dilution (1:20) was set to 100 % and the ODs of the remaining sera were calculated relative to this. The sera of animals that received OVA-expressing iPSCs or RMA cells comprised similar levels of OVA-specific antibodies to OVA-immunized control mice (129/Sv). The anti-OVA titers of hosts inoculated with wt iPSCs were similar to normal sera of non-treated control mice. No differences in the sera of animals that either did or did not reject the iPSC OVA clones were found (Figure 32 B).

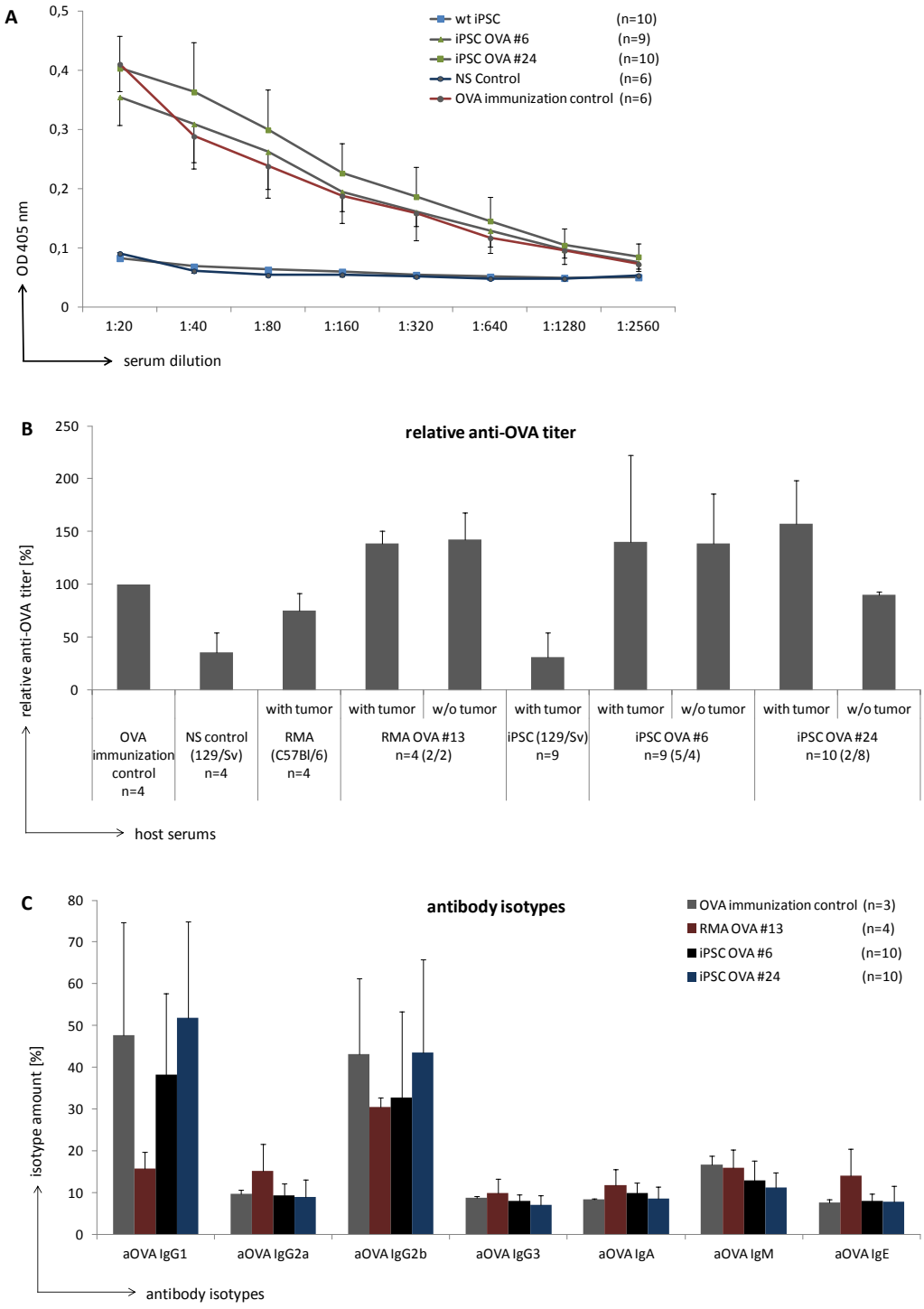

Figure 32: Generation of OVA-specific antibodies in syngeneic hosts

(A) Diagram shows the mean ODs and SEM for OVA-specific antibodies in different serum dilutions as detected by ELISA. Sera were collected from syngeneic hosts after transplantation of wt iPSCs and OVA-expressing iPSCs. Normal sera (NS) of 129/Sv mice were used as negative control. Sera of 129/Sv mice immunized at least 4 times with recombinant OVA protein were used as reference control.

(B) Diagram represents relative anti-OVA titers and SD in the serum of syngeneic hosts after iPSC OVA inoculation compared to the mean anti-OVA titers of four 129/Sv mice immunized with recombinant OVA protein. The normal serum of four 129/Sv mice was used as negative control. In braces the partition of the total numbers regarding engraftment/rejection are shown.

(C) Diagram depicts isotype distribution of OVA-specific antibodies generated in syngeneic hosts and SD. Isotype distribution was calculated using ODs of isotype-specific secondary antibodies relative to the OD of the total of OVA-specific antibodies as determined in ELISA.

Therefore, antibodies alone seemed to have no effect on the engraftment success of cells expressing a minor histocompatibility antigen. However, the presence of OVA-specific antibodies in the sera of the hosts demonstrates that the inoculated OVA-expressing iPSCs were immunogenic and able to induce an antibody response.

Moreover, the host serum was analyzed for the distribution of antibody isotypes using isotype-specific secondary antibodies in ELISAs. The major part of OVA-specific antibodies in the sera of 129/Sv mice, that received iPSCs for transplantation, consisted of IgG1 and IgG2b isotypes. The isotype distribution in these sera was similar to control sera of animals immunized with recombinant OVA protein. In contrast, in sera of C57Bl/6 mice, inoculated with RMA OVA cells, lower amounts of the IgG1 isotype were detected (Figure 32 B). The isotype distribution demonstrated that a class switch occurred in B cells. Since the OVA protein represents a thymus-dependent antigen, B cells need the interaction with antigen-specific $CD4^+$ T helper cells for the class switch. Thus, albeit the iPSCs inhibited T cell proliferation *in vitro* they became immunogenic *in vivo*.

5 Discussion

5.1 MHC class I expression in PSCs

As mentioned earlier, MHC mismatch represents a major immunological hurdle for transplantations. Therefore, the expression of these molecules on different pluripotent stem cell (PSC) lines was determined by qPCR and flow cytometry. In accordance with previously reported findings no cell surface expression MHC class I molecules on ESCs, derived from 4 different mouse strains (FVB, 129/Sv, C57Bl/6 and Stra8-eGFP/Rosa26 mice) was detected in flow cytometry (Abdullah et al, 2007; Magliocca et al, 2006; Tian et al, 1997). Furthermore, three iPSC lines (TTF-iPSCs derived from tail-tip fibroblasts of 129/Sv mice as well as iPSCs derived from 129/Sv and C57Bl/6 MEFs) and maGSCs derived from 4 different mouse strains (FVB, 129/Sv, C57Bl/6 and Stra8-eGFP/Rosa26 mice) were negative for the expression of MHC class I molecules. Thus, lack of MHC class I molecules in flow cytometry is a common feature of murine PSCs and not restricted to ESCs.

Despite their negativity for MHC class I molecules in flow cytometry, low amounts of *H2D, H2K* and *β2m* mRNAs were detectable in all analyzed murine PSC lines. Suarez-Alvarez et al. reported that *β2m* transcripts were not detectable in the human ESC line Shef-1 and the human iPSC line MSUH-002 and concluded that a lack of *β2m* in these cells might limit the expression of MHC class I molecules on the cell surface (Suarez-Alvarez et al, 2010). However, that seems to be not the case in the different murine PSC lines analyzed in this study. Furthermore, results of our group, regarding MHC class I gene expression, revealed that *β2m* transcripts were readily detectable in six different human iPSC lines and the hESC line H9 (Hamann, 2012). Therefore, lack of *β2m* mRNA expression is not a common feature of human PSC lines and seems to be no species-specific difference.

Moreover, the MHC class I gene expression upon IFNγ stimulation was analyzed in different PSC lines. Elevated levels of *H2D, H2K* and *β2m* transcripts were detected in the majority of the analyzed PSCs. However, not all analyzed PSC lines responded to IFNγ stimulation with increased MHC class I gene expression. *H2D* and *β2m* mRNA amounts were not increased in ESCs and maGSCs derived from Stra8 mice. In addition, no increased *H2D* and *H2K* transcript levels were found in ESCs derived from C57Bl/6 mice. Abdullah et al. reported that the expression of MHC class I heavy chain and *β2m* transcripts increased following stimulation with IFNγ (20 ng/ml; 48 hrs) in the CGR8 ESC line (Abdullah et al, 2007). Moreover, it was reported that MHC class I molecules were inducible on the undifferentiated RW-4 mESC line (Bonde & Zavazava, 2006). However, the cell surface expression of MHC class I molecules did not increase upon IFNγ

stimulation in two other studies (Nussbaum et al, 2007; Tian et al, 1997). The results demonstrate that variations between different PSC lines (also within one species) exist, providing a possible explanation for the contradicting results published so far. Notably, even the very low cell surface expression of MHC class I molecules is sufficient for recognition by activated CTLs (Abdullah et al, 2007; Dressel et al, 2009).

5.2 Antigen processing is impaired in PSCs

Antigen processing and its presentation via the MHC class I pathway are associated with the cell surface expression of MHC class I molecules and largely defines the susceptibility of cells to the cytotoxicity of CTLs. In order to analyze the ability of PSCs to process and present intracellular antigens, an Ovalbumin (OVA) expression construct as endogenously expressed model antigen was introduced into different PSC types. CTLs derived from transgenic OT-I mice, which express a T cell receptor (TCR) that is specific for the OVA-derived SIINFEKL peptide in a MHC class I context, were used as effector cells. Their ability to kill OVA-expressing PSCs was used as read out for the ability of PSCs to present OVA-derived peptides. The functionality of the experimental set up was demonstrated using OVA-expressing RMA target cells as positive control. Indeed RMA OVA cells were efficiently killed by OT-I CTLs, even more efficiently than SIINFEKL-pulsed wt RMA cells that served as standard positive control. Western blot analyses and flow cytometry revealed that the RMA OVA clone expressed higher amounts of the OVA-eGFP transgene than the majority of tested PSC clones. Therefore, one could argue that the OVA-expressing RMA clone was killed by peptide-specific CTLs to higher extend due to higher OVA expression. However, the flow cytometric analyses showed that the MPI-II OVA #1 clone expressed similar OVA levels to the RMA OVA clone, which did not result in a higher susceptibility to the killing of peptide-specific CTLs. Moreover, the MPI-II OVA #1 clone was not lysed in a higher extend as the MPI-II OVA #4 clone which expressed lower amounts of OVA-eGFP. Therefore, the possibility that a lower occurrence of specific peptides combined with the limitation of weak MHC class I molecule expression in PSCs limited the read out of this assay is unlikely. This conclusion was supported by results of qPCR. In all OVA-expressing clones the *OVA-eGFP* gene was highly expressed (with Ct values of 22 or less) and consistently higher than the housekeeping gene *Hprt*. Moreover, using CTLs to evaluate the cell surface expression of SIINFEKL/H2K^{b} ensures a highly sensitive read out for antigen presentation, since as few as about three MHC class I complexes presenting SIINFEKL are sufficient for CTLs to lyse this cell (Brower et al, 1994). The usage of CTLs derived from

transgenic OT-I mice ensures a high effector population since almost 100 % of these CTLs express a T cell receptor specific for the OVA-derived SIINFEKL peptide in a MHC class I/H2K^b context.

IPSCs as well as both ESC lines, which endogenously expressed OVA as model antigen, were apparently unable to process and present this antigen since they were resistant to killing by OVA (SIINFEKL)-specific CTLs. In contrast, OVA-expressing maGSCs were at least partially able to process and present OVA peptides since these cells were killed by cognate CTLs, albeit to a small extend. However, their antigen presenting capability was impaired, since they were not as susceptible to peptide-specific CTLs as wt maGSCs pulsed with SIINFEKL peptide. Since the MHC class I gene expression in maGSCs was similar to ESCs and iPSCs, and all PSC lines were negative for MHC class I molecules on the cell surface in flow cytometry, additional differences between these pluripotent cell types must exist. In addition to maGSCs, also ESCs and iPSCs were moderately killed by peptide-specific CTLs following incubation with exogenous SIINFEKL peptide, demonstrating that PSCs were not generally protected against the cytotoxic activity of CTLs.

To analyze possible reasons for the inability of PSCs to present antigens, the expression of genes encoding proteins of the peptide loading complex were analyzed. Transcripts of Calnexin, Calreticulin, TAPBP and ERp57 were detectable in all PSCs. Therefore, the failure in antigen presentation did not result from missing expression of these chaperones. These findings are partially contrary to those reported by Suarez-Alvarez et al. in the human ESC line Shef-1 and the human iPSC (hiPSC) line MSUH-002. They reported lacking gene expression of *TAPBP* and *Calr* in hESCs and lacking *Calr* gene expression in hiPSCs (Suarez-Alvarez et al, 2010). However, findings of our group demonstrated that *Calr* was expressed to a varying extend in six different hiPSC lines and the hESC line H9. Therefore, this variation likely depends on the specific cell line used for the gene expression studies and lack of expression of these genes is not a general feature of human PSCs. In accordance to the findings of Suerez-Alvarez et al., no *TAPBP* expression was detectable in the majority of these hiPSC lines. Only in H9 hESCs and IMR hiPSCs trace amounts of *TAPBP* transcripts were detected (Hamann, 2012). Whether or not the expression of *TAPBP* is generally different between murine and human PSCs has to be tested in further studies.

The *Tap1* gene was expressed only in small amounts compared to RMA cells and *Tap2* transcripts were virtually absent in all murine PSCs analyzed in this study. Due to the lack of suitable antibodies the qPCR results could not be verified on protein level. However, the apparent absence of *Tap2* expression could be a reason for the strong impairment of PSCs in antigen presentation, since the transport of peptides into the lumen of the ER is a crucial event in antigen presentation and critically depends on TAP2. Furthermore, the low *Tap* gene expression provides an explanation for undetectable MHC class I expression in general. It is known that TAP deficiency leads to loss of MHC class I surface expression, since the transport of newly synthesized MHC class

I molecules is not induced until peptide loading has occurred (Van Kaer et al, 1992). One way to prove this hypothesis, would be to reconstitute *Tap* expression in OVA-expressing PSCs and test their susceptibility to get killed by peptide-specific CTLs. However, three different OVA-expressing maGSC OVA clones (only two of which were shown) were at least slightly able to present antigens, suggesting that additional reasons for the inability of PSCs to present antigens might exist.

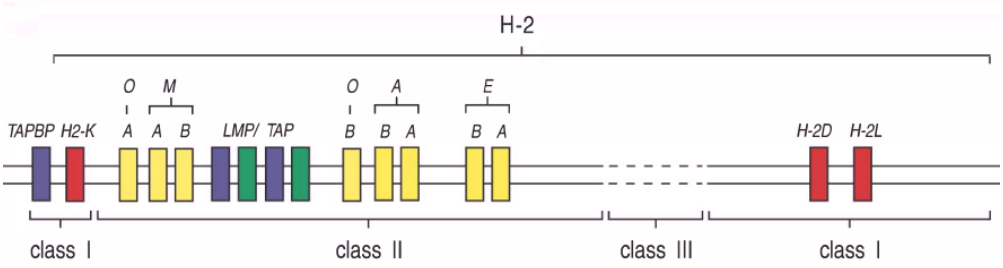

Figure 33: Location of the *Tap* and the *LMP* genes within the MHC class II locus
(adapted from (Murphy, 2012))

In addition to peptide loading complex related genes, the gene expression of the immuno-proteasomal subunits *LMP2* and *LMP7* was analyzed. *LMP2* transcripts were detected only in trace amounts and the gene of the immunoproteasomal subunit *LMP7* was not expressed in PSCs. Since the *Tap* genes and the *LMP* genes are located next to each other within the MHC class II locus, it seems possible that the whole gene locus is silenced in PSCs (Figure 33). However, it is unlikely that the missing LMP expression caused the inability of PSCs to present antigens. Even though it was shown that compared with the standard proteasome the immunoproteasome generates peptides favored for TAP and MHC class I binding in a higher frequency, a complete loss of antigen presentation due to a lack of LMP subunits was not reported (Fehling et al, 1994; Kincaid et al, 2012; Rock & Goldberg, 1999). Thus, the standard proteasome is able to generate peptides for presentation on MHC class I molecules. Furthermore, also other proteases, such as the IFNγ-inducible leucine aminopeptidase or the tripeptidyl peptidase II, contribute to the generation of peptides for antigen presentation (Beninga et al, 1998; Geier et al, 1999; Glas et al, 1998).

Since iPSCs might represent the pluripotent cell type with most therapeutic potential, their capability to process and present antigens was analyzed in more detail. The stimulation with IFNγ had no impact on the ability of iPSCs to present antigens. Following 48 hrs of IFNγ stimulation no increased lysis of OVA-expressing iPSCs exposed to OT-I CTLs was detectable. Moreover, the MHC class I surface expression was not increased. These findings are in accordance with previous studies regarding ESCs, in which surface expression of MHC class I molecules did not change upon

IFNγ stimulation (Abdullah et al, 2007; Nussbaum et al, 2007; Tian et al, 1997). However, the expression of MHC class I genes in TTF-iPSCs was enhanced upon IFNγ stimulation but did not result in enhanced cell surface expression of MHC class I molecules. This finding suggests that other reasons, additional to low gene expression, must be responsible for the low surface expression of MHC class I molecules. The low *Tap* expression is one possible explanation and could have contributed to the finding that the expression of MHC class I molecules did not increase on the cell surface of TTF-iPSCs following IFNγ stimulation.

Using formation of embryoid bodies (EBs), the impact of differentiation on the ability of PSCs to present antigens should be determined. EB formation, using the hanging drop method, resembles aspects of embryonic development. The formed cellular aggregates spontaneously differentiate along the three germ lineages and cells with origin of endoderm, ectoderm, and mesoderm arise (Keller, 1995; Martin & Evans, 1975). However, following 14 days of differentiation the expression od the OVA transgene got almost completely lost in PSCs. This most likely resulted from extensive epigenetic changes during the differentiation process, resulting in silencing of the genomic loci in which the OVA-eGFP transgene had integrated. To overcome this problem, in future experiments the transgene would have to be inserted by homologous recombination into a genomic locus, known to retain transcriptional activity after PSC differentiation. Another possibility would be to express the transgene without integration into the genome, using a self-replicating episomal vector.

5.3 Expression of proteins inhibiting CTL-mediated cytotoxicity

The results of the ^{51}chromium release assays demonstrated that the investigated PSC lines were only susceptible to CTL-mediated lysis, when they were incubated with exogenous SIINFEKL peptide. Therefore, the inability of CTLs to lyse OVA-expressing PSCs must result from the inability of PSCs to present antigens. In contrast, it has been reported that GGR8 mESCs presented viral epitopes to CTLs upon infection with the LCM virus and were resistant to peptide-specific CTLs, due to the expression of Serpin 6 (SPI-6) (Abdullah et al, 2007). SPI-6 is a potent inhibitor of granzyme B, thereby blocking the granule exocytosis pathway that enables NK cells and CTLs to lyse target cells (Medema et al, 2001a). To investigate, whether this is a common mechanism of mESCs, maGSCs and iPSCs to evade CTL-mediated cytotoxicity, the *SPI-6* gene expression in the different PSC lines was analyzed. However, only trace amounts of *SPI-6* transcripts were detected in all PSCs. Furthermore, in previous studies of our group no SPI-6 protein was detectable in the cell lysate of a variety of murine PSCs (Dressel et al, 2009; Dressel et al, 2010). Therefore, in the

PSC lines analyzed in this study, SPI-6 is unlikely to be the mediator of cytotoxicity suppression. The reason for this discrepancy is unknown, but may largely depend on cell culture conditions and particularly on the specific cell lines used for the investigations. Moreover, viral infection of ESCs could have contributed to changes in their immunological properties and hence, do not resemble conditions which are expected upon transplantation of those cells. Thus, the endogenously expressed model antigen OVA used in this thesis is more suitable to investigate the immunogenicity of PSCs in transplantation studies.

Cathepsin B (CtsB) is another protein, known to inhibit CTL-mediated cytotoxicity. It inhibits the pore-forming activity of perforin (see 1.3). *CtsB* transcripts were found in all analyzed PSCs and also mature CtsB protein in all PSC lysates. However, CtsB expression was detected to similar extends in RMA cells, which were efficiently killed. Furthermore, also PSCs pulsed with the OVA-derived SIINFEKL peptides were moderately killed by peptide-specific CTLs. Therefore, CtsB expression apparently did not render the analyzed PSC lines resistant to CTL-mediated cytotoxicity.

5.4 Immunogenicity of PSCs

5.4.1 PSCs suppress T cell proliferation *in vitro*

In co-culture assays with splenocytes derived from OT-I mice, OVA-expressing PSCs completely failed to induce the proliferation of naive antigen-specific $CD8^+$ T cells, despite addition of the cytokine IL-2. In contrast, OVA-expressing RMA cells efficiently induced proliferation of antigen-specific $CD8^+$ T cells. This finding is in accordance with the previous finding that PSCs are unable to present antigens in context of MHC class I molecules since signaling from the TCR detecting its specific peptide in MHC class I context is crucial for the activation of T cells. Nevertheless, it was analyzed whether a lack of co-stimulatory signals could contribute to lacking T cell proliferation. Activation of T cells requires signals from both, the TCR and from co-stimulatory molecules. It was shown, that T cells stimulated by TCR without associated co-stimulation become anergic, resulting in unresponsiveness and lacking proliferation (Schwartz, 1993). The co-stimulatory molecule CD86 was neither expressed on the cell surface nor on the transcript level. However, the co-stimulatory molecule CD80 was detected on the surface of ESCs, iPSCs and maGSCs. *CD80* transcripts were also detectable in all PSC lines. The expression of co-stimulatory molecules in PSCs was even higher than in RMA cells and antigen-specific $CD8^+$ T cells which were cultured together with RMA OVA cells were efficiently activated. Thus, the failure of PSCs to stimulate T cell proliferation directly was not due to missing expression of co-stimulatory molecules on the cell surface. These

findings are contrary to studies, in which the immunogenicity of human ESCs was characterized. In one study the expression of CD80 and CD86 was very low and in two further studies it was reported to be completely absent (Deuse et al, 2011; Grinnemo et al, 2006; Li et al, 2004). At this time it remains to be determined whether this is a general difference between murine and human ESCs or whether it depends on the characteristics of the specific cell-lines that were analyzed.

More likely than by direct stimulation, antigen-specific $CD8^+$ T cells should have become activated by APCs via cross-presentation. When OVA-expressing PSCs die during culture, OVA protein is released and becomes accessible to APCs within the splenocyte fraction used in these assays. Therefore, T cells were expected to become activated by APCs, even when PSCs were not able to stimulate T cells directly. The APCs would take up the OVA protein, process it and subsequently present the resulting peptides on MHC class I complexes to $CD8^+$ T cells. In addition to cross-presentation, APCs would also present antigens to $CD4^+$ T cells via the MHC class II antigen presenting pathway (see 1.4.2). However, neither in co-culture with OVA-expressing PSCs nor in co-culture with OVA-expressing RMA cells the proliferation of $CD4^+$ T cells was induced. Since RMA lymphoma cells are very robust, only few cells die during culture and the resulting OVA amounts, accessible for APC might have been too low or absent. Furthermore, RMA cells are unable to stimulate $CD4^+$ T cells directly, since no MHC class II molecules are expressed on their cell surface, even upon IFNγ stimulation (Ossendorp et al, 1998).

To exclude the possibility, that the OVA amounts released by PSC were not sufficient for antigen-specific stimulation, defined amounts of recombinant OVA protein was added to the co-culture of PSCs and antigen-specific $CD4^+$ and $CD8^+$ T cells. Even under these conditions T cells failed to proliferate in the presence of PSCs. This result demonstrates that PSCs were not only unable to stimulate T cells directly but actively suppressed the activation of antigen-specific T cells.

The suppressive activity of PSCs could have been mediated by direct cell-cell contact or by the release of soluble substances. To address this question, PSCs were separated from splenocytes by a permeable membrane in co-culture assays. These membranes (with a pore size of 0.4 µm) were permeable for soluble molecules but not for cells. The findings of these assays suggest that soluble substance were not responsible for the suppressive effect of PSCs on T cell proliferation. Whereas the proliferation of $CD4^+$ and $CD8^+$ T cells cultured in direct contact to PSCs was completely inhibited, proliferation of $CD4^+$ and $CD8^+$ T cells separated from PSCs by the membrane was not. Furthermore, the culture of $CD4^+$ and $CD8^+$ T cells in medium conditioned by ESCs and maGSCs did not result in the suppression of T cell proliferation. However, it is also possible that soluble substances that inhibit T cell proliferation are released only, following an initializing signal mediated by cell-cell contact. A modification of the Transwell co-culture assay could answer this question in future experiments, using direct co-culture of PSCs and T cells and

additional T cells separated from both by the permeable membrane. If the proliferation of separated T cells is inhibited in this approach one can assume, that the direct interaction of PSCs and T cells induced the expression of soluble substances responsible for inhibition of separated T cells.

5.4.2 Expression of amino acid depleting enzymes

Several mechanisms have been reported, by which ESCs suppress T cell activation. The findings of the co-culture assays demonstrate that maGSC and iPSCs share this property with ESCs. Therefore, it was investigated whether one of the mechanisms reported for ESCs could be responsible for the immune-modulating activity of the different PSC lines which were analyzed in this study. It was reported that high expression of Arginase 1 results in depletion of L-arginine, thereby providing a mechanism in the human ESC lines HES-1 and HES-2 to suppress T cell activity (Yachimovich-Cohen et al, 2010). However, *Arg1* transcripts were completely absent in both analyzed murine ESC lines. Furthermore, no *Arg1* transcripts were detectable in the analyzed maGSC and iPSC lines. Thus, Arginase 1-mediated T cell suppression might be a mechanism specific for human ESCs.

Similar to Arg1, Indoleamine 2,3-dioxygenase (IDO) act on T cell activity by depletion of amino acids from their environment (Munn & Mellor, 2007). IDO catabolizes tryptophan and its up-regulation is associated with immune-escape mechanisms of several carcinomas (Brandacher et al, 2006; Ozaki et al, 1988; Pan et al, 2008; Witkiewicz et al, 2008). However, only low amounts of both, mRNA and protein, was expressed in all analyzed PSCs. Furthermore, in RMA cells similar amounts of IDO compared to PSCs were found. As mentioned before, RMA cells were not able to suppress T cell proliferation. Therefore, it is unlikely that expression of IDO alone is responsible for the suppression of T cell proliferation.

5.4.3 Expression of soluble factors

Koch et al. reported that the inhibitory effect of mESCs on T cell proliferation results from the release of TGFβ (Koch et al, 2008). Indeed, moderate amounts of *TGFβ* transcripts were detectable in all analyzed PSC lines. However, RMA cells possessed at least 3-fold higher transcript levels of TGFβ and were unable to inhibit T cell proliferation. Therefore, TGFβ expression was unlikely the reason for the suppressive activity of PSCs observed in co-culture assays. This conclusion is in accordance with a report of Han et al., in which TGFβ release was analyzed by

ELISA and it was concluded that TGFβ did not contribute to the immunosuppressive properties of mESCs and iPSCs (Han et al, 2011).

Similar results were obtained for the cytokine-like molecule Galectin-1 (Gal-1). So far the release of Gal-1 has not been analyzed for PSC-mediated immunosuppression but was reported to be expressed on a variety of tumors and associated with reduced infiltrating T cells (Chiang et al, 2008; Jung et al, 2007; Le et al, 2005; Saussez et al, 2007; Spano et al, 2010). Furthermore, albeit the underlying mechanisms are not completely understood, it was demonstrated that Gal-1 expression enables tumor cells to induce apoptosis in T cells (Cooper et al, 2010; Kovacs-Solyom et al, 2010). In order to investigate whether Gal-1 contributed to PSCs immunogenicity, the *Gal-1* expression was analyzed by qPCR. In all PSC lines high amounts of *Gal-1* transcripts were detected, especially in both maGSC lines. However, again the gene expression in RMA cells, unable to inhibit T cell proliferation, was even higher.

It was demonstrated, that secreted Semaphorin-3A (Sema-3A) has the capacity to inhibit the activity of T cells (Catalano et al, 2006). Indeed Sema-3A transcripts were found in all analyzed PSC lines but again also high levels in RMA cells which contradicts a possible role of Sema-3A in PSC-mediated T cell inhibition.

In summary, transcripts of all analyzed soluble substances were detected in the different PSC lines but also in RMA cells, suggesting that these substances are not responsible for PSC-mediated inhibition of T cell proliferation. In addition, the co-culture assays with PSCs and by a membrane separated T cells suggested that soluble substances did not mediate the observed immunosuppressive functions of PSCs. However, the gene expression studies are not sufficient to clearly demonstrate whether the investigated substances are the main actors in PSC-mediated T cell inhibition. It is possible that differences in the post-transcriptional regulation of these gene products exist between RMA cells and PSCs. Therefore, these studies were mainly performed to identify possible new candidates involved in inhibition of T cell function. Especially *Gal-1* was highly expressed in PSCs and was until now not associated with the immunogenicity of PSCs. Therefore, Gal-1 but also Sema-3A are interesting new candidates for further studies.

5.4.4 Expression of inhibitory ligands

Fas ligand expression represents a potent mechanism to induce apoptosis in Fas receptor bearing target cells (see 1.3). However, no Fas ligand expression was detected on the surface of all analyzed PSC lines, independent of their origin (129/Sv or C57Bl/6 mice). Thus, the results of flow cytometry suggest that the inhibition of T cell proliferation did not result from the induction of

apoptosis in T cells via Fas engagement. This conclusion is in accordance with the observation that the murine ESC lines HM1, CGR8 and αPIG44 were negative for FasL in flow cytometry (Frenzel et al, 2009). In addition, in human ESCs FasL was not detectable, neither on transcript level nor on the cell surface (Drukker et al, 2006; Grinnemo et al, 2006). In contrast, other groups reported that mESCs as well as rat ESC-like cells induce apoptosis of NK cells or T cells by expression of Fas ligand (Bonde & Zavazava, 2006; Fandrich et al, 2002).

The gene expression of additional ligands, namely PD-L1, PD-L2, RCAS1, B7-H3 and B7-H4, was analyzed in order to investigate whether one of them contributed in PSC-mediated T cell inhibition. All these ligands were reported to inhibit T cell function but except PD-L1 none of these candidates was analyzed so far regarding its contribution to PSC-mediated immunosuppression. However, since previously reported mechanisms were unlikely to be responsible for the observations made in co-culture assays, new candidate genes involved in PSC's immunogenicity should been identified. Han et al. demonstrated by RT-PCR that the murine ESC line SCRC-1002 and MSCs contained *PD-L1* transcripts. However, anti-PD-L1 blocking antibodies failed to abrogate immunosuppressive activity of ESCs and MSCs (Han et al, 2011).

Nearly no transcripts of *PD-L1* were found in the different murine PSC lines analyzed in this thesis except for maGSC (C57Bl/6) cells, which expressed trace amounts of *PD-L1*. Furthermore, PSCs were negative for *PD-L2* transcripts. Hence, PD ligands are unlikely responsible for mediating immunosuppressive functions of PSCs. The expression of *RCAS1*, a tumor associated antigen known to induce apoptosis in T cells, was low in all analyzed PSCs. Furthermore, transcript amounts varied between different PSC origins. Especially in maGSCs and iPSCs derived from C57Bl/6 mice higher amounts of *RCAS1* transcripts were detectable compared with other PSC lines. However, RMA cells possessed similar amounts of *RCAS1* transcripts as PSCs, suggesting that RCAS1 expression was not responsible for the T cell suppressive effects observed in co-culture assays. Therefore, RCAS1 was not chosen for further investigations, but a contribution of this ligand to the immunosuppressive activity of PSCs cannot generally be excluded.

In contrast, in all PSC lines high levels of *B7-H3* transcripts were detected, whereas no *B7-H3* transcripts were detected in RMA cells. Therefore, the contribution of the B7-H3 ligand to PSC-mediated T cell inhibition was further analyzed. However, despite high transcript levels no B7-H3 ligands on the cell surface of PSCs were detected by flow cytometry. These data suggests, that B7-H3 is post-transcriptionally regulated which was also concluded by Hofmeyer et al. before (Hofmeyer et al, 2008). Furthermore, the immunological role of B7-H3 remains controversial. It was shown, that B7-H3 inhibits T cell activation and high expression of B7-H3 is associated with immune evasion of a variety of tumors (Leitner et al, 2009; Prasad et al, 2004; Zang et al, 2010; Zang et al, 2007). In contrast, it was reported that B7-H3 expression stimulates T cell responses

(Chapoval et al, 2001; Luo et al, 2004). In one study it was reported that B7-H3 binds to the Triggering receptor expressed on myeloid cells (TREM)-like transcript 2 (TREML2), which is expressed on $CD8^+$ T cells and on activated $CD4^+$ T cells. The interaction with B7-H3 expressing cells enhanced IFNγ production and proliferation of $CD8^+$ T cells and the addition of an anti-B7-H3 antibody suppressed this stimulating activity (Hashiguchi et al, 2008). Although B7-H3 was not detected on the surface of PSCs, its expression could have been induced in PSCs upon co-culture. Hence, the same anti-B7-H3 antibody was used in co-culture experiments to block possible interactions between PSCs and splenocytes via B7-H3. However, an effect on T cell activation was not observed in these blocking experiments. The proliferation of T cells was neither enhanced nor reduced. Therefore, the data suggest that B7-H3 is not responsible for PSC-mediated immunosuppression, despite high levels of B7-H3 transcripts in PSCs. Transcripts of B7-H4, another member of the B7 family, were only expressed in trace amounts in PSCs. In iPSC (C57Bl/6) and maGSC (129/Sv) cells B7-H4 transcripts were completely absent. Thus, B7-H4 is unlikely the mediator of T cell inhibition observed in co-culture assays.

The findings of the co-culture assays demonstrate that ESCs, iPSCs and maGSCs have a suppressive effect on T cell proliferation, as previously reported for ESCs. S. Kadereit and A. Trounson assumed that PSCs become susceptible to OT-I CTLs due to the expression of antigen-specific TCRs on 100 % of this effector population, thereby possibly overriding inhibitory effects of ESCs (Kadereit & Trounson, 2011). However, also allogeneic CTLs, representing an effector population with a lower number of specific T cells, were able to kill PSCs (unpublished data). Furthermore, despite an equal effector to target ratio to ^{51}chromium release assays in the co-culture experiments, all analyzed PSC lines possessed the ability to suppress the proliferation of OT-I and OT-II T cells *in vitro*. Moreover, the findings of ^{51}chromium release assays demonstrated that PSCs were not able to escape CTL-mediated cytotoxicity after incubation with SIINFEKL peptides. Therefore, an immune privilege of PSCs rather results from their ability to suppress activation of T cells than to suppress their cytotoxic activity by expression of SPI-6 or CtsB. Although, the fundamental mechanism of immunosuppressive activity remains controversial, high expression of new candidate-genes like *Gal-1* and *B7-H3* was shown, which might contribute to PSC-mediated immunosuppressive function.

5.5 Expression of mHC antigens decrease engraftment in syngeneic hosts

Immune rejection and teratoma growth are the major hurdles that have to be overcome, before clinical implementation of iPSC-derived grafts can be established. Although iPSCs could

theoretically be transplanted in an autologous setting, which would be less immunogenic than transplantation of ESC-derived allografts, the presence of minor histocompatibility antigens is possible. The expression of differentiation antigens or any other proteins specifically expressed only during embryogenesis could elicit immune rejection of those cells. Since such antigens are unlikely to be encountered by the immune system before, no tolerance towards these antigens is established. An example for such an antigen is Oct4, a key factor of pluripotency. Dhodapkar et al. detected OCT4-specific T cells in the majority (more than 80 %) of healthy human donors. The majority of these T cells were CD4 positive and specific for highly conserved sequences of Oct4 (Dhodapkar et al, 2010).

In addition, the risk of teratoma formation in the recipient rises in autologous transplantations due to diminished immune surveillance. Using OVA, expressed in iPSCs as model antigen, the outcome of syngeneic transplanted iPSCs expressing a defined mHC antigen was further analyzed by teratoma growth assays. The wt iPSCs engrafted in about 90 % (n=12) of syngeneic hosts and formed rapidly growing teratomas. Despite possessing a male phenotype, the majority of iPSCs successfully engrafted also in female hosts. This is most likely due to low expression of Y-chromosome-derived genes during early embryogenesis. Most of the Y-chromosomal transcription is firstly initialized upon forming of the bipotential gonads in the embryo e. g. the SRY (sex determining region of Y) gene (Gilbert, 2003). Since iPSCs largely resemble the epigenetic state of ESCs (Li et al, 2011) it is likely that these genes are also barely expressed in iPSCs.

The transplantation of two OVA-expressing iPSC clones resulted in rejection in 65 % (13/20) of the hosts. Therefore, the expression of a mHC antigen was largely sufficient to reject these cells. Moreover, tumor growth of OVA-expressing iPSCs was diminished in all immunocompetent animals, since tumors remained significantly smaller in size and weight, compared to tumors formed after inoculation of wt iPSCs. Interestingly, only female hosts rejected inoculated iPSC OVA-derived tumor cells completely within 100 days. Therefore, additional, Y-chromosome-derived mHC antigens seemed to have enhanced the rejection process. The pluripotency and viability of iPSCs and iPSC OVA cells was demonstrated using teratoma growth assays in immunodeficient mice that were performed in parallel. In 100 % (9/9) of inoculated immunodeficient hosts rapidly growing tumors were detected. In contrast to immunocompetent hosts, the tumors formed after inoculation of wt and OVA-expressing iPSCs in immunodeficient hosts, did not differ in size and weight. Immunohistochemistry of dissected tumor tissue further demonstrated the viability of tumor cells, since a large part was positive for the proliferation marker Ki67. In summary, these findings demonstrate that the inability of iPSC OVA clones to engraft in the majority of hosts or the iPSC OVA-derived tumors remained smaller, respectively, was not due to reduced viability of these cells. Therefore, the immunogenicity of these cells

increased upon expression of a mHC antigen and the recipient's immune system was able to impede tumor growth or even reject these cells. The immunohistochemical stainings furthermore demonstrated the recruitment of different leukocyte populations like T cells, B cells and macrophages to the tumor tissue. These findings demonstrate that iPSC derived tumors are indeed immunogenic, what was also shown by flow cytometric analysis of tumor cells.

In vitro studies with host derived splenocytes and RMA OVA cells as target cell line suggested that the rejection of iPSC OVA-derived tumors depended on the cytotoxic activity of antigen-specific T cells. Especially hosts which rejected iPSC OVA-derived tumors contained $CD8^+$ T cells specific for OVA-derived antigens and furthermore, these $CD8^+$ T cells were able to kill cells presenting OVA-derived antigens. Therefore, antigen-specific T cells arose in syngeneic hosts and became properly activated due to mHC expression. In contrast, pluripotent OVA-expressing iPSCs were not killed by peptide-specific CTLs *in vitro*. This finding suggests that during differentiation into teratoma cells *in vivo,* at least at a specific stage of differentiation, the ability of iPSC-derived cells to present antigens increased. Since iPSCs differentiated *in vitro* into EBs virtually lost their transgene expression after 14 days, the ability of iPSCs to present OVA-derived antigens might be only possible during a limited period of time during differentiation (Figure 34). This hypothesis is supported by the finding of Abdullah et al. that the murine ESC line CGR8 only transiently express MHC class I molecules at days four to six after induction of differentiation and decline back to undetectable levels thereafter (Abdullah et al, 2007).

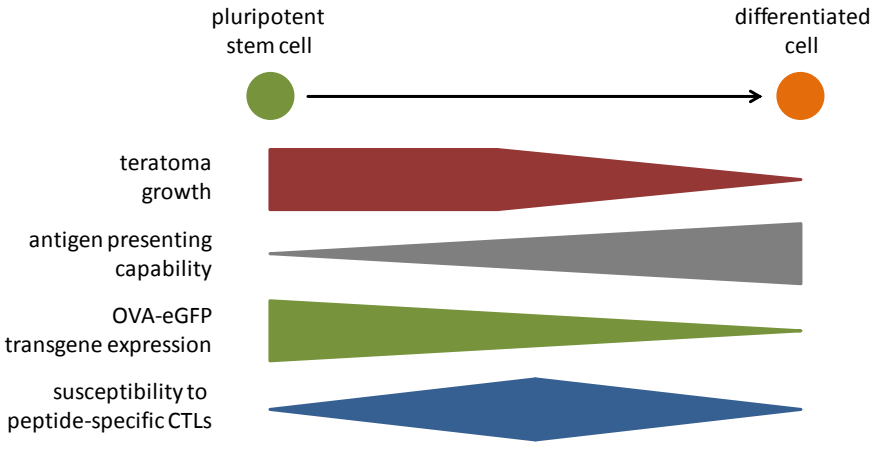

Figure 34: Schematic overview of the immunogenicity of iPSCs over the course of time following transplantation
(adapted from (Dressel, 2011))

The sera of host animals were analyzed for OVA-specific antibodies by ELISA. Indeed, the sera of animals that were inoculated with OVA-expressing iPSCs contained antibodies against OVA,

independent of teratoma formation or rejection. The titer of OVA-specific antibodies was similar to that, found in serum of animals immunized at least four times with recombinant OVA protein. This finding demonstrates that iPSCs or their derivatives, expressing a mHC antigen, are immunogenic and able to induce an antibody response in the host. The majority of detected antibodies had an IgG1 or an IgG2b isotype. The occurrence of these antibody isotypes demonstrates that a class switch occurred in peptide-specific B cells. Since the OVA protein is a thymus-dependent antigen, B cells need the interaction with antigen-specific $CD4^+$ T cells to induce the class switch. Therefore, not only antigen-specific B cells but also antigen-specific $CD4^+$ T cells became properly activated in syngeneic hosts upon transplantation of iPSCs or iPSC-derived cells expressing OVA as single mHC antigen. The data suggest that the inhibitory effects of iPSCs on the activation of $CD4^+$ T cells, observed in co-culture experiments, are only locally and transiently and get lost upon differentiation of iPSCs. It remains unclear whether antibody generation contributes to the rejection of iPSC OVA cell derived tumors, although the findings demonstrate that OVA-specific antibodies alone are not sufficient to induce immune rejection of iPSC OVA derived tumor cells. In summary, despite the immunosuppressive effects of iPSCs observed in co-culture assays *in vitro*, iPSCs or their derivatives which expressed a mHC antigen were able to induce an immune resonse *in vivo*.

The reasons for spontaneous engraftment of OVA-expressing cells in some animals remain unclear, but may largely depend on kind and progress of differentiation within the tumor as well as the immune system of the host. Nevertheless, these data demonstrate that a single mHC antigen is sufficient to frequently induce immune rejection in syngeneic hosts and rejection of these cells likely depends on CTLs. However, rejection must not occur and might be avoidable by immunomodulation of the recipient when differentiated cells are transplanted.

6 Summary and conclusions

PSC-derived transplants could be a promising tool in cell replacement therapies in order to treat a broad variety of diseases associated with irreversible tissue injury. However, especially immunological issues have to be considered before stem cell transplantations could be successfully implemented into clinical applications. In this thesis the different pluripotent stem cell types ESCs, iPSCs and maGSCs were further characterized for their immunological properties and the immunogenic potential of iPSCs expressing a mHC antigen was unveiled.

MHC class I molecules were undetectable by flow cytometry on all analyzed murine PSCs, suggesting that this is a common feature of murine PSCs. However, despite undetectable expression of MHC class I molecules on the cell surface, after exogenous loading with the SIINFEKL peptide all PSC lines were susceptible to peptide-specific CTLs, demonstrating that minor amounts of MHC class I molecules exist on the cell surface of PSCs. Although, the expression of MHC class I genes was low, the qPCR results demonstrated that the low MHC class I cell surface expression is not due to a lack of MHC class I gene transcription. Therefore, additional reasons for the low cell surface expression of MHC class I molecules must exist. The results of ^{51}chromium release assays demonstrated that murine ESCs and iPSCs were unable to process and present antigens derived from an endogenously expressed protein (OVA). In contrast, the analyzed maGSC line was able to process and present antigens to a small extent. However, maGSCs were impaired in their ability to present antigens, since they were not as susceptible to the killing of peptide-specific CTLs as maGSCs which were exogenously loaded with the SIINFEKL peptide. Gene expression studies, analyzing the transcript amounts of peptide loading complex member genes, revealed that the *Tap1* gene was only low expressed and *Tap2* transcripts were virtually absent in PSCs. This finding not only provides a possible explanation for the inability of PSCs to process and present antigens, but also for the low expression of MHC class I molecules on their cell surface since successful peptide loading is crucial for the transport of these complexes to the cell surface. However, despite nearly lacking *Tap2* gene expression the analyzed maGSC OVA clones were at least slightly lysed by OVA-specific CTLs, suggesting that additional reasons for the impairment in antigen presentation of PSCs might exist.

Moreover, PSCs were not only unable to stimulate the proliferation of naive peptide-specific T cells directly but actively suppressed T cell activation *in vitro* and this suppressive mechanism is mediated by an at least initial cell-cell contact of PSCs and T cells. The contribution of previously reported mechanisms mediating such an immunosuppressive activity of ESCs was not confirmed for the different analyzed PSC lines. Thus, the mechanism which enables PSCs to suppress T cell proliferation remains unclear.

IPSCs probably have the highest therapeutic potential, since autologous cells for transplantation are available for every patient. Moreover, their use is not restricted due to ethical concerns. Therefore, this PSC type and particularly the impact of mHC expression on the outcome of transplantation was analyzed in more detail. The findings of the transplantation studies in immunocompetent syngeneic hosts demonstrated that mHC antigens, endogenously expressed in iPSCs, are indeed sufficient to induce immune rejection of these cells or at least significantly decrease teratoma growth. The rejection depended mainly on the cytotoxicity of peptide-specific CTLs, which were found in all hosts which rejected OVA-expressing iPSC transplants. Moreover, these mHC-expressing iPSCs were able to induce an antibody response against the model antigen OVA in the host. OVA-specific antibodies were generated to similar extends in animals which were immunized at least four times with OVA protein. The isotype distribution of these antibodies showed high levels of IgG1 and IgG2b antibodies, demonstrating that an immunoglobulin (Ig) class switch occurred in OVA-specific B cells. Consequently, also active OVA-specific $CD4^+$ T cells must have arisen in the host, since interaction with those cells is crucial to induce the Ig class switch in B cells specific for a protein-derived antigen. In summary, these data demonstrate that iPSCs expressing a mHC antigen are indeed immunogenic.

7 References

Abdullah Z, Saric T, Kashkar H, Baschuk N, Yazdanpanah B, Fleischmann BK, Hescheler J, Kronke M, Utermohlen O (2007) Serpin-6 expression protects embryonic stem cells from lysis by antigen-specific CTL. *J Immunol* **178:** 3390-3399

Ackerman AL, Giodini A, Cresswell P (2006) A role for the endoplasmic reticulum protein retrotranslocation machinery during crosspresentation by dendritic cells. *Immunity* **25:** 607-617

Balaji KN, Schaschke N, Machleidt W, Catalfamo M, Henkart PA (2002) Surface cathepsin B protects cytotoxic lymphocytes from self-destruction after degranulation. *J Exp Med* **196:** 493-503

Barnden MJ, Allison J, Heath WR, Carbone FR (1998) Defective TCR expression in transgenic mice constructed using cDNA-based alpha- and beta-chain genes under the control of heterologous regulatory elements. *Immunol Cell Biol* **76:** 34-40

Beninga J, Rock KL, Goldberg AL (1998) Interferon-gamma can stimulate post-proteasomal trimming of the N terminus of an antigenic peptide by inducing leucine aminopeptidase. *J Biol Chem* **273:** 18734-18742

Birnboim HC, Doly J (1979) A rapid alkaline extraction procedure for screening recombinant plasmid DNA. *Nucleic Acids Res* **7:** 1513-1523

Bonde S, Zavazava N (2006) Immunogenicity and engraftment of mouse embryonic stem cells in allogeneic recipients. *Stem Cells* **24:** 2192-2201

Boyd AS, Wood KJ (2009) Variation in MHC expression between undifferentiated mouse ES cells and ES cell-derived insulin-producing cell clusters. *Transplantation* **87:** 1300-1304

Bradley A, Evans M, Kaufman MH, Robertson E (1984) Formation of germ-line chimaeras from embryo-derived teratocarcinoma cell lines. *Nature* **309:** 255-256

Brandacher G, Perathoner A, Ladurner R, Schneeberger S, Obrist P, Winkler C, Werner ER, Werner-Felmayer G, Weiss HG, Gobel G, Margreiter R, Konigsrainer A, Fuchs D, Amberger A (2006) Prognostic value of indoleamine 2,3-dioxygenase expression in colorectal cancer: effect on tumor-infiltrating T cells. *Clin Cancer Res* **12:** 1144-1151

Brivanlou AH, Gage FH, Jaenisch R, Jessell T, Melton D, Rossant J (2003) Stem cells. Setting standards for human embryonic stem cells. *Science* **300:** 913-916

Bronte V, Zanovello P (2005) Regulation of immune responses by L-arginine metabolism. *Nat Rev Immunol* **5:** 641-654

Brower RC, England R, Takeshita T, Kozlowski S, Margulies DH, Berzofsky JA, Delisi C (1994) Minimal requirements for peptide mediated activation of CD8+ CTL. *Mol Immunol* **31:** 1285-1293

Brunlid G, Pruszak J, Holmes B, Isacson O, Sonntag KC (2007) Immature and neurally differentiated mouse embryonic stem cells do not express a functional Fas/Fas ligand system. *Stem Cells* **25:** 2551-2558

Catalano A, Caprari P, Moretti S, Faronato M, Tamagnone L, Procopio A (2006) Semaphorin-3A is expressed by tumor cells and alters T-cell signal transduction and function. *Blood* **107:** 3321-3329

Chapoval AI, Ni J, Lau JS, Wilcox RA, Flies DB, Liu D, Dong H, Sica GL, Zhu G, Tamada K, Chen L (2001) B7-H3: a costimulatory molecule for T cell activation and IFN-gamma production. *Nat Immunol* **2:** 269-274

Cheng IF, Kaiser D, Huebscher D, Hasenfuss G, Guan K, Schafer K (2012) Differentiation of multipotent adult germline stem cells derived from mouse testis into functional endothelial cells. *J Vasc Res* **49:** 207-220

Chiang WF, Liu SY, Fang LY, Lin CN, Wu MH, Chen YC, Chen YL, Jin YT (2008) Overexpression of galectin-1 at the tumor invasion front is associated with poor prognosis in early-stage oral squamous cell carcinoma. *Oral Oncol* **44:** 325-334

Colbert JD, Matthews SP, Miller G, Watts C (2009) Diverse regulatory roles for lysosomal proteases in the immune response. *Eur J Immunol* **39:** 2955-2965

Coligan JE (2005) *Short Protocols in Immunology*: John Wiley & Sons.

Cooper D, Ilarregui JM, Pesoa SA, Croci DO, Perretti M, Rabinovich GA (2010) Multiple functional targets of the immunoregulatory activity of galectin-1: Control of immune cell trafficking, dendritic cell physiology, and T-cell fate. *Methods Enzymol* **480:** 199-244

Cresswell P (1996) Invariant chain structure and MHC class II function. *Cell* **84:** 505-507

Crotzer VL, Blum JS (2009) Autophagy and its role in MHC-mediated antigen presentation. *J Immunol* **182:** 3335-3341

Davidson HW, Reid PA, Lanzavecchia A, Watts C (1991) Processed antigen binds to newly synthesized MHC class II molecules in antigen-specific B lymphocytes. *Cell* **67:** 105-116

Denzin LK, Cresswell P (1995) HLA-DM induces CLIP dissociation from MHC class II alpha beta dimers and facilitates peptide loading. *Cell* **82:** 155-165

DESA/PD. (2011) World Population Prospects: The 2010 Revision, Press Release (3 May 2011): "World Population to reach 10 billion by 2100 if Fertility in all Countries Converges to Replacement Level". United Nations, Department of Economic and Social Affairs, Population Division.

Deuse T, Seifert M, Tyan D, Tsao PS, Hua X, Velden J, Eiermann T, Volk HD, Reichenspurner H, Robbins RC, Schrepfer S (2011) Immunobiology of naive and genetically modified HLA-class-I-knockdown human embryonic stem cells. *J Cell Sci* **124:** 3029-3037

Dhodapkar KM, Feldman D, Matthews P, Radfar S, Pickering R, Turkula S, Zebroski H, Dhodapkar MV (2010) Natural immunity to pluripotency antigen OCT4 in humans. *Proc Natl Acad Sci U S A* **107:** 8718-8723

Dihazi H, Dihazi GH, Nolte J, Meyer S, Jahn O, Muller GA, Engel W (2009) Multipotent adult germline stem cells and embryonic stem cells: comparative proteomic approach. *J Proteome Res* **8:** 5497-5510

Dong H, Zhu G, Tamada K, Chen L (1999) B7-H1, a third member of the B7 family, co-stimulates T-cell proliferation and interleukin-10 secretion. *Nat Med* **5:** 1365-1369

Dressel R (2011) Effects of histocompatibility and host immune responses on the tumorigenicity of pluripotent stem cells. *Semin Immunopathol* **33:** 573-591

Dressel R, Guan K, Nolte J, Elsner L, Monecke S, Nayernia K, Hasenfuss G, Engel W (2009) Multipotent adult germ-line stem cells, like other pluripotent stem cells, can be killed by cytotoxic T lymphocytes despite low expression of major histocompatibility complex class I molecules. *Biol Direct* **4:** 31

Dressel R, Nolte J, Elsner L, Novota P, Guan K, Streckfuss-Bomeke K, Hasenfuss G, Jaenisch R, Engel W (2010) Pluripotent stem cells are highly susceptible targets for syngeneic, allogeneic, and xenogeneic natural killer cells. *FASEB J* **24:** 2164-2177

Dressel R, Schindehutte J, Kuhlmann T, Elsner L, Novota P, Baier PC, Schillert A, Bickeboller H, Herrmann T, Trenkwalder C, Paulus W, Mansouri A (2008) The tumorigenicity of mouse embryonic stem cells and in vitro differentiated neuronal cells is controlled by the recipients' immune response. *PLoS One* **3:** e2622

Drukker M, Katchman H, Katz G, Even-Tov Friedman S, Shezen E, Hornstein E, Mandelboim O, Reisner Y, Benvenisty N (2006) Human embryonic stem cells and their differentiated derivatives are less susceptible to immune rejection than adult cells. *Stem Cells* **24:** 221-229

Du C, Wang Y (2011) The immunoregulatory mechanisms of carcinoma for its survival and development. *J Exp Clin Cancer Res* **30:** 12

Ehring B, Meyer TH, Eckerskorn C, Lottspeich F, Tampe R (1996) Effects of major-histocompatibility-complex-encoded subunits on the peptidase and proteolytic activities of human 20S proteasomes. Cleavage of proteins and antigenic peptides. *Eur J Biochem* **235:** 404-415

Engelhard VH (1994) Structure of peptides associated with class I and class II MHC molecules. *Annu Rev Immunol* **12:** 181-207

Evans MJ, Kaufman MH (1981) Establishment in culture of pluripotential cells from mouse embryos. *Nature* **292:** 154-156

Fallarino F, Grohmann U, Vacca C, Bianchi R, Orabona C, Spreca A, Fioretti MC, Puccetti P (2002) T cell apoptosis by tryptophan catabolism. *Cell Death Differ* **9:** 1069-1077

Fandrich F, Lin X, Chai GX, Schulze M, Ganten D, Bader M, Holle J, Huang DS, Parwaresch R, Zavazava N, Binas B (2002) Preimplantation-stage stem cells induce long-term allogeneic graft acceptance without supplementary host conditioning. *Nat Med* **8:** 171-178

Fehling HJ, Swat W, Laplace C, Kuhn R, Rajewsky K, Muller U, von Boehmer H (1994) MHC class I expression in mice lacking the proteasome subunit LMP-7. *Science* **265:** 1234-1237

Ferguson TA, Griffith TS (1997) A vision of cell death: insights into immune privilege. *Immunol Rev* **156:** 167-184

Fischbach GD, Fischbach RL (2004) Stem cells: science, policy, and ethics. *J Clin Invest* **114:** 1364-1370

Frenzel LP, Abdullah Z, Kriegeskorte AK, Dieterich R, Lange N, Busch DH, Kronke M, Utermohlen O, Hescheler J, Saric T (2009) Role of natural-killer group 2 member D ligands and intercellular adhesion molecule 1 in natural killer cell-mediated lysis of murine embryonic stem cells and embryonic stem cell-derived cardiomyocytes. *Stem Cells* **27:** 307-316

Fukuda M, Tanaka A, Hamao A, Suzuki S, Kusama K, Sakashita H (2004) Expression of RCAS1 and its function in human squamous cell carcinoma of the oral cavity. *Oncol Rep* **12:** 259-267

Geier E, Pfeifer G, Wilm M, Lucchiari-Hartz M, Baumeister W, Eichmann K, Niedermann G (1999) A giant protease with potential to substitute for some functions of the proteasome. *Science* **283:** 978-981

Gilbert SF (2003) *Developmental Biology*, Seventh Edition edn. Sunderland, MA 01375 USA: Sinauer Associates Inc.

Glas R, Bogyo M, McMaster JS, Gaczynska M, Ploegh HL (1998) A proteolytic system that compensates for loss of proteasome function. *Nature* **392:** 618-622

Glaser T, Opitz T, Kischlat T, Konang R, Sasse P, Fleischmann BK, Engel W, Nayernia K, Brustle O (2008) Adult germ line stem cells as a source of functional neurons and glia. *Stem Cells* **26:** 2434-2443

Grandea AG, 3rd, Van Kaer L (2001) Tapasin: an ER chaperone that controls MHC class I assembly with peptide. *Trends Immunol* **22:** 194-199

Griffith TS, Ferguson TA (1997) The role of FasL-induced apoptosis in immune privilege. *Immunol Today* **18:** 240-244

Grinnemo KH, Kumagai-Braesch M, Mansson-Broberg A, Skottman H, Hao X, Siddiqui A, Andersson A, Stromberg AM, Lahesmaa R, Hovatta O, Sylven C, Corbascio M, Dellgren G (2006) Human embryonic stem cells are immunogenic in allogeneic and xenogeneic settings. *Reprod Biomed Online* **13:** 712-724

Guan K, Nayernia K, Maier LS, Wagner S, Dressel R, Lee JH, Nolte J, Wolf F, Li M, Engel W, Hasenfuss G (2006) Pluripotency of spermatogonial stem cells from adult mouse testis. *Nature* **440:** 1199-1203

Guan K, Wagner S, Unsold B, Maier LS, Kaiser D, Hemmerlein B, Nayernia K, Engel W, Hasenfuss G (2007) Generation of functional cardiomyocytes from adult mouse spermatogonial stem cells. *Circ Res* **100:** 1615-1625

Guermonprez P, Saveanu L, Kleijmeer M, Davoust J, Van Endert P, Amigorena S (2003) ER-phagosome fusion defines an MHC class I cross-presentation compartment in dendritic cells. *Nature* **425:** 397-402

Hamann C (2012) Expression profiling of genes involved in antigen presentation in human pluripotent stem cells. Master of Science Thesis, Department of Cellular and Molecular Immunology, Georg-August University, Göttingen

Han KH, Ro H, Hong JH, Lee EM, Cho B, Yeom HJ, Kim MG, Oh KH, Ahn C, Yang J (2011) Immunosuppressive mechanisms of embryonic stem cells and mesenchymal stem cells in alloimmune response. *Transpl Immunol* **25:** 7-15

Hashiguchi M, Kobori H, Ritprajak P, Kamimura Y, Kozono H, Azuma M (2008) Triggering receptor expressed on myeloid cell-like transcript 2 (TLT-2) is a counter-receptor for B7-H3 and enhances T cell responses. *Proc Natl Acad Sci U S A* **105:** 10495-10500

Hentze H, Soong PL, Wang ST, Phillips BW, Putti TC, Dunn NR (2009) Teratoma formation by human embryonic stem cells: evaluation of essential parameters for future safety studies. *Stem Cell Res* **2:** 198-210

Hofmeyer KA, Ray A, Zang X (2008) The contrasting role of B7-H3. *Proc Natl Acad Sci U S A* **105:** 10277-10278

Hogquist KA, Jameson SC, Heath WR, Howard JL, Bevan MJ, Carbone FR (1994) T cell receptor antagonist peptides induce positive selection. *Cell* **76:** 17-27

Houde M, Bertholet S, Gagnon E, Brunet S, Goyette G, Laplante A, Princiotta MF, Thibault P, Sacks D, Desjardins M (2003) Phagosomes are competent organelles for antigen cross-presentation. *Nature* **425:** 402-406

Iyer R, Jenkinson CP, Vockley JG, Kern RM, Grody WW, Cederbaum S (1998) The human arginases and arginase deficiency. *J Inherit Metab Dis* **21 Suppl 1:** 86-100

Jung EJ, Moon HG, Cho BI, Jeong CY, Joo YT, Lee YJ, Hong SC, Choi SK, Ha WS, Kim JW, Lee CW, Lee JS, Park ST (2007) Galectin-1 expression in cancer-associated stromal cells correlates tumor invasiveness and tumor progression in breast cancer. *Int J Cancer* **120:** 2331-2338

Kadereit S, Trounson A (2011) In vitro immunogenicity of undifferentiated pluripotent stem cells (PSC) and derived lineages. *Semin Immunopathol* **33:** 551-562

Kanatsu-Shinohara M, Inoue K, Lee J, Yoshimoto M, Ogonuki N, Miki H, Baba S, Kato T, Kazuki Y, Toyokuni S, Toyoshima M, Niwa O, Oshimura M, Heike T, Nakahata T, Ishino F, Ogura A, Shinohara T (2004) Generation of pluripotent stem cells from neonatal mouse testis. *Cell* **119:** 1001-1012

Kaufman DL, Evans GA (1990) Restriction endonuclease cleavage at the termini of PCR products. *Biotechniques* **9:** 304, 306

Keller GM (1995) In vitro differentiation of embryonic stem cells. *Curr Opin Cell Biol* **7:** 862-869

Khromov T, Pantakani DV, Nolte J, Wolf M, Dressel R, Engel W, Zechner U (2011) Global and gene-specific histone modification profiles of mouse multipotent adult germline stem cells. *Mol Hum Reprod* **17:** 166-174

Kincaid EZ, Che JW, York I, Escobar H, Reyes-Vargas E, Delgado JC, Welsh RM, Karow ML, Murphy AJ, Valenzuela DM, Yancopoulos GD, Rock KL (2012) Mice completely lacking immunoproteasomes show major changes in antigen presentation. *Nat Immunol* **13:** 129-135

Kisselev AF, Akopian TN, Woo KM, Goldberg AL (1999) The sizes of peptides generated from protein by mammalian 26 and 20 S proteasomes. Implications for understanding the degradative mechanism and antigen presentation. *J Biol Chem* **274:** 3363-3371

Koch CA, Geraldes P, Platt JL (2008) Immunosuppression by embryonic stem cells. *Stem Cells* **26:** 89-98

Kolossov E, Bostani T, Roell W, Breitbach M, Pillekamp F, Nygren JM, Sasse P, Rubenchik O, Fries JW, Wenzel D, Geisen C, Xia Y, Lu Z, Duan Y, Kettenhofen R, Jovinge S, Bloch W, Bohlen H, Welz A, Hescheler J, Jacobsen SE, Fleischmann BK (2006) Engraftment of engineered ES cell-derived cardiomyocytes but not BM cells restores contractile function to the infarcted myocardium. *J Exp Med* **203:** 2315-2327

Kovacs-Solyom F, Blasko A, Fajka-Boja R, Katona RL, Vegh L, Novak J, Szebeni GJ, Krenacs L, Uher F, Tubak V, Kiss R, Monostori E (2010) Mechanism of tumor cell-induced T-cell apoptosis mediated by galectin-1. *Immunol Lett* **127:** 108-118

Kovacsovics-Bankowski M, Rock KL (1995) A phagosome-to-cytosol pathway for exogenous antigens presented on MHC class I molecules. *Science* **267:** 243-246

Kropshofer H, Vogt AB, Moldenhauer G, Hammer J, Blum JS, Hammerling GJ (1996) Editing of the HLA-DR-peptide repertoire by HLA-DM. *EMBO J* **15:** 6144-6154

Lankat-Buttgereit B, Tampe R (2002) The transporter associated with antigen processing: function and implications in human diseases. *Physiol Rev* **82:** 187-204

Lawrenz B, Schiller H, Willbold E, Ruediger M, Muhs A, Esser S (2004) Highly sensitive biosafety model for stem-cell-derived grafts. *Cytotherapy* **6:** 212-222

Le QT, Shi G, Cao H, Nelson DW, Wang Y, Chen EY, Zhao S, Kong C, Richardson D, O'Byrne KJ, Giaccia AJ, Koong AC (2005) Galectin-1: a link between tumor hypoxia and tumor immune privilege. *J Clin Oncol* **23:** 8932-8941

Lee J, Kim HK, Rho JY, Han YM, Kim J (2006) The human OCT-4 isoforms differ in their ability to confer self-renewal. *J Biol Chem* **281:** 33554-33565

Leitner J, Klauser C, Pickl WF, Stockl J, Majdic O, Bardet AF, Kreil DP, Dong C, Yamazaki T, Zlabinger G, Pfistershammer K, Steinberger P (2009) B7-H3 is a potent inhibitor of human T-cell activation: No evidence for B7-H3 and TREML2 interaction. *Eur J Immunol* **39:** 1754-1764

Li L, Baroja ML, Majumdar A, Chadwick K, Rouleau A, Gallacher L, Ferber I, Lebkowski J, Martin T, Madrenas J, Bhatia M (2004) Human embryonic stem cells possess immune-privileged properties. *Stem Cells* **22:** 448-456

Li Y, Zhang Q, Yin X, Yang W, Du Y, Hou P, Ge J, Liu C, Zhang W, Zhang X, Wu Y, Li H, Liu K, Wu C, Song Z, Zhao Y, Shi Y, Deng H (2011) Generation of iPSCs from mouse fibroblasts with a single gene, Oct4, and small molecules. *Cell Res* **21:** 196-204

Liew CG, Draper JS, Walsh J, Moore H, Andrews PW (2007) Transient and stable transgene expression in human embryonic stem cells. *Stem Cells* **25:** 1521-1528

Liu Y, Cheng D, Li Z, Gao X, Wang H (2012) The gene expression profiles of induced pluripotent stem cells (iPSCs) generated by a non-integrating method are more similar to embryonic stem cells than those of iPSCs generated by an integrating method. *Genet Mol Biol* **35:** 693-700

Ljunggren HG, Stam NJ, Ohlen C, Neefjes JJ, Hoglund P, Heemels MT, Bastin J, Schumacher TN, Townsend A, Karre K, et al. (1990) Empty MHC class I molecules come out in the cold. *Nature* **346:** 476-480

Luo L, Chapoval AI, Flies DB, Zhu G, Hirano F, Wang S, Lau JS, Dong H, Tamada K, Flies AS, Liu Y, Chen L (2004) B7-H3 enhances tumor immunity in vivo by costimulating rapid clonal expansion of antigen-specific CD8+ cytolytic T cells. *J Immunol* **173:** 5445-5450

Magliocca JF, Held IK, Odorico JS (2006) Undifferentiated murine embryonic stem cells cannot induce portal tolerance but may possess immune privilege secondary to reduced major histocompatibility complex antigen expression. *Stem Cells Dev* **15:** 707-717

Mammolenti M, Gajavelli S, Tsoulfas P, Levy R (2004) Absence of major histocompatibility complex class I on neural stem cells does not permit natural killer cell killing and prevents recognition by alloreactive cytotoxic T lymphocytes in vitro. *Stem Cells* **22:** 1101-1110

Maric MA, Taylor MD, Blum JS (1994) Endosomal aspartic proteinases are required for invariant-chain processing. *Proc Natl Acad Sci U S A* **91:** 2171-2175

Martin GR (1981) Isolation of a pluripotent cell line from early mouse embryos cultured in medium conditioned by teratocarcinoma stem cells. *Proc Natl Acad Sci U S A* **78:** 7634-7638

Martin GR, Evans MJ (1975) Differentiation of clonal lines of teratocarcinoma cells: formation of embryoid bodies in vitro. *Proc Natl Acad Sci U S A* **72:** 1441-1445

Matsui Y, Zsebo K, Hogan BL (1992) Derivation of pluripotential embryonic stem cells from murine primordial germ cells in culture. *Cell* **70:** 841-847

Matsuzaki J, Gnjatic S, Mhawech-Fauceglia P, Beck A, Miller A, Tsuji T, Eppolito C, Qian F, Lele S, Shrikant P, Old LJ, Odunsi K (2010) Tumor-infiltrating NY-ESO-1-specific CD8+ T cells are negatively regulated by LAG-3 and PD-1 in human ovarian cancer. *Proc Natl Acad Sci U S A* **107:** 7875-7880

Medema JP, de Jong J, Peltenburg LT, Verdegaal EM, Gorter A, Bres SA, Franken KL, Hahne M, Albar JP, Melief CJ, Offringa R (2001a) Blockade of the granzyme B/perforin pathway through overexpression of the serine protease inhibitor PI-9/SPI-6 constitutes a mechanism for immune escape by tumors. *Proc Natl Acad Sci U S A* **98:** 11515-11520

Medema JP, Schuurhuis DH, Rea D, van Tongeren J, de Jong J, Bres SA, Laban S, Toes RE, Toebes M, Schumacher TN, Bladergroen BA, Ossendorp F, Kummer JA, Melief CJ, Offringa R (2001b) Expression of the serpin serine protease inhibitor 6 protects dendritic cells from cytotoxic T lymphocyte-induced apoptosis: differential modulation by T helper type 1 and type 2 cells. *J Exp Med* **194:** 657-667

Meissner A, Wernig M, Jaenisch R (2007) Direct reprogramming of genetically unmodified fibroblasts into pluripotent stem cells. *Nat Biotechnol* **25:** 1177-1181

Mellor AL, Munn DH (1999) Tryptophan catabolism and T-cell tolerance: immunosuppression by starvation? *Immunol Today* **20:** 469-473

Meyer S, Nolte J, Opitz L, Salinas-Riester G, Engel W (2010) Pluripotent embryonic stem cells and multipotent adult germline stem cells reveal similar transcriptomes including pluripotency-related genes. *Mol Hum Reprod* **16:** 846-855

Mombaerts P, Iacomini J, Johnson RS, Herrup K, Tonegawa S, Papaioannou VE (1992) RAG-1-deficient mice have no mature B and T lymphocytes. *Cell* **68:** 869-877

Moss CX, Tree TI, Watts C (2007) Reconstruction of a pathway of antigen processing and class II MHC peptide capture. *EMBO J* **26:** 2137-2147

Munn DH, Mellor AL (2007) Indoleamine 2,3-dioxygenase and tumor-induced tolerance. *J Clin Invest* **117:** 1147-1154

Munn DH, Shafizadeh E, Attwood JT, Bondarev I, Pashine A, Mellor AL (1999) Inhibition of T cell proliferation by macrophage tryptophan catabolism. *J Exp Med* **189:** 1363-1372

Murphy K (2012) *Janeway's Immunobiology*, 8th edn.: Garland Science, Taylor & Francis Group, LLC.

Nagata S (1996) Fas-mediated apoptosis. *Adv Exp Med Biol* **406:** 119-124

Nakagawa M, Koyanagi M, Tanabe K, Takahashi K, Ichisaka T, Aoi T, Okita K, Mochiduki Y, Takizawa N, Yamanaka S (2008) Generation of induced pluripotent stem cells without Myc from mouse and human fibroblasts. *Nat Biotechnol* **26:** 101-106

Narayan K, Su KW, Chou CL, Khoruzhenko S, Sadegh-Nasseri S (2009) HLA-DM mediates peptide exchange by interacting transiently and repeatedly with HLA-DR1. *Mol Immunol* **46:** 3157-3162

Neefjes J, Jongsma ML, Paul P, Bakke O (2011) Towards a systems understanding of MHC class I and MHC class II antigen presentation. *Nat Rev Immunol* **11:** 823-836

Norbury CC, Hewlett LJ, Prescott AR, Shastri N, Watts C (1995) Class I MHC presentation of exogenous soluble antigen via macropinocytosis in bone marrow macrophages. *Immunity* **3:** 783-791

Nussbaum J, Minami E, Laflamme MA, Virag JA, Ware CB, Masino A, Muskheli V, Pabon L, Reinecke H, Murry CE (2007) Transplantation of undifferentiated murine embryonic stem cells in the heart: teratoma formation and immune response. *FASEB J* **21:** 1345-1357

Okita K, Ichisaka T, Yamanaka S (2007) Generation of germline-competent induced pluripotent stem cells. *Nature* **448:** 313-317

Okita K, Nakagawa M, Hyenjong H, Ichisaka T, Yamanaka S (2008) Generation of mouse induced pluripotent stem cells without viral vectors. *Science* **322:** 949-953

Ossendorp F, Mengede E, Camps M, Filius R, Melief CJ (1998) Specific T helper cell requirement for optimal induction of cytotoxic T lymphocytes against major histocompatibility complex class II negative tumors. *J Exp Med* **187:** 693-702

Ozaki Y, Edelstein MP, Duch DS (1988) Induction of indoleamine 2,3-dioxygenase: a mechanism of the antitumor activity of interferon gamma. *Proc Natl Acad Sci U S A* **85:** 1242-1246

Pamer E, Cresswell P (1998) Mechanisms of MHC class I--restricted antigen processing. *Annu Rev Immunol* **16:** 323-358

Pan K, Wang H, Chen MS, Zhang HK, Weng DS, Zhou J, Huang W, Li JJ, Song HF, Xia JC (2008) Expression and prognosis role of indoleamine 2,3-dioxygenase in hepatocellular carcinoma. *J Cancer Res Clin Oncol* **134:** 1247-1253

Pfaffl MW (2001) A new mathematical model for relative quantification in real-time RT-PCR. *Nucleic Acids Res* **29:** e45

Pfeifer JD, Wick MJ, Roberts RL, Findlay K, Normark SJ, Harding CV (1993) Phagocytic processing of bacterial antigens for class I MHC presentation to T cells. *Nature* **361:** 359-362

Pieters J (1997) MHC class II compartments: specialized organelles of the endocytic pathway in antigen presenting cells. *Biol Chem* **378:** 751-758

Plumas J, Chaperot L, Richard MJ, Molens JP, Bensa JC, Favrot MC (2005) Mesenchymal stem cells induce apoptosis of activated T cells. *Leukemia* **19:** 1597-1604

Prasad DV, Nguyen T, Li Z, Yang Y, Duong J, Wang Y, Dong C (2004) Murine B7-H3 is a negative regulator of T cells. *J Immunol* **173:** 2500-2506

Praveen PV, Yaneva R, Kalbacher H, Springer S (2010) Tapasin edits peptides on MHC class I molecules by accelerating peptide exchange. *Eur J Immunol* **40:** 214-224

Resnick JL, Bixler LS, Cheng L, Donovan PJ (1992) Long-term proliferation of mouse primordial germ cells in culture. *Nature* **359:** 550-551

Riese RJ, Wolf PR, Bromme D, Natkin LR, Villadangos JA, Ploegh HL, Chapman HA (1996) Essential role for cathepsin S in MHC class II-associated invariant chain processing and peptide loading. *Immunity* **4:** 357-366

Robertson NJ, Brook FA, Gardner RL, Cobbold SP, Waldmann H, Fairchild PJ (2007) Embryonic stem cell-derived tissues are immunogenic but their inherent immune privilege promotes the induction of tolerance. *Proc Natl Acad Sci U S A* **104:** 20920-20925

Rock KL, Goldberg AL (1999) Degradation of cell proteins and the generation of MHC class I-presented peptides. *Annu Rev Immunol* **17:** 739-779

Rock KL, Rothstein L, Gamble S, Fleischacker C (1993) Characterization of antigen-presenting cells that present exogenous antigens in association with class I MHC molecules. *J Immunol* **150:** 438-446

Sadasivan B, Lehner PJ, Ortmann B, Spies T, Cresswell P (1996) Roles for calreticulin and a novel glycoprotein, tapasin, in the interaction of MHC class I molecules with TAP. *Immunity* **5:** 103-114

Sant AJ, Miller J (1994) MHC class II antigen processing: biology of invariant chain. *Curr Opin Immunol* **6:** 57-63

Saric T, Frenzel LP, Hescheler J (2008) Immunological barriers to embryonic stem cell-derived therapies. *Cells Tissues Organs* **188:** 78-90

Saussez S, Decaestecker C, Lorfevre F, Cucu DR, Mortuaire G, Chevalier D, Wacreniez A, Kaltner H, Andre S, Toubeau G, Camby I, Gabius HJ, Kiss R (2007) High level of galectin-1 expression is a negative prognostic predictor of recurrence in laryngeal squamous cell carcinomas. *Int J Oncol* **30:** 1109-1117

Schmid D, Pypaert M, Munz C (2007) Antigen-loading compartments for major histocompatibility complex class II molecules continuously receive input from autophagosomes. *Immunity* **26:** 79-92

Schubert U, Anton LC, Gibbs J, Norbury CC, Yewdell JW, Bennink JR (2000) Rapid degradation of a large fraction of newly synthesized proteins by proteasomes. *Nature* **404:** 770-774

Schwartz RH (1993) T cell anergy. *Sci Am* **269:** 62-63, 66-71

Sfanos KS, Bruno TC, Meeker AK, De Marzo AM, Isaacs WB, Drake CG (2009) Human prostate-infiltrating CD8+ T lymphocytes are oligoclonal and PD-1+. *Prostate* **69:** 1694-1703

Shen L, Sigal LJ, Boes M, Rock KL (2004) Important role of cathepsin S in generating peptides for TAP-independent MHC class I crosspresentation in vivo. *Immunity* **21:** 155-165

Sherman MA, Weber DA, Jensen PE (1995) DM enhances peptide binding to class II MHC by release of invariant chain-derived peptide. *Immunity* **3:** 197-205

Shi F, Shi M, Zeng Z, Qi RZ, Liu ZW, Zhang JY, Yang YP, Tien P, Wang FS (2011) PD-1 and PD-L1 upregulation promotes CD8(+) T-cell apoptosis and postoperative recurrence in hepatocellular carcinoma patients. *Int J Cancer* **128:** 887-896

Shi Y, Desponts C, Do JT, Hahm HS, Scholer HR, Ding S (2008) Induction of pluripotent stem cells from mouse embryonic fibroblasts by Oct4 and Klf4 with small-molecule compounds. *Cell Stem Cell* **3:** 568-574

Spano D, Russo R, Di Maso V, Rosso N, Terracciano LM, Roncalli M, Tornillo L, Capasso M, Tiribelli C, Iolascon A (2010) Galectin-1 and its involvement in hepatocellular carcinoma aggressiveness. *Mol Med* **16:** 102-115

Stadtfeld M, Nagaya M, Utikal J, Weir G, Hochedlinger K (2008) Induced pluripotent stem cells generated without viral integration. *Science* **322:** 945-949

Streckfuss-Bömeke K, Vlasov A, Hulsmann S, Yin D, Nayernia K, Engel W, Hasenfuss G, Guan K (2009) Generation of functional neurons and glia from multipotent adult mouse germ-line stem cells. *Stem Cell Res* **2:** 139-154

Suarez-Alvarez B, Rodriguez RM, Calvanese V, Blanco-Gelaz MA, Suhr ST, Ortega F, Otero J, Cibelli JB, Moore H, Fraga MF, Lopez-Larrea C (2010) Epigenetic mechanisms regulate MHC and antigen processing molecules in human embryonic and induced pluripotent stem cells. *PLoS One* **5:** e10192

Takahashi K, Yamanaka S (2006) Induction of pluripotent stem cells from mouse embryonic and adult fibroblast cultures by defined factors. *Cell* **126:** 663-676

Taylor GS, Long HM, Haigh TA, Larsen M, Brooks J, Rickinson AB (2006) A role for intercellular antigen transfer in the recognition of EBV-transformed B cell lines by EBV nuclear antigen-specific CD4+ T cells. *J Immunol* **177:** 3746-3756

Tewari MK, Sinnathamby G, Rajagopal D, Eisenlohr LC (2005) A cytosolic pathway for MHC class II-restricted antigen processing that is proteasome and TAP dependent. *Nat Immunol* **6:** 287-294

Thomson JA, Itskovitz-Eldor J, Shapiro SS, Waknitz MA, Swiergiel JJ, Marshall VS, Jones JM (1998) Embryonic stem cell lines derived from human blastocysts. *Science* **282:** 1145-1147

Tian L, Catt JW, O'Neill C, King NJ (1997) Expression of immunoglobulin superfamily cell adhesion molecules on murine embryonic stem cells. *Biol Reprod* **57:** 561-568

Townsend A, Ohlen C, Foster L, Bastin J, Ljunggren HG, Karre K (1989) A mutant cell in which association of class I heavy and light chains is induced by viral peptides. *Cold Spring Harb Symp Quant Biol* **54 Pt 1:** 299-308

Trowsdale J, Betz AG (2006) Mother's little helpers: mechanisms of maternal-fetal tolerance. *Nat Immunol* **7:** 241-246

Van Kaer L, Ashton-Rickardt PG, Ploegh HL, Tonegawa S (1992) TAP1 mutant mice are deficient in antigen presentation, surface class I molecules, and CD4-8+ T cells. *Cell* **71:** 1205-1214

van Parijs L, Perez VL, Abbas AK (1998) Mechanisms of peripheral T cell tolerance. *Novartis Found Symp* **215:** 5-14; discussion 14-20, 33-40

Vandesompele J, De Preter K, Pattyn F, Poppe B, Van Roy N, De Paepe A, Speleman F (2002) Accurate normalization of real-time quantitative RT-PCR data by geometric averaging of multiple internal control genes. *Genome Biol* **3:** RESEARCH0034

Watts C (2012) The endosome-lysosome pathway and information generation in the immune system. *Biochim Biophys Acta* **1824:** 14-21

Wernig M, Meissner A, Foreman R, Brambrink T, Ku M, Hochedlinger K, Bernstein BE, Jaenisch R (2007) In vitro reprogramming of fibroblasts into a pluripotent ES-cell-like state. *Nature* **448:** 318-324

Witkiewicz A, Williams TK, Cozzitorto J, Durkan B, Showalter SL, Yeo CJ, Brody JR (2008) Expression of indoleamine 2,3-dioxygenase in metastatic pancreatic ductal adenocarcinoma recruits regulatory T cells to avoid immune detection. *J Am Coll Surg* **206:** 849-854; discussion 854-846

Wu DC, Boyd AS, Wood KJ (2008) Embryonic stem cells and their differentiated derivatives have a fragile immune privilege but still represent novel targets of immune attack. *Stem Cells* **26:** 1939-1950

Wu K, Kryczek I, Chen L, Zou W, Welling TH (2009) Kupffer cell suppression of CD8+ T cells in human hepatocellular carcinoma is mediated by B7-H1/programmed death-1 interactions. *Cancer Res* **69:** 8067-8075

Yachimovich-Cohen N, Even-Ram S, Shufaro Y, Rachmilewitz J, Reubinoff B (2010) Human embryonic stem cells suppress T cell responses via arginase I-dependent mechanism. *J Immunol* **184:** 1300-1308

Zang X, Sullivan PS, Soslow RA, Waitz R, Reuter VE, Wilton A, Thaler HT, Arul M, Slovin SF, Wei J, Spriggs DR, Dupont J, Allison JP (2010) Tumor associated endothelial expression of B7-H3 predicts survival in ovarian carcinomas. *Mod Pathol* **23:** 1104-1112

Zang X, Thompson RH, Al-Ahmadie HA, Serio AM, Reuter VE, Eastham JA, Scardino PT, Sharma P, Allison JP (2007) B7-H3 and B7x are highly expressed in human prostate cancer and associated with disease spread and poor outcome. *Proc Natl Acad Sci U S A* **104:** 19458-19463

Zechner U, Nolte J, Wolf M, Shirneshan K, Hajj NE, Weise D, Kaltwasser B, Zovoilis A, Haaf T, Engel W (2009) Comparative methylation profiles and telomerase biology of mouse multipotent adult germline stem cells and embryonic stem cells. *Mol Hum Reprod* **15:** 345-353

Zhang Y, Huang S, Gong D, Qin Y, Shen Q (2010) Programmed death-1 upregulation is correlated with dysfunction of tumor-infiltrating CD8+ T lymphocytes in human non-small cell lung cancer. *Cell Mol Immunol* **7:** 389-395

Zhao T, Zhang ZN, Rong Z, Xu Y (2011) Immunogenicity of induced pluripotent stem cells. *Nature* **474:** 212-215

Zhou D, Li P, Lin Y, Lott JM, Hislop AD, Canaday DH, Brutkiewicz RR, Blum JS (2005) Lamp-2a facilitates MHC class II presentation of cytoplasmic antigens. *Immunity* **22:** 571-581

Zhou H, Wu S, Joo JY, Zhu S, Han DW, Lin T, Trauger S, Bien G, Yao S, Zhu Y, Siuzdak G, Scholer HR, Duan L, Ding S (2009) Generation of induced pluripotent stem cells using recombinant proteins. *Cell Stem Cell* **4:** 381-384

Zovoilis A, Nolte J, Drusenheimer N, Zechner U, Hada H, Guan K, Hasenfuss G, Nayernia K, Engel W (2008) Multipotent adult germline stem cells and embryonic stem cells have similar microRNA profiles. *Mol Hum Reprod* **14:** 521-529